Universo Primitivo
Proceedings 2020

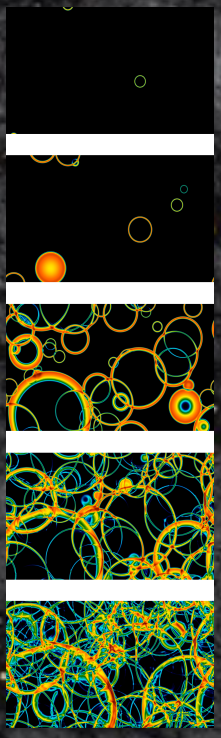
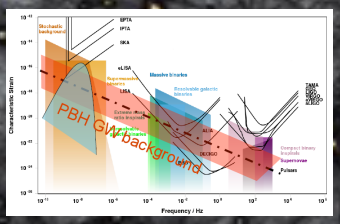

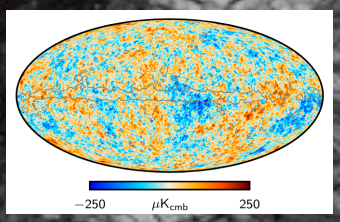

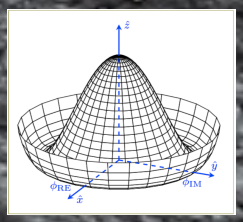
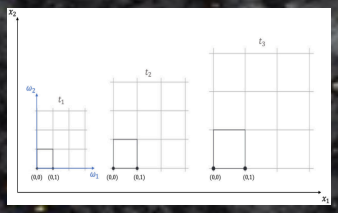
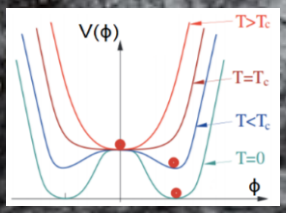

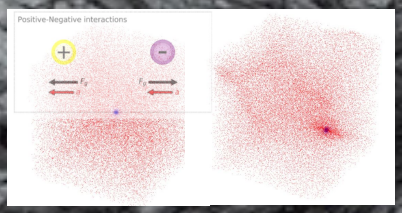

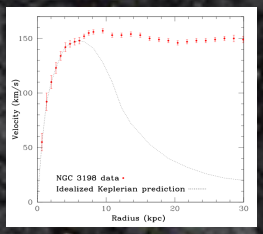

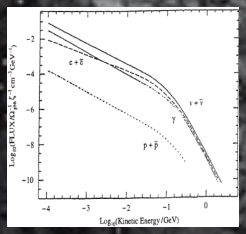

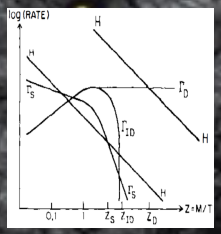

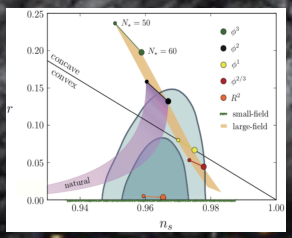

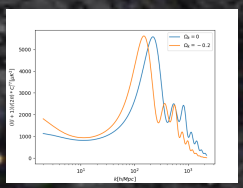
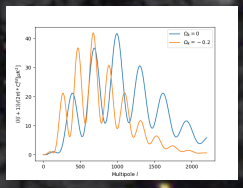
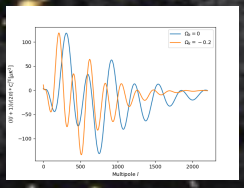
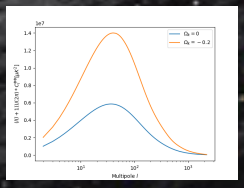
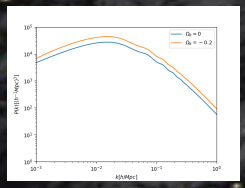

Participants: João Viana, Henrique Miranda, Sara Nóbrega, André Baptista, Diogo Calado, Afonso do Vale, João Dias, Johannes Brinz; Luis Atayde, Pedro Garcia, Pedro Martins, Hellene Rehahn, Sona Ertlova. **Editor**: António da Silva

Index of presentations

Day 1: 05/02/2020, 9h00-13h30, C8.2.4

i. João Viana, "Electroweak phase transition and the Highs mechanism”
ii. Henrique Miranda, "Primordial Black Holes and their Cosmological Implications”
iii. Sara Nóbrega, "Predictions of linear primordial Gravitational Waves related to the standard single-field slow-roll inflationary scenario"
iv. Diogo Calado, "A brief review on GUT and Electroweak Baryogenesis and the Deep Underground Neutrino Experiment"
v. André Baptista, "Electroweak Baryogenesis”

Day 2: 06/02/2020, 9h00-17h30, C8.2.14 (morning), C8.2.3 (afternoon)

vi. Afonso do Vale, "Dark Matter - Observational overview and possible candidates"
vii. João Dias, "Prospects for the unification of dark matter and dark energy using negative mass particles"
viii. Johannes Brinz, "The expansion of space"
ix. Luis Atayde, "A review of CAMB: a CMB Boltzmann code to compute anisotropies in the cosmic microwave background"
x. Pedro Garcia, "Electroweak phase transition and the Highs mechanism"
xi. Pedro Martins, "Formation of Primordial Black Holes”
xii. Hellene Rehahn, "Cosmic Neutrino Background"

Proceedings

Electroweak phase transition and the Higgs mechanism

João Viana [1], 49547

[1] Faculdade de Ciências da Universidade de Lisboa; fc49547@alunos.fc.ul.pt

Received: date; Accepted: date; Published: date

Abstract: The Higgs mechanism was proposed by 1962 by Philip Warren Anderson. In 1964 three groups, independently, demonstrated how one could explain the mass generation of the bosons W^+, W^- and Z using the Higgs mechanism. We are going to apply the Higgs mechanism to an Abelian Example $U(1)$ and to the Electroweak Standard Model proposed by S. L. Glashow, A. Salam and S. Winberg and show how the symmetry breaking generates mass for the W^+, W^- and Z bosons. Afterwards we will discuss what type of electroweak phase transitions there can be, and their consequences.

1. Electroweak phase transition

The electroweak phase transition happened very early after the Big Bang, the universe was approximately $10^{-11}\,s$ long and its temperature was approximately $160\,GeV$ [1] , and it happened when the Higgs field ϕ stopped having a non-zero vacuum expectation value (v.e.v.).

A simplistic explanation is that at early stages the universe was very hot and energetic and because of that the Higgs potential was shaped like a bowl.

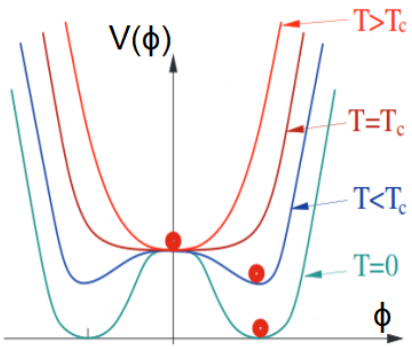

Fig. 1. Change of the potential $V(\phi)$ of the Higgs field ϕ with the temperature of the universe.

Since the universe was shaped like bowl it caused it to have a zero v.e.v. ($\langle\phi\rangle = 0$). As the universe cooled down, the field potential changed its shape to a "Mexican hat". This shape has a non-zero v.e.v. ($\langle\phi\rangle \neq 0$), this means that, even in vacuum, the energy of the Higgs field is not zero. This change from $\langle\phi\rangle = 0 \rightarrow \langle\phi\rangle \neq 0$ triggered the Higgs mechanism and caused some particles to have mass.

2. Higgs Mechanism

Quantum field theory was very successful understanding the electromagnetic field and the strong force but there was a inconsistency: the gauge bosons Z, W^+ and W^- should be massless, in reality these bosons have a very large mass ($\sim 80 - 90\,GeV$), which comparable to some molecules. In 1964 three separate groups were able to show how, by symmetry breaking caused by the Higgs field, one can be able to generate mass of the gauge bosons $W^\pm$ and Z, leptons and quarks. The mass of some other particles, like neutrons and protons, come mainly from the binding energy of the gluons: $E = mc^2$.

Without getting into many mathematical details, which we will discuss in the next section, the Higgs mechanism states that the breaking in symmetry cause the bosons to interact with the field, this interaction "slows" them down and they stop being able to travel at the speed of light (because their mass is generated, $m \neq 0$). The stronger the boson interacts with the field, the bigger their mass will be.

3. Abelian Example of the Higgs Mechanism

We will start with an abelian example with global $U(1)$ gauge symmetry, this example will be based on the work done by [2], [3] and [4]. We will couple a complex scalar field ϕ of electric charge q to a electromagnetic field A^μ. The Lagrangian of the field will be:

$$\mathcal{L} = -\frac{1}{4}F_{\mu\nu}F^{\mu\nu} + D_\mu\phi^* D^\mu\phi - V(\phi) \tag{3.1}$$

Where $-\frac{1}{4}F_{\mu\nu}F^{\mu\nu}$ is the kinetic term of the electromagnetic field with

$$F_{\mu\nu} = \partial_\mu A_\nu - \partial_\nu A_\mu \tag{3.2}$$

The term $D_\mu\phi^* D^\mu\phi$ is the coupling of the electromagnetic field and the scalar field with

$$D_\mu\phi(x) = \partial_\mu\phi(x) + iqA_\mu(x)\phi(x), \quad D_\mu\phi^*(x) = \partial_\mu\phi^*(x) - iqA_\mu(x)\phi^*(x) \tag{3.3}$$

The coupling of the complex scalar field to itself is given by

$$V(\phi) = \frac{\lambda}{2}(\phi^*\phi)^2 + m^2(\phi^*\phi) \tag{3.4}$$

We require $\lambda > 0$ for stability. If $m^2 > 0$ then the theory is simply quantum electrodynamics with a massless photon and a charged scalar field ϕ with mass m .We will suppose that $m^2 < 0$ [5]. This will mean that the potential is shaped like a "Mexican Hat Potential".

From this we can easily see that the Lagrangian is invariant under $U(1)$ rotations, $\phi \to e^{i\theta}\phi$ and under local $U(1)$ gauge transformations:

$$\begin{aligned} A_\mu(x) &\to A_\mu(x) - \partial_\mu\eta(x) \\ \phi(x) &\to e^{iq\eta(x)}\phi(x) \end{aligned} \tag{3.5}$$

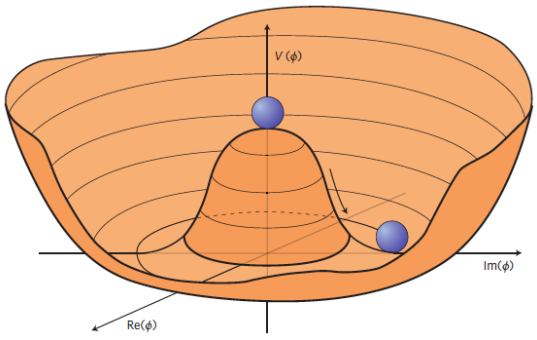

Fig. 2. Higgs "Mexican Hat" Potential given by $V(\phi) = \frac{\lambda}{2}(\phi^*\phi)^2 + m^2(\phi^*\phi)$ with $\lambda > 0$ and $m^2 < 0$. We have a local maximum at $\phi = 0$ and a global mininum at $|\phi| = \sqrt{-m^2/\lambda}$

It is trivial to see that that the potential has a local maximum at $\phi = 0$ and a global minimum at $|\phi| = \sqrt{\frac{-m^2}{\lambda}} = \frac{v}{\sqrt{2}}$

Because of this the system will "fall" into the valley of minimal energy which will give a non-zero vacuum expectation value $\langle\phi\rangle \neq 0$, therefore the $U(1)$ global gauge symmetry of the theory will be broken. If we had global $U(1)$ symmetry this spontaneous breakdown would lead to a massless Goldstone scalar [4].

Now we will parameterize ϕ as

$$\phi = \frac{v+h}{\sqrt{2}}e^{i\frac{\chi}{v}} \tag{3.6}$$

Where h and χ are scalar fields and have no v.e.v. (vacuum expected value). After making the substitution, rearranging the Lagrangian (3.1) and making the following gauge transformation:

$$A_\mu \to A_\mu - \frac{1}{ev}\partial_\mu \chi$$

We get

$$\begin{aligned}\mathcal{L} = &-\frac{1}{4}F_{\mu\nu}F^{\mu\nu} + \frac{e^2v^2}{2}A_\mu A^\mu \\ &+ \frac{1}{2}\left(\partial_\mu h \partial^\mu h - 2\mu^2 h^2\right) + \frac{1}{2}\partial_\mu\chi\partial^\mu\chi + (h,\chi \text{ interaction})\end{aligned} \tag{3.7}$$

In the Lagrangian we can identify a photon with mass $m_A = ev$, a scalar field h with mass $m_h = \sqrt{2}\mu = \sqrt{2\lambda}v$ and a massless scalar field χ.

4. Higgs mechanism in the Electroweak Standard Model

Now we explore the Electroweak Standard Model proposed by S. L. Glashow, A. Salam and S. Winberg. Before the electroweak phase transition we had the electroweak unification and it is based on a $SU(2)_L \otimes U(1)_Y$:

$$\mathcal{L}_{SM} = \mathcal{L}_{gauge} + \mathcal{L}_f + \mathcal{L}_{Higgs} + \mathcal{L}_{Yuk} \tag{4.1}$$

The theory contains three $SU(2)_L$ gauge bosons, W^i_μ , $i = 1, 2, 3$, that couple to the weak-isospin T and one $U(1)_Y$ gauge boson, B_μ, that couple to the hypercharge Y.

The first term, $\mathcal{L}_{gauge}$ is given by

$$\mathcal{L}_{\text{gauge}} = -\frac{1}{4}F^{\mu\nu}F_{\mu\nu} - \frac{1}{4}G^{i\mu\nu}G^i_{\mu\nu} \tag{4.2}$$

Where

$$G^i_{\mu\nu} = \partial_\mu W^i_\nu - \partial_\nu W^i_\mu - g\epsilon^{ijk}W^j_\mu W^k_\nu \tag{4.3}$$

$$F_{\mu\nu} = \partial_\mu B_\nu - \partial_\nu B_\mu \tag{4.4}$$

The term $\mathcal{L}_f$ corresponds to the fermion term an it is given by

$$\mathcal{L}_f = i\bar{\Psi}_L \not{D}\Psi_L + i\bar{\psi}_R \not{D}\psi_R \tag{4.5}$$

The $\not{D}$ is called the *Feynman slash notation* and is given by

$$\not{D} \overset{\text{def}}{=} \gamma^\mu D_\mu \tag{4.6}$$

With γ being the Dirac matrices

$$\gamma^0 = \begin{pmatrix} 1 & 0 & 0 & 0 \\ 0 & 1 & 0 & 0 \\ 0 & 0 & -1 & 0 \\ 0 & 0 & 0 & -1 \end{pmatrix}, \quad \gamma^1 = \begin{pmatrix} 0 & 0 & 0 & 1 \\ 0 & 0 & 1 & 0 \\ 0 & -1 & 0 & 0 \\ -1 & 0 & 0 & 0 \end{pmatrix}$$

$$\gamma^2 = \begin{pmatrix} 0 & 0 & 0 & -i \\ 0 & 0 & i & 0 \\ 0 & i & 0 & 0 \\ -i & 0 & 0 & 0 \end{pmatrix}, \quad \gamma^3 = \begin{pmatrix} 0 & 0 & 1 & 0 \\ 0 & 0 & 0 & -1 \\ -1 & 0 & 0 & 0 \\ 0 & 1 & 0 & 0 \end{pmatrix}$$

It is useful to define a product of the four gamma matrices as γ^5 as

$$\gamma^5 := i\gamma^0\gamma^1\gamma^2\gamma^3 = \begin{pmatrix} 0 & 0 & 1 & 0 \\ 0 & 0 & 0 & 1 \\ 1 & 0 & 0 & 0 \\ 0 & 1 & 0 & 0 \end{pmatrix}$$

Where the covariant derivative acts on Ψ_L and ψ_R , respectively, as

$$D_\mu \Psi_L = \left(\partial_\mu + igW_\mu + ig' Y_L B_\mu\right) \Psi_L, \quad D_\mu \psi_R = \left(\partial_\mu + ig' Y_R B_\mu\right) \psi_R \tag{4.7}$$

The L/R refer to the left/right chiral projections of Ψ:

$$\Psi_L = \frac{1-\gamma^5}{2}\Psi, \quad \psi_R = \frac{1+\gamma^5}{2}\Psi \tag{4.8}$$

In the electroweak gauge theory the left-handed quarks and leptons (Ψ_L) are arranged in doublets:

$$q_L = \begin{pmatrix} u \\ d \end{pmatrix}_L, \quad l_L = \begin{pmatrix} \nu_e \\ e^- \end{pmatrix}_L$$

While the right handed quarks and leptons (ψ_R) are arranged in singlets:

$$u_R, d_R, \nu_{eR}, e_R^-$$

The gauge transformations are:

$$\begin{aligned} \Psi_L \to \Psi_L' &= e^{iY_L\theta(x)} U_L \Psi_L \\ \psi_R \to \psi_R' &= e^{iY_R\theta(x)} \psi_R \end{aligned} \tag{4.9}$$

The transformation U_L only acts on the doublet of $U(2)_L$ and is

$$U_L = e^{i\frac{\sigma_i}{2}\beta^i} \tag{4.10}$$

With σ_i being the Pauli matrices.

The hypercharge Y is fixed in such a way that the sum of the hypercharge Y with the third component of the weak iso-spin give the electromagnetic charge:

$$Q = T_3 + Y \quad \text{(some authors definition is } \tfrac{Y}{2} \text{ instead of } Y) \tag{4.11}$$

For left-handed doublets T_3 is $\frac{\sigma_3}{2}$ (i.e. $T_3 = \pm\frac{1}{2}$), while for right-handed singlets $T_3 = 0$. Hence the hypercharge eigenvalues for the leptons are

$$Y(l_L) = -\frac{1}{2}, \quad Y(l_R) = -1$$

$$Y(q_L) = \frac{1}{6}, \quad Y(u_R) = \frac{2}{3}, \quad Y(d_R) = -\frac{1}{3}$$

The transformation properties of B_μ and W_μ (W_μ can be written in terms of the generators: $W_\mu = W_\mu^i \sigma_i/2$) are fixed by the gauge symmetry of the fermion Lagrangian:

$$\begin{aligned} B_\mu &\to B_\mu' = B_\mu - \tfrac{1}{g'}\partial_\mu\theta \\ W_\mu &\to W_\mu' = U_L W_\mu U_L^\dagger + \tfrac{1}{g}\left(\partial_\mu U_L\right) U_L^\dagger \end{aligned} \tag{4.12}$$

The Higgs part of the Lagrangian is:

$$\mathcal{L}_{\text{Higgs}} = \left(D^\mu\phi\right)^\dagger \left(D_\mu\phi\right) - V(\phi) \tag{4.13}$$

To spontaneously we are gonna consider ϕ to be a $SU(2)_L$ gauge spinor with $U(1)_R$ hypercharge $Y(\phi) = \frac{1}{2}$:

$$\phi = \begin{pmatrix} \phi^+ \\ \phi^0 \end{pmatrix} \tag{4.14}$$

The covariant derivative of the field becomes

$$D_\mu \phi = \left(\partial_\mu + ig\frac{\sigma_i}{2} W_\mu^i + i\frac{1}{2} g' B_\mu \right) \phi \tag{4.15}$$

Renormalizability and requiring $SU(2)_L \otimes U(1)_Y$ invariance sets the Higgs potential as:

$$V(\phi) = \frac{\lambda}{2} \left(\phi^\dagger \phi \right)^2 + m^2 \left(\phi^\dagger \phi \right) \tag{4.16}$$

We require $\lambda > 0$ to have vacuum stability. Like before by setting $m^2 < 0$ the field will acquire a non-zero v.e.v. which will spontaneously break the symmetry. Since there are infinite solutions to $\phi^\dagger \phi = v/2$ we arbitrary chose:

$$\langle \phi \rangle = \frac{1}{\sqrt{2}} \begin{pmatrix} 0 \\ v \end{pmatrix} \tag{4.17}$$

Since we need conservation of electric charge only a neutral scalar field could acquire a v.e.v.. So ϕ^0 is so be considered as the neutral component of the doublet, and we have that $Q(\phi) = 0$. Hence electromagnetism is unbroken by the scalar v.e.v.

$$SU(2)_L \otimes U(1)_Y \to U(1)_Q$$

Now, the Z and $W^\pm$ masses will be generated just like in the section 3. We will write the doublet scalar in the unitary gauge:

$$\phi = \frac{1}{\sqrt{2}} \begin{pmatrix} 0 \\ v + h \end{pmatrix} \tag{4.18}$$

Since we are more interested in the contributions for the bosons masses we will omit the h related terms

$$\begin{aligned} (D^\mu \phi)^\dagger (D_\mu \phi) &= \left| \left(\partial_\mu + \frac{i}{2} g \frac{\sigma_k}{2} W_\mu^k + \frac{i}{2} g' B_\mu \right) \frac{1}{\sqrt{2}} \begin{pmatrix} 0 \\ v \end{pmatrix} \right|^2 \\ &= \frac{v^2}{8} \left[g^2 \left(\left(W_\mu^1 \right)^2 + \left(W_\mu^2 \right)^2 \right) + \left(g W_\mu^3 - g' B_\mu \right)^2 \right] \end{aligned} \tag{4.19}$$

From here we can define the charged boson $W_\mu^\pm$ as:

$$W_\mu^\pm \equiv \frac{1}{\sqrt{2}} \left(W_\mu^1 \pm i W_\mu^2 \right) \tag{4.20}$$

and the term in g^2 becomes

$$\frac{1}{2} \left(\frac{gv}{2} \right)^2 W_\mu^\dagger W^\mu \tag{4.21}$$

and thus boson $W^\pm$ mass is generated, and given by

$$m_{w^\pm} = \tfrac{gv}{2} \tag{4.22}$$

The second term we can write in matricial form like :

$$\frac{v^2}{8}\left(gW_\mu^3 - g'B_\mu\right)^2 = \frac{1}{2}\begin{pmatrix} W_\mu & B_m u \end{pmatrix} M^2 \begin{pmatrix} W_\mu \\ B_m u \end{pmatrix} \tag{4.23}$$

With

$$M^2 = \frac{v^2}{4}\begin{pmatrix} g^2 & -g'g \\ -g'g & g'^2 \end{pmatrix} \tag{4.24}$$

This matrix has eigenvalues

$$m_A^2 = 0 \quad \text{and} \quad m_Z^2 = \tfrac{v^2}{4}(g^2 + g'^2)$$

and, therefore, we define the bosons A and Z as being the eigenvectors of the matrix

$$Z_\mu \equiv \frac{1}{\sqrt{g^2+g'^2}}\left(gW_\mu^3 - g'B_\mu\right) \qquad \text{with mass} \quad m_Z = \frac{v}{2}\sqrt{g^2+g'^2}$$
$$A_\mu \equiv \frac{1}{\sqrt{g^2+g'^2}}\left(g'W_\mu^3 + gB_\mu\right) \qquad \text{with mass} \quad m_A = 0$$

Were are going to introduce the *Weinberg angle* or *weak mixing angle*

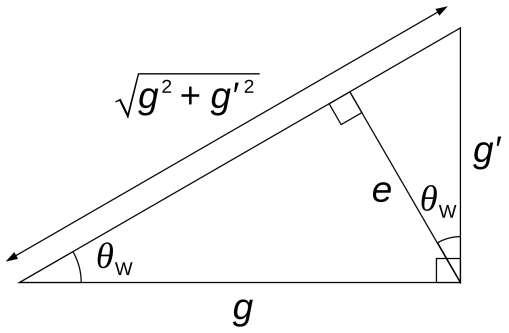

Fig. 3. Schematic of the Weinberg angle or weak mixing angle, used to relate the contribution of the electroweak unification bosons B and W^3 to the bosons A and Z.

And allow us to describe the relations between the contributions of the electroweak unification bosons B and W^3 to the bosons A and Z in a matricial form which resembles a rotation by the angle θ_W, the weak mixing angle.

$$\begin{pmatrix} A^\mu \\ Z^\mu \end{pmatrix} = \begin{pmatrix} \cos\theta_W & \sin\theta_W \\ -\sin\theta_W & \cos\theta_W \end{pmatrix}\begin{pmatrix} B^\mu \\ W^\mu \end{pmatrix} \tag{4.25}$$

The value of the mixing angle and be empirically found [6]:

$$\cos\theta_W = \tfrac{m_{W^\pm}}{m_Z} \approx 0.882 \tag{4.26}$$

5. Nature of the Electroweak phase transition

Now one must discuss the nature of the phase transition and its consequences. We have two possibilities:

- second-order phase transition or crossover
- first-order phase transition

These terms has a similar meaning as in classical physics. Classically, a first-order phase transition happens when the system has a discontinuity on the first derivative of the free energy, here, by first-order phase transition, we

mean that the $\langle\phi\rangle$ changes in a non-continuous way and does not let the Universe have a constant thermodynamical equilibrium. With second order transition we mean that $\langle\phi\rangle$ changes continuously with time and the Universe is always in constantly in thermal equilibrium.

We can write some simplistic changes to the Higgs potential that illustrate this difference

The potential of the second-order phase transition is:

$$V(T,H) = \lambda\left(H^2 - v^2\right)^2 + bT^2H^2 \tag{5.1}$$

The potential of the first-order phase transition is:

$$V(T,H) = \lambda\left(H^2 - v^2\right)^2 + bT^2H^2 + aTH^3 \tag{5.2}$$

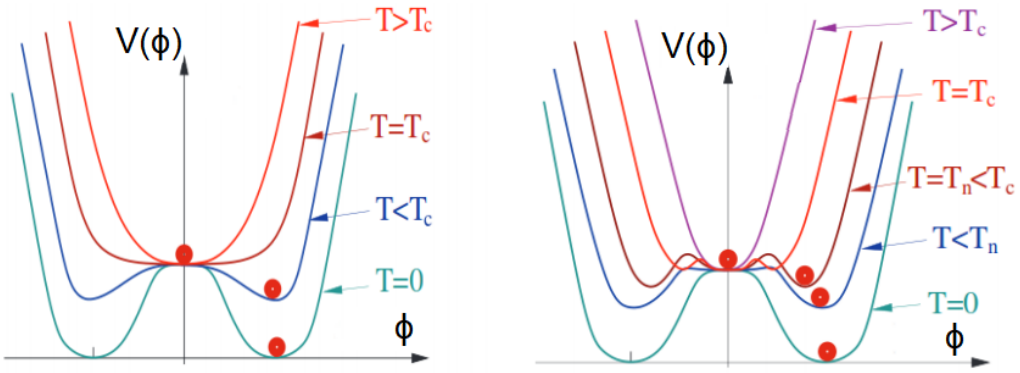

Fig. 4. Left: Variation of the Higgs potential in a second-order phase transition. Right: Variation of the Higgs potential in a first-order phase transition

In the **second-order transition** (5.1) for $T > T_c$ there exists only one global minimum at $\phi = 0$. As the temperature goes down and becomes slightly bigger than T_c, the potential changes its shape and starts having a local maximum at $\phi = 0$ and a global minimum very close to 0. As the temperature continues to go down the global minimum moves away from $\phi = 0$ until it reaches it final state ($T \sim 0\,GeV$) with $\phi = v$. In this case $\langle\phi\rangle$ follows continuously the minimum of the potential from 0 to v.

For the **first-order transition** (5.2) for $T > T_c$ there exists only one global minimum at $\phi = 0$. When the temperature reaches T_c appears a local minimum, since it is not a global minimum the v.e.v. is not able to change and stays a zero. As times goes on the local minimum moves further away from $\phi = 0$ but the potential gets smaller. When $T = T_n$ this local minimum is promoted to global minimum. This means that the v.e.v. jumps suddenly from $\langle\phi\rangle = 0$ to a value different from zero, in a non continuous way.

According to the standard model, the electroweak phase transition is of second order. But this means that baryogenesiss should never have occurred [7]. Because of this we need to make extension to the standard model.

According to [8], anomalous weak interaction during the first-order transition is able to explain baryogenesis. But, if a first-order phase transition happened, it would make the Higgs mass unrealistic ($m_H < 66.5 \pm 1.4\,GeV$ [9]; $m_H < 42\,GeV$ [10]). Which is far from what is measure in LHC ($m_H \approx 125\,GeV$).

The real nature of the electroweak phase transition is still an unknown and a subject of great discussion. It is clear that changes need to be made to the Standard Model.

References

1. Melo, I. Higgs potential and fundamental physics. Lecture Notes, 2016.
2. Nguyen, K. The Higgs Mechanism. Lecture Notes, 2009.
3. Kaplunovsky, V. Glashow–Weinberg–Salam Theory. Lecture Notes, 2015.
4. Kaplunovsky, V. HIGGS MECHANISM. Lecture Notes, 2019.
5. Dawson, S. Introduction to Electroweak Symmetry Breaking, 1999, [arXiv:hep-ph/hep-ph/9901280].

6. Okun, L.B. *Leptons and Quarks*; North Holland, 1982.
7. Kisslinger, L.S. *Astrophysics And The Evolution Of The Universe (Second Edition)*; Wspc, 2016.
8. Nelson, A.; Kaplan, D.; Cohen, A. Why there is something rather than nothing: Matter from weak interactions. *Nuclear Physics B* **1992**, *373*, 453 – 478. doi:https://doi.org/10.1016/0550-3213(92)90440-M.
9. Fodor, Z. Electroweak phase transitions. *Nuclear Physics B - Proceedings Supplements* **2000**, *83-84*, 121 – 125. Proceedings of the XVIIth International Symposium on Lattice Field Theory, doi:https://doi.org/10.1016/S0920-5632(00)91603-7.
10. Das, S.; Fox, P.J.; Kumar, A.; Weiner, N. The dark side of the electroweak phase transition. *Journal of High Energy Physics* **2010**, *2010*. doi:10.1007/jhep11(2010)108.

Proceedings

Primordial Black Holes and their Cosmological Implications

Henrique Miranda [1]

[1] Faculdade de Ciências da Universidade de Lisboa, Campo Grande, P-1749-016 Lisbon, Portugal; fc49545@alunos.fc.ul.pt

Received: date; Accepted: date; Published: date

Abstract: Density perturbations in hybrid inflation models with two stages of inflation can be very large and the resulting density inhomogeneities lead to a copious production of black holes. In these models the amount of black holes produced can be extremely small, but it could be large enough to have relevant cosmological and astrophysical implications. With a certain choice of parameters these black holes may constitute the dark matter in the universe. For some other models where the masses of the black holes are very low, their evaporation can be responsible for the post-inflationary reheating. The aim of this paper is to explore the formation of primordial black holes, the possible implications for cosmology and astrophysics and their possible detection.

Keywords: Cosmology; Hybrid Inflation; Primordial Black Holes; Dark Matter; Gravitational Waves

1. Introduction

The acceleration of the scale factor could drive the universe towards homogeneity, isotropy and spatial flatness at large scales. For this reason, a time of inflation in the early universe is an attractive idea in modern cosmology. Briefly, inflation is a theory of exponential expansion of space in the early universe. The inflationary epoch lasted from 10^{-36} s after the conjectured Big Bang singularity to some time between 10^{-33} s and 10^{-32} s after the singularity. Following the inflationary period, the universe continued to expand, but the expansion was no longer accelerated [1].

Hybrid inflation is a type of inflation. Hybrid inflation models can have very large density perturbations which can lead to a copious production of black holes. This type of black holes are called primordial black holes and their existence was first proposed in 1966 [2]. The theory behind their origin was first studied in depth by Stephen Hawking in 1971 [3]. Depending on the model, primordial black holes could have initial masses ranging from 10^{-8} kg (the so-called Planck relics) to more than thousands of solar masses. However, primordial black holes originally having a mass lower than 10^{11} kg would not have survived to the present due to Hawking radiation, which causes complete evaporation in a time much shorter than the age of the Universe [4]. Primordial black holes belong to the class of MAssive Compact Halo Objects (MACHOs). They are naturally a good dark matter candidate: they are non-baryonic, nearly collisionless and stable , they have non-relativistic velocities, and they form very early in the history of the Universe (typically less than one second after the Big Bang) [5]. Primordial black holes are also good candidates for being the seeds of the supermassive black holes at the center of massive galaxies, as well of intermediate-mass black holes [6].

In this paper, firstly it will be explored what is a hybrid inflation model and the conditions that lead to density perturbations, through the analysis of two different models. For particular conditions, the primordial black holes have cosmological and astrophysical implications that too will be explored. Finally, it will be discussed the detectability of such primordial black holes.

2. Hybrid Inflation

In the past it was presumed that inflation began in the false vacuum state after the high temperature phase transitions in the early universe [7], that is, it was assumed initial thermal equilibrium. However, this assumption should not be considered [8]. So all possible conditions started to be considered and not only those that assumed initial thermal equilibrium and then it was seen if some of these conditions led to inflation. This process is called chaotic inflation [9]. The class of chaotic inflation provides the most general framework for the development of inflationary cosmology.

Examples of potentials of simple chaotic models are:

$$V(\phi) = \frac{m^2\phi^2}{2}, V(\phi) = \frac{\lambda\phi^4}{4} \tag{1}$$

In these models inflation occurs at $\phi > M_P$. Chaotic inflation near $\phi = 0$ can be considered in models with potentials which could be used for implementation of the new inflation (The term "new inflation" refers to inflation at small ϕ) scenario, for example:

$$V(\phi) = -\frac{m^2\phi^2}{2} + \frac{\lambda\phi^4}{4} \tag{2}$$

However, with this potential even if inflation can be achieved at small ϕ the spectrum has a unacceptably large negative tilt and so the problem of having inflation at $\phi = 0$ arises again. A scenario in which this problem vanishes is with hybrid inflation [10], [11]. When considering hybrid inflation, the initial conditions for inflation are not determined by thermal effects, hence hybrid inflation belongs to the general class of chaotic inflation models and also hybrid inflation may occur for values of ϕ much smaller than M_P.

A distinctive feature of hybrid inflation is that it describes the evolution of two scalar fields, ϕ and ψ . In hybrid inflation, one scalar field (ψ) is responsible for most of the energy density (thus determining the rate of expansion), while the other field (ϕ) is responsible for the slow roll (thus determining the period of inflation and its termination). So fluctuations in the field ψ would not affect inflation termination, while fluctuations in the field ϕ would not affect the rate of expansion. Therefore, hybrid inflation is not eternal [12]. When the slowly moving field ϕ reaches some critical value ϕ_c, it triggers a rapid motion of the field ψ , inducing a transition to a “waterfall” regime. Then the energy density of the field ψ rapidly decreases, and inflation ends.

3. Primordial Black Hole Formation Scenarios

An interesting hybrid inflationary model [13] has the following effective potential:

$$V(\phi, \psi) = M^4 cos^2\left(\frac{\psi}{\sqrt{2}f}\right) + \frac{1}{2}m^2\phi^2 + \frac{1}{4}\lambda^4\phi^2\psi^2 \tag{3}$$

In the case of this model, the effective potential is symmetric with respect to the change $\psi \to -\psi$, so the field ψ can roll with equal probability towards its positive and negative values, at the moment of the phase transition. This is a topological defect, called domain wall. During the long stage of rolling of the field ψ to its minimum, all topological defects in this model appear to be inflating. Independently of the nature of these defects (domain walls, strings, monopoles, either topologically stable or not) their exponential expansion leads to density perturbations $\delta\rho/\rho = \mathcal{O}(1)$ on the exponentially large scale corresponding to the moment of the phase transition. This may result in a copious black hole formation. The appearance of inflating topological defects demonstrates that the existence of the second stage of inflation in the hybrid scenario may lead to large density perturbations. The phase transition at $\phi = \phi_c$ leads to the appearance of a characteristic spike in the spectrum of density perturbations [13]. A spike in the spectrum of density perturbations is a mechanism that can lead to the formation of primordial black holes [4], but there are other mechanims such as first-order phase transitions [14], resonant reheating [15], tachyonic preheating [16] or some curvaton scenarios [17]. The mechanisms that will be explored are the spike in the spectrum of density perturbations and the accretion and merging of already formed primordial black holes.

3.1. Spikes in the Primordial Power Spectrum

This mechanism of formation of primordial black holes will be explored by comparison between two different models, a model with a effective potential given by equation (3) and a model with the following effective potential [6]:

$$V(\phi, \psi) = \Lambda\left[\left(1 - \frac{\psi^2}{M^2}\right)^2 + \frac{(\phi - \phi_c)}{\mu_1} - \frac{(\phi - \phi_c)^2}{\mu_2^2} + \frac{2\phi^2\psi^2}{M^2\phi_c^2}\right] \tag{4}$$

Where μ_1 and μ_2 are mass parameters. Initially, inflation takes place along the valley $\psi = 0$. After the critical value ϕ_c this potential develops a tachyonic instability, forcing the field trajectories to reach one of the global minima, located at $\phi = 0, \psi = \pm M$. As said before, the phase transition leads to the appearance of a characteristic spike in the spectrum of density perturbations. In Ref. [4], it was concluded that in the case that the primordial curvature fluctuation spectrum has a pronounced spike at some particular scale, it is possible to generate primordial black holes whenever those high curvature fluctuations reentered the horizon during the radiation era, since nothing could prevent their gravitational collapse. The mass of those primordial black holes would be given very approximately by the total mass within the horizon at the time of reentry. In Figure 1 is pictured the power spectrum of curvature fluctuations for the mentioned models and for the ΛCDM model.

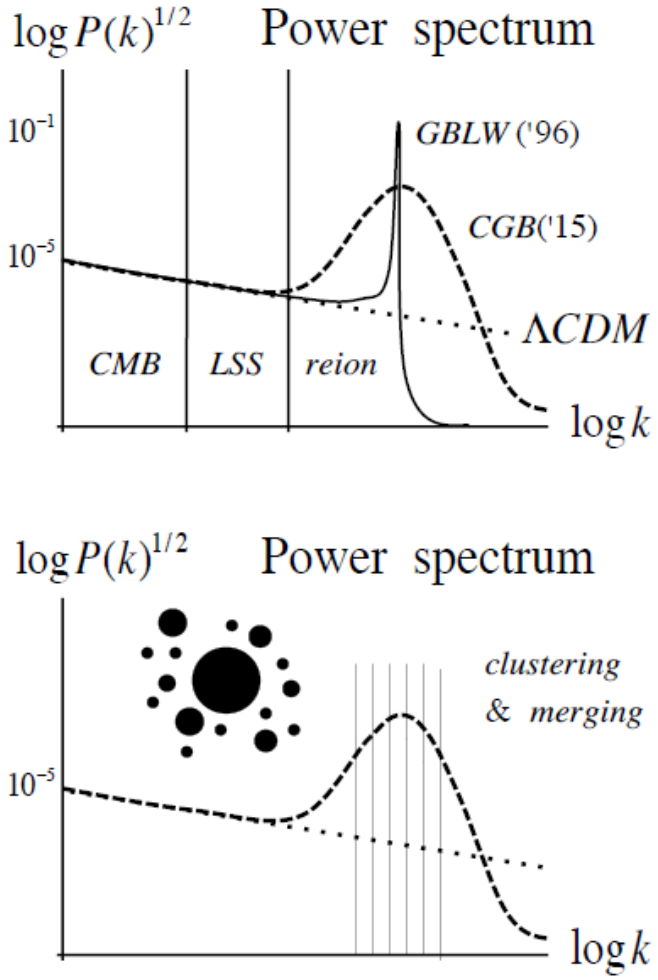

Figure 1. The primordial power spectrum of curvature fluctuations induced during inflation. Those fluctuations that enter during the radiation era collapse to form black holes within a range of masses, and spatially clustered around the more massive ones. The dotted line corresponds to the Gaussian primordial spectrum predicted by inflation and at the core of the ΛCDM paradigm, and consistent with the observed CMB anisotropies; the continuous line corresponds to the original model of GBLW (1996) [4], with a sharp spike in the spectrum, that gives rise to a monochromatic mass spectrum, and the dashed line corresponds to the recent proposal of CGB (2015) [6] for a broad spike in the spectrum, giving rise to a broad mass spectrum of primordial black holes, which are strongly clustered. From Ref. [18].

In the model proposed in Ref. [4], the power spectrum has a sharp spike which gives rise to a monochromatic mass spectrum, however in the model in Ref. [6] rather than a single sharp spike in the matter power spectrum, there is a large spike which could generate a broad spectrum of primordial black hole masses, which are strongly clustered.

The width of the spike in the matter power spectrum that gives rise to the mass range of primordial black hole depends on the particular inflationary model behind the origin of curvature fluctuations that gave rise to the formation of structure in the universe. Some models of inflation may have a phase transition 20 e-folds before the end of inflation, triggered by a symmetry breaking field, like in hybrid inflation [19], and this will give rise to a very pronounced spike in the spectrum, whose width will depend on the parameters of the model.

3.2. Accretion and Merging

As stated before, considering a model with a large spike in the power spectrum will lead to a broad spectrum of primordial black hole masses that are strongly clustered. This population of primordial black holes can evolve through accretion and merging with each other. The primordial black holes can accrete gas and radiation via Bondi-Hoyle accretion during the radiation era, but at a rate that is negligible. The rate of accretion increases during the matter era, but stays below the Eddington limit. In case the primordial black holes acquire an accretion disk of gas, and the outflows are along the axis, like in quasars and microquasars [20], they can accrete much faster. Massive primordial black holes originate in clusters and so they can find each other and merge more easily, by gravitational attraction, emitting gravitational waves in the process, and generating a stochastic background [21].

Thus, both through accretion and merging, the masses of the black holes grow at an important rate, and so their mass distribution is shifted towards larger values since recombination. Furthermore, since the primordial black holes form a fluid of zero pressure, their density contrast grows like any matter component, linear with the scale factor during the matter era. Changes in the spin distribution are also expected. Primordial black holes arise from the gravitational collapse of an isotropic gas upon horizon crossing of order-one fluctuations in curvature and so they are born without spin, but the subsequent mergers will create a spin. The spin acquired through merging can be significant, but since the mergers occur from a random distribution of orientations of the orbits it is likely that the final spin distribution will be centered around the zero-spin configuration with a dispersion that depends on the merging history and mass distribution.

4. Cosmological and Astrophysical Implications

In the previous section was discussed that the density perturbations created at the moment of the phase transition are very large. For the model of Ref. [13] with parameters that correspond to the second stage of inflation lasting 20 - 30 Hubble times H^{-1}, one has density perturbations $\delta\rho/\rho = \mathcal{O}(1)$. In such a situation one can expect copious production of huge black holes, which should lead to disastrous cosmological consequences. However, the problem of copious production of black holes can be solved by choosing the parameters in such a way that the second stage of inflation is completely eliminated. Nonetheless, considering that the second stage of inflation does exist leads to some very interesting possibilities.

4.1. Primordial Black Holes as Dark Matter Candidates

Considering models where the second stage of inflation lasts for about 10 Hubble times (In this case the probability of the black hole formation is sufficiently small, so that the amount of black holes does not contradict the cosmological bounds on the black hole abundance) one obtains $M_{BH} = 2 \times 10^{20}\ g = 10^{-13}\ M_{\odot}$. Using the average density of our galaxy $\rho_g \sim 10^{-25}\ g/cm^3$ we find that these small black holes may populate the halo of our galaxy and be separated from each other an average of $10^{15}\ cm$. They could very well constitute the missing mass in our galaxy. So it is possible that the black holes produced in the hybrid inflation scenario may serve as the dark matter candidates. Bear in mind that changing slightly the parameters of the model, changes simultaneously the scale and the height of the spike in the black hole spectrum. So values of the black hole masses and the distances between them can be made substantially different by modification of the hybrid inflation model.

4.2. Reheating from Black Hole Evaporation

Considering models where the second stage of inflation lasts for about 2 to 3 Hubble times, then the black holes formed from the large density perturbations may be small enough to evaporate quickly. With the parameters of the model used in Ref. [13] even the smallest black holes are very heavy and evaporate too late.

However, by considering hybrid inflation with a short second stage of inflation and a sufficiently large Hubble constant, the black holes produced during inflation can be made very small, so that they evaporate before nucleosynthesis, reheating the universe. Even if the probability of formation of such black holes is suppressed, the fraction of matter in such micro black holes at the moment of their evaporation may be quite substantial, since the fraction of energy in radiation rapidly decreases in an expanding universe. If this is true it will lead to important modifications of the thermal history of the universe and raises the possibility that the baryon asymmetry of the universe was produced in the process of black hole evaporation [22], [23].

4.3. The Seed of Super Massive Black Holes

It is believed that at the center of galaxies exist supermassive black holes, going from 10^6 $M_\odot$ to 10^9 $M_\odot$ and that they descent from less massive black holes in quasars at high redshift. However, it does not exist an explanation for the existence of super massive black holes at redshifts up to approximately $z > 8$ [24]. Their existence as fully formed galaxies before 500 Myr is a challenge for standard ΛCDM model. It is unlikely that stellar evolution alone can explain the existence of such massive black holes so quickly, therefore several proposals suggest that they are built up from smaller black holes that act as seeds of the galactic supermassive black hole [25].

To explain the existence of such massive black holes so quickly, it is needed black holes seeds of at least 10^3 $M_\odot$ at $z \approx 15$, assuming uninterrupted accretion at the Eddington limit. The model proposed in Ref. [6] provides a mechanism for the formation of those seeds, in the tail of the black hole mass distribution. The abundance of stellar-mass primordial black holes is low prior to recombination, but smaller black holes can grow by merging and it is possible that a significant fraction of the smaller mass black holes grow to become intermediate mass black holes at approximately $z > 15$. Then by continuing to merge with each other and accrete matter they can form supermassive black holes. Thus with this model is possible to get a number of supermassive black holes, roughly 1 for 10^{12} stellar-mass black hole in galaxies, which is expected for a primordial black hole dark matter component. This model therefore predicts that supermassive black holes should be observed at the center of galaxies at very early times.

5. Observational Constraints of Primordial Black Holes

As said before primordial black holes are non-relativistic and effectively nearly collisionless, so they are good candidates for dark matter. The mass spectrum of primordial black holes is severely constrained by several types of observations. Some of this constraints are:

- *Lifetime of primordial black holes*
  The timescale of evaporation of primordial black holes due to Hawking radiation is of the order of $t_{ev}(M) \sim G^2M^3/\hbar c^4$. Considering primordial black holes with a mass of $M_{PBH} \simeq 5 \times 10^{11}\ kg$, they evaporate in a time much shorter than the age of the Universe [26], [27] and therefore cannot contribute significantly to dark matter today.

- *Light elements abundances*
  The Big Bang nucleosynthesis might be affected by the evaporation of primordial black holes. Primordial black holes heavier than $M_{PBH} = 10^7\ kg$ do not evaporate before the Big Bang nucleosynthesis, so they can affect light element abundances through the emission of mesons and anti-nucleons and through the hadro-dissociation and photo-dissociation processes. Strong bounds have been established on primordial black holes abundance from Big Bang nucleosynthesis [27], but those only concern primordial black hole with masses approximately lower than $M_{PBH} = 10^{11}\ kg$ which are not good candidates for dark matter due to early evaporation.

- *Extragalactic photon background*
  Observable extragalatic gamma-ray radiation can be emitted by evaporating primordial black holes at the present epoch. The Hawking radiation produced by a primordial black hole with mass of $M_{PBH} \simeq 10^{13}\ kg$ is responsible for the emission of $\sim 100\ MeV$ radiation. This radiation should have been observed with the EGRET and Fermi Large Area telescopes if $\Omega_{PBH} > 0.01$ [27].

Primordial black holes cannot account for the totality of dark matter if $M_{PBH} < 7 \times 10^{12}\ kg$. To obtain this value it was assumed a uniform distribution of primordial black holes throughout the Universe, which is not realistic since dark matter clusters, like galaxies, galaxy clusters and superclusters.

- *Galactic background radiation*
  Primordial black holes are expected to have clustered with galactic halos, and thus there should also be a galactic background of gamma radiation, which should be anisotropic and in principle separable from the extra-galactic emission. The constraints from galactic background radiation are close but less competitive than Big Bang nucleosynthesis and extragalactic ones. A distinctive signature of primordial black holes could also be seen in the ratio of antiprotons to protons, in the energy range between 100 MeV and 10 GeV, in the galactic cosmic ray spectrum [27]. This gives typically similar constraints on the abundance of primordial black holes.

- *Femtolensing of gamma-ray bursts*
  Gravitational femtolensing of gamma-ray bursts can be induced by compact objects. In the Fermi Gamma-Ray Burst Monitor experiment there has been a lack of femtolensing detection, which is evidence that in the mass range between $M_{PBH} = 10^{14}\ kg$ and $M_{PBH} = 10^{17}\ kg$, primordial black holes cannot account for a large fraction of dark matter [28].

- *Star Formation*
  Suppose that star formation takes place in an environment dominated by dark matter, that is constituted partially or totally of primordial black holes. In that case, the primordial black holes could be captured by stars and at the end of the star evolution they would destroy in a very short time by accretion the compact remnant (a white dwarf or a neutron star). The constraints resulting from the observation of neutron stars and white dwarfs in globular clusters does not allow primordial black holes in the mass range between $M_{PBH} = 10^{13}\ kg$ and $M_{PBH} = 10^{19}\ kg$ to constitute totally the dark matter.

- *Capture of primordial black holes by neutron stars*
  As primordial black holes can be captured by stars, they can also be captured by neutron stars, which are accreted onto the primordial black hole and destroyed in a very short time. Primordial black holes cannot account entirely for dark matter in the range between $M_{PBH} = 10^{15}\ kg$ and $M_{PBH} = 10^{21}\ kg$, assuming large dark matter densities and low velocities, conditions that can be fulfilled in the cores of globular clusters.

- *Microlensing surveys*
  Assuming that the dark matter in the galactic halo is mostly composed by primordial black holes, it is expected gravitational microlensing events of stars in the Magellanic cloud. Gravitational microlensing was not observed by the EROS microlensing survey nor by the MACHO collaboration, so they put a limit on the abundance of primordial black holes between $M_{PBH} = 10^{23}\ kg$ and $M_{PBH} = 10^{31}\ kg$.

- *Cosmic microwave background spectral distortions*
  The recombination history can be modified by X-rays emitted by gas accretion near primordial black holes, which lead to cosmic microwave background spectral distortions and cosmic microwave background temperature anisotropies [29]. The COBE/FIRAS experiment can constrain the distortions and it was concluded that primordial black holes heavier than $M_{PBH} = 10\ M_{\odot}$ cannot contribute to more than a few percent of the dark matter and that primordial black holes with approximately the Sun's mass cannot contribute to more than about 10 % of dark matter. However these bounds assume that primordial black hole masses do not change with time. But, as said before, merging and accretion since recombination can in principle lead to primordial black hole masses with masses significantly larger than $M_{PBH} = 10\ M_{\odot}$ today while being sub-solar before recombination, thus evading both microlensing and cosmic microwave background constraints.

The principal constraints on the fraction of dark matter due to massive primordial black hole are summarized on Figure 2.

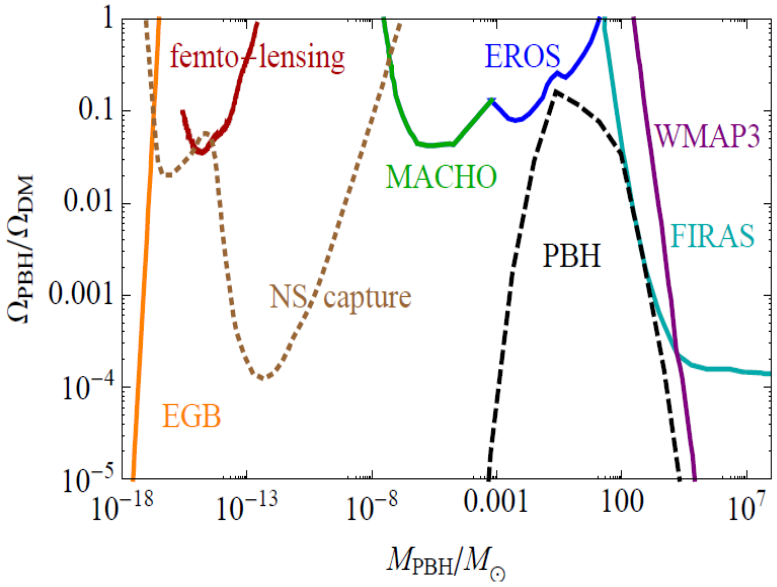

Figure 2. Limits on the abundance of primordial black holes today, from extragalactic photon background (orange), femtolensing (red), microlensing by MACHO (green) and EROS (blue) and cosmic microwave background distortions by FIRAS (cyan) and WMAP3 (purple). The constraints from star formation and capture by neutron stars in globular clusters are displayed for $\rho_{DM}^{Glob.Cl} = 2 \times 10^3\ GeVcm^{-3}$ (brown). The black dashed line corresponds to a particular scenario of primordial black hole formation considered in Ref. [6]. From Ref. [6]

The constraints from star formation and capture by neutron stars are displayed as brown dotted lines, since they can be avoided in the case that the dark matter density inside globular clusters is low enough. In this conditions, exists a gap between $M_{PBH} = 10^{17}\ kg$ and $M_{PBH} = 10^{23}\ kg$ where there is no constraint. The primordial black holes can be identified to the dark matter component in this interval. It is important to keep in mind these limits were obtained under the implicit assumption of a mono-chromatic distribution of primordial black holes [30]. In the scenario proposed in Ref. [6], the primordial black holes mass spectrum is very broad, covering typically five orders of magnitudes, and it is still unknown how the current constraints must be adapted for such broad mass spectra.

6. Gravitational Waves and Detection of Primordial Black Holes

Most of the stellar black holes, black holes originated as consequence of stellar evolution, have masses of the order of the stars (Figure 3), only a few are heavier than 10 $M_{\odot}$. The mass of these black holes usually is determined from the X-ray emission of their accretion disk. The gravitational collapse of population III supermassive stars, with very low metallicity, is responsible for the arise of the more massive black holes. Even if the progenitor star has a mass of 250 $M_{\odot}$, it is difficult to produce black holes heavier than 10 $M_{\odot}$.

The LIGO interferometer detected the merge of several massive black holes [31], [32]. LIGO detected the merging of three massive black holes binary systems (Figure 3). The masses of the black holes before merging are not equal, they range from 8 to 36 $M_{\odot}$, and the final black hole masses range from 23 to 62 $M_{\odot}$. The masses of these black holes are somewhat larger than expected from remnants of supernovae explosions and stellar evolution [33], so it is possible that LIGO has discovered a whole new population of massive black holes, formed in the early universe [18]. It is possible that the massive black holes detected by LIGO are of primordial origin, since their mass is contained in the mass distribution of primordial black holes (Figure 4).

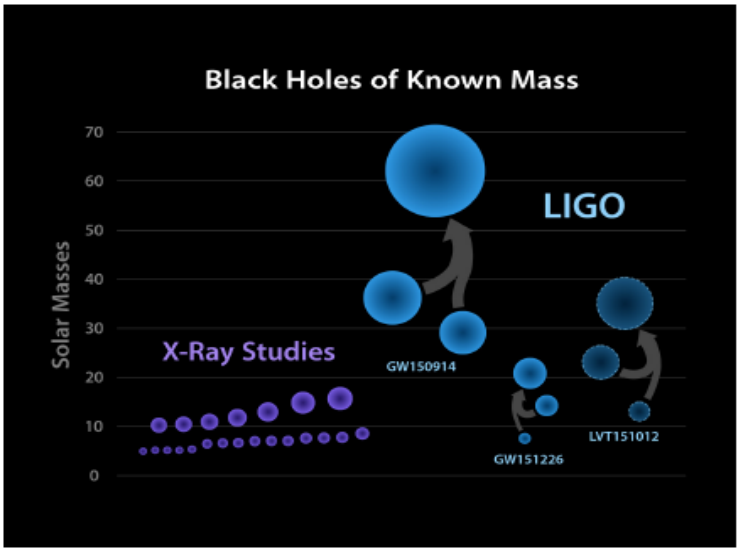

Figure 3. The Black Holes of Known Mass detected by LIGO. It seems likely they correspond to a new population of black holes unheard of before. While IMBH and SMBH were known to populate the centers of globular clusters and galaxies, respectively, this new class of black holes in binaries had not been detected before. From Ref. [18].

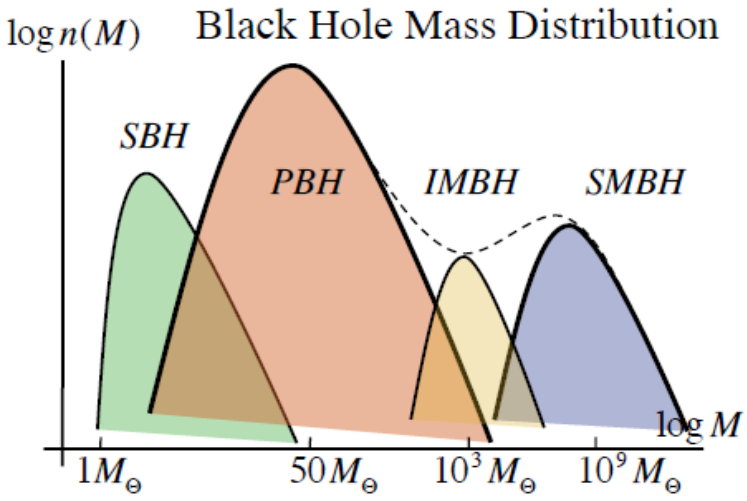

Figure 4. The mass distribution of black holes in our universe can be classified in three large groups, Stellar Black Holes, that arise from the gravitational collapse of stellar systems, the Primordial Black Holes that were formed in the early Universe, the Supermassive Black Holes at the centers of Quasars and the Intermediate Black Holes at the centers of Globular Clusters. From Ref. [18].

Primordial black holes have three different sources of gravitational waves at very different frequencies [18]:

1. As it was discussed in section 3, the broad spikes in the curvature fluctuation power spectrum is generated during inflation from the slow-roll motion of the inflaton field and possibly other fields coupled to it. Scalar fluctuations have a large enough amplitude to create a sizeable gravitational wave background with a spike at frequencies associated with the size of the horizon at reentry that will have redshifted today.

2. The formation of primordial black holes itself leads to a gravitational wave stochastic background.

3. The gravitational collapse that gives rise to the primordial black holes at horizon reentry during the radiation era produces also a small fraction of energy in the form of gravitational waves.

In Figure 5 it can be seen that the gravitational waves stochastic background arising from the merging of primordial black holes during the matter era is just below the Advanced LIGO sensitivity, but could eventually be detected at lower frequencies by LISA and that the gravitational waves stochastic background created from the violent gravitational collapse that formed the primordial black holes upon horizon entry of large fluctuations during the radiation era is in the range of sensitivity of the future Square Kilometre Array (SKA).

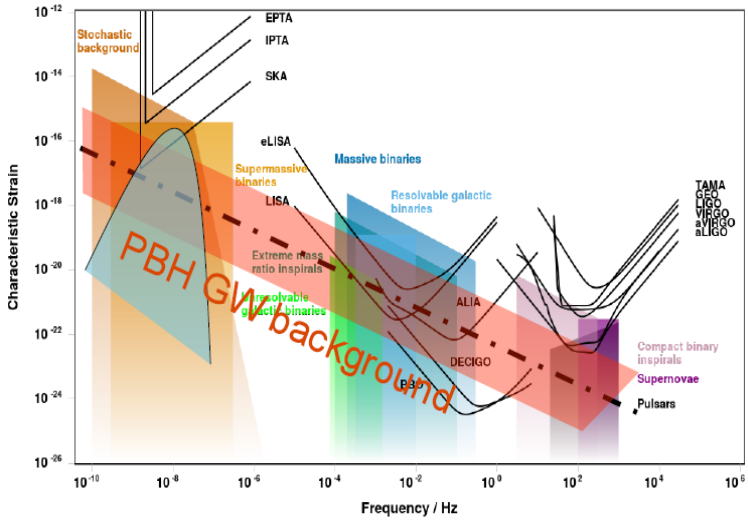

Figure 5. The stochastic background of gravitational waves from the merging of primordial black holes since recombination spans many orders of magnitude, from below the nanohertz to above the kilohertz. The range is covered by ground interferometers, satellites and pulsar timing arrays. Also shown in grey is the stochastic background of gravitational waves created from the violent gravitational collapse that formed the primordial black holes upon horizon entry of large fluctuations during the radiation era. From Ref. [18].

7. Conclusions

Hybrid inflation models describe the evolution of two scalar fields, ϕ and ψ. The existence of the second stage of inflation leads to the appearance of inflating topological defects which may lead to large density perturbations. Primordial black holes can arise from spikes in the spectrum of density perturbations. It has been studied the possibility that the existence of these primordial black holes has cosmological and astrophysical implications, such as the possibility that they are the main component of dark matter, their possible influence on the thermal history of the universe and that they may act as seeds of the galactic supermassive black holes. Different type of observations constrained the mass spectrum of primordial black holes between $M_{PBH} = 10^{17}\ kg$ and $M_{PBH} = 10^{23}\ kg$ and they can be identified to the dark matter component in this interval. It is possible that the the massive black holes detected by LIGO are of primordial origin, since their mass is contained in the mass distribution of primordial black holes. Assuming that they have a primordial origin with the future terrestrial and space gravitational waves interferometers we may be able to characterise their distribution and properties, providing clues about their origin and the early stages of the evolution of the Universe.

In conclusion, primordial black holes are a good candidate for collisionless cold dark matter. In the case that primordial black holes are in fact responsible for dark matter, and their properties can be measured, then the dynamics occurring in the last stages of inflation may be studied by astrophysical and cosmological observations, opening a new window into the early universe.

References

1. Kolb, E.W.; Turner M.S. The Early Universe. Westview Press, 1990.
2. Zel'dovitch, Y. B. and Novikov, I. D. The Hypothesis of Cores Retarded During Expansion and the Hot Cosmological Model. Soviet Astronomy 1966, 10, 602-603.
3. Hawking S. Gravitationally collapsed objects of very low mass. Mon. Not. R. Astron. Soc. 1971, 152, 75-78.

4. García-Bellido, J.; Linde A. D. and Wands D. Density perturbations and black hole formation in hybrid inflation. Phys. Rev. 1996, D 54, 6040-6058.
5. Overduin, J. M. and Wesson, P. S. Dark Matter and Background Light. Physics Reports. 2004, 402 (5–6): 267–406.
6. Clesse, S. and García-Bellido, J. Massive Primordial Black Holes from Hybrid Inflation as Dark Matter and the seeds of Galaxies. Phys. Rev. 2015, D 92, 023524.
7. Guth, A. H. Inflationary universe: A possible solution to the horizon and flatness problems. Phys. Rev. 1981, D 23, 347-356.
8. Linde, A.D. Particle Physics and Infltionary Cosmology. Contemp. Concepts Phys. 2005, 5, 1-362.
9. Linde, A.D. Chaotic inflation. Phys. Lett. 1983, 129B, 177-181.
10. Linde, A.D. Hybrid Inflation. Phys. Rev. 1994, D 49, 748-754.
11. Jeannerot, R. Supersymmetric SO(10) model with inflation and cosmic strings. Phys. Rev. 1996, D 53, 5426.
12. Linde, A.D. and Fischler, W. Prospects of Inflation. Physica Scripta. 2005, 117, 40–48.
13. Randall, L.; Soljacic, M. and Guth, A. H. Supernatural inflation: inflation from supersymmetry with no very small parameters. Nucl. Phys. 1996, B 472, 377-408.
14. Jedamzik, K. and Niemeyer, J. C. Primordial black hole formation during first-order phase transitions. Phys. Rev. 1999, D 59, 124014.
15. Suyama, T.; Tanaka, T.; Bassett, B. and Kudoh H. Are black holes overproduced during preheating? Phys. Rev. 2005, D 71, 063507.
16. Suyama, T.; Tanaka, T.; Bassett, B. and Kudoh H. Black hole production in tachyonic preheating. JCAP 2006, 0604.
17. Kohri, K.; Lin, C.-M. and Matsuda, T. Primordial black holes from the inflating curvaton. Phys. Rev. 2013, D 87, 103527.
18. García-Bellido, J. Massive Primordial Black Holes as Dark Matter and their detection with Gravitational Waves. J. Phys. 2017, 840, 012032.
19. Goncharov, A.S. and Linde, A.D. A Simple Realization Of The Inflationary Universe Scenario In Su(1,1) Supergravity. Class. Quantum Grav. 1984, 1, L75-L79.
20. Luo, Y.; Hanasoge, S.; Tromp, J. and Pretorius, F. Detectable Seismic Consequences of the Interaction of a Primordial Black Hole with Earth. Astrophys. J. 2012, 751, 16.
21. Clesse, S. and Garbrecht, B. Slow roll during the waterfall regime: The small coupling window for supersymmetric hybrid inflation. Phys. Rev. 2012, D 86, 023525.
22. Hawking, S. Black hole explosions? Nature 1974, 248, 30-31.
23. Barrow, J.; Copeland, E.; Kolb, E. and Liddle, A. Baryogenesis in extended inflation. II. Baryogenesis via primordial black holes. Phys. Rev. 1991, D 43, 984.
24. Fan, X.; et al. A Survey of z > 5.7 Quasars in the Sloan Digital Sky Survey. II. Discovery of Three Additional Quasars at z > 6. Astron. J. 2003, 125, 1649.
25. Rubin, S. G.; Sakharov, A. S. and Khlopov M. Y. The formation of primary galactic nuclei during phase transitions in the early universe. J. Exp. Theor. Phys. 2001, 92, 921-929.
26. Carr, B. J. Some cosmological consequences of primordial black-hole evaporations. Astrophys. J. 1976, 206, 8.
27. Carr, B.; Kohri, K.; Sendouda, Y. and Yokoyama, J. New cosmological constraints on primordial black holes. Phys. Rev. 2010, D 81, 104019.
28. Barnacka, A.; Glicenstein, J. and Moderski, R. New constraints on primordial black holes abundance from femtolensing of gamma-ray bursts. Phys. Rev. 2012, D 86, 043001.
29. Ricotti, M.; Ostriker, J. P. and Mack, K. J. Effect of Primordial Black Holes on the Cosmic Microwave Background and Cosmological Parameter Estimates. Astrophys. J. 2007, 680, 2.
30. Capela, F.; Pshirkov, M. and Tinyakov, P. Constraints on primordial black holes as dark matter candidates from capture by neutron stars. Phys. Rev. 2013, D 87, 123524.
31. Abbott, B. P.; et al. [LIGO Scientific and Virgo Collaborations], Observation of Gravitational Waves from a Binary Black Hole Merger. Phys. Rev. Lett. 2016, 116, 061102.
32. Abbott, B. P.; et al. [LIGO Scientific and Virgo Collaborations], GW151226: Observation of Gravitational Waves from a 22-Solar-Mass Binary Black Hole Coalescence. Phys. Rev. Lett. 2016, 116, 241103.
33. Abbott, B. P.; et al. [LIGO Scientific and Virgo Collaborations], Astrophysical Implications of the Binary Black-Hole Merger GW150914. Astrophys. J. 2016, 818, L22.

Proceedings

Predictions of linear primordial Gravitational Waves related to the standard single-field slow-roll inflationary scenario

Sara Nóbrega [1]

[1] FCUL; fc49536@alunos.fc.ul.pt

Abstract: Here is reviewed some of the fundamental aspects about gravitational waves (GW) from primordial times regarding slow-roll inflation. One of the predictions of any inflation-model is a spectrum of primordial GW. The features of such a signal encode unique information about the physics of the early Universe thus being a powerful source to understand the origin and evolution of it. These GW are tensor perturbations/fluctuations to the spatial metric, which are characterized by a nearly scale-invariant power-spectrum on super-horizon scales. Developing a perturbation theory within GR, besides a set of perturbations coupled to the energy density of the Universe, tensor perturbations are produced. The latter are due to fluctuations of the metric tensor and constitute the so called gravitational wave background. The amplitude of the GW signal is usually described by the tensor-to-scalar ratio r. The current best bound on r comes from the joint analysis of Planck, BICEP2 (Background Imaging of Cosmic Extragalactic Polarization) , Keck Array and other data, with $r < 0.07$[1]. The production of a stochastic background of gravitational waves is a fundamental prediction of any cosmological inflationary model. Thus, the observational signature of the inflationary GW background would be a major step for inflationary cosmology and the possibility of a future direct detection, by experiments such as LIGO or LISA, cannot be ruled out.

Keywords: Gravitational Waves; Inflation; Slow-Roll

---

1. Introduction

It is known that inflation produces the seeds for the large structures we see today in the Universe and that these structures have origin in tiny fluctuations in the inflation field. But why does inflation produce fluctuations? Treating inflation quantum-mechanically, by the uncertainty principle, there are spatially varying fluctuations in the inflation field itself, $\delta\phi(t,x) \equiv \phi(t,x) - \overline{\phi}(t)$, where $\phi(t)$ is the inflation field. Inflation will zoom out this tiny spatial differences, so when inflation ends, different regions of space will have had inflated by different amounts. This also leads to differences in the local densities, $\delta\rho(t,x)$ and in the CMB temperature, $\delta T(x)$. It is worth remarking that the theory wasn't engineered to produce the CMB fluctuations, but their origin is instead a natural consequence of treating inflation quantum mechanically. One of the most important predictions of inflation is a spectrum of primordial GW. During inflation and preheating, GW can be produced in two ways: from vacuum fluctuations of the gravitational field (the scope of this report) or by a classical mechanism. The first is related to the single-field slow-roll inflation. For this kind of production, different predictions for the tensor power-spectrum follow from different theories of gravity underlying the inflationary model. However, GW produced in a classical regime only occur when a source term is present in the GW equation of motion. These won't be treated here.

But why are primordial gravitational waves important and why should we care? First of all, primordial GW are not a prediction of non-inflationary models, so if we detected them, we would be closer than ever to prove that inflation actually happened. Logically, the study of observational signatures of primordial GW would not only provide a way to probe the inflation paradigm but would also help us realize wich inflationary-models are correct. GW themselves arise from quantum fluctuations in the gravitational field, so their detection would be the first experimental evidence of quantum gravity. Also, primordial GW represent a very useful tool to constrain different aspects of the early Universe and of the underlying fundamental physics theory. It is known that classical GW could be generated in the reheating phase. Through GW, we can study the reheating mechanisms and its parameters. Detecting them would also have consequences for high energy and fundamental physics. The energy scale on wich inflation occurs is much higher that the one we use in our accelerators. Detecting the parameter r, the tensor-to-scalar ratio, would

provide evidence for the existence of physics beyond the SM and give us a clue about the energy regime of this new physics. These are some of the reasons why primordial GW might open a new observational window and a new era in cosmology and because of that they are the object of a growing experimental effort, and their detection would be a major goal for cosmology in the next decades. Second-order GW will not be treated here but combining scalar perturbations of first order we get a source for GW at second order.

2. Discussion

2.1. First Considerations

2.1.1. Relativistic Perturbation Theory

When treating scales larger that the Hubble Radius (explained later) we shall make use GR instead of Newtonian physics. First of all, let's see how a small perturbation $\delta g_{\mu\lambda}$ changes the metric. Assuming a FRW metric $\overline{g}_{\mu\lambda}$:

$$g_{\mu\lambda} = \overline{g}_{\mu\lambda} + \delta g_{\mu\lambda} \tag{1}$$

The line element for a flat FRW back-ground spacetime is:

$$ds^2 = a^2(\tau)[d\tau^2 - \delta_{ij}dx^i dx^j] \tag{2}$$

where τ represents the comoving time.

The perturbed metric can therefore be written as:

$$ds^2 = a^2(\tau)[(1+2A)d\tau^2 - 2B_i dx^i d\tau - (\delta_{ij} + h_{ij})dx^i dx^j] \tag{3}$$

where A (scalar), B_i (vector) and h_{ij} (symmetric tensor) are functions of space and time. For tensor perturbations of the spatial metric:

$$ds^2 = a^2(\tau)[d\tau^2 - (\delta_{ij} + 2h_{ij})dx^i dx^j] \tag{4}$$

The metric perturbations in equation 3 aren't uniquely defined because they depend on the choice of coordinates, or "the gauge choice". Making a different choice of coordinates, we can change the values of the perturbation variables and may even introduce fake perturbations that can arise by an inconvenient choice of coordinates, even if the background is homogeneous. So we need a more physical way to identify true perturbations. One way to do this is to define perturbations in such a way that they don't change under a change of coordinates. This constitutes the gauge problem and it is addressed by gauge transformations. The complete mathematical scope of gauge transformations won't be addressed here but it is worth mentioning that one way to avoid the gauge problems is to define special combinations of metric perturbations that don't transform under a change of coordinates (Bardeen variables). These gauge-invariant variables can be considered as the 'real' spacetime perturbations since they cannot be removed by a gauge transformation.

2.2. Comoving Curvature Perturbation

There is a quantity, named *comoving curvature perturbation*, which is conserved on super-Hubble scales for adiabatic fluctuations. This quantity is an important link between the fluctuations that we observe in the late-time Universe and the primordial seed fluctuations created by inflation, which I want to present here.

Considering an arbitrary gauge and working out the intrinsic curvature of surfaces of constant time, the induced metric γ_{ij} is the spatial part of equation 3, i.e.,

$$\gamma_{ij} \equiv a^2[(1+2C)\delta_{ij} + 2E_{ij}] \tag{5}$$

where $E_{ij} \equiv \partial_{(i}\partial_{j)}E$ (scalar perturbations). The 3-D Ricci scalar associated with γ_{ij} is

$$a^2 R_{(3)} = -4\nabla^2 (C - \frac{1}{3}\nabla^2 E) \tag{6}$$

where the *curvature perturbation* is defined as $C - \frac{1}{3}\nabla^2 E$ and R is the comoving curvature perturbation. It is convenient to have a gauge-invariant expression for R, so that it can be evaluated from any gauge. The correct gauge-invariant expression for the comoving curvature perturbation is:

$$R = C - \frac{1}{3}\nabla^2 E + H(B + v) \tag{7}$$

where H here denotes the Hubble parameter concerning the comoving time.

Let's consider a coordinate transformation of the form $X^\mu \mapsto X^\mu + \xi^\mu$, where $\xi^0 \equiv T$ and $\xi^i \equiv \partial^i L$. We need the transformations:

$$C \mapsto C - HT - \frac{1}{3}\nabla^2 L \tag{8}$$

$$E \mapsto E - L \tag{9}$$

So, we get: $R = C - \frac{1}{3}\nabla^2 E + H(B + v) \mapsto (C - HT - \frac{1}{3}\nabla^2 L) - \frac{1}{3}\nabla^2 (E - L) + H(B - v) = C - \frac{1}{3}\nabla^2 E + H(B + v) = R$

This quantity is indeed gauge-invariant, and since B and v vanish in the comoving gauge, we can always add linear combinations of these to $C - \frac{1}{3}\nabla^2 E$ to form a gauge invariant combination that equals R.

It also known that the quantity R doesn't evolve on super-Hubble scales, that is, $k << H$. This is important because it means that the value of R that is computed at horizon crossing during inflation is not altered until later times.

On small scales, fluctuations in the inflaton field are described by a collection of harmonic oscillators. Quantum fluctuations induce a non-zero variance in the amplitudes of these oscillators:

$$\langle |\delta\phi_k|^2 \rangle \equiv \langle 0||\delta\phi_k|^2|0\rangle \tag{10}$$

The inflationary expansion stretches these fluctuations to superhorizon scales. In comoving coordinates, the fluctuations have constant wavelengths, but the Hubble radius shrinks, creating super-Hubble fluctuations in the process.

At horizon crossing, $k = aH$, it is convenient to switch from inflaton fluctuations to fluctuations in the conserved curvature perturbations R. The relationship between R and $\delta\phi$ is simplest in spatially flat gauge:

$$R = -\frac{H}{\dot{\phi}'}\delta\phi \tag{11}$$

The variance of curvature perturbations therefore is:

$$\langle |R_k|^2 \rangle = (\frac{H}{\dot{\phi}'})^2 \langle |\delta\phi_k|^2 \rangle \tag{12}$$

where $\delta\phi$ are the inflaton fluctuations in spatially flat gauge.

The fact that the quantity R is conserved on superhorizon scales allow us to know or at least relate the predictions on the horizon exit and horizon re-entry. Actually, in this time interval, the physics is not really well-known and there is a lot of uncertainty relating the equations for the perturbations. Curiously, we are only able to connect late-time observables to inflationary theories because the wavelenghts of the perturbations were outside the horizon during the period from well before the end of inflation until near present.

3. The Physics of Inflation

Considering an isotropic and homogeneous Universe, the Friedman-Robertson-Walker (FRW) metric gives us:

$$ds^2 = -dt^2 + a^2(t)[\frac{dr^2}{1-Kr^2} + r^2(d\theta^2 + sin^2\theta d\phi^2)] \tag{13}$$

where t is the cosmic time, r, ϕ, θ are the comoving spherical coordinates, K the curvature of the 3D space-time and $a(t)$ is the scale factor.

The Friedman equation and the acceleration equation are, respectively :

$$H^2 = \frac{8\pi G}{3}\rho - \frac{K}{a^2} \tag{14}$$

$$\frac{\ddot{a}}{a} = -\frac{4\pi G}{3}(\rho + 3P) \tag{15}$$

The main and basic requirement to have an inflationary period is to have $\ddot{a} > 0$, that is, an accelerated expansion. So, regarding the acceleration equation, if $\ddot{a} > 0$, then $(\rho + 3P) < 0$, so $\rho < -3P$, which leads to $P < -\frac{\rho}{3}$. We know that, for radiation, w=1/3 and for matter w=0, (with $w = \frac{P}{\rho}$) so the inflation can't be provided by ordinary matter or radiation.

Simplifying and assuming $P \simeq -\rho$ we get: $a(t) = a_I e^{H(t-t_0)}$. A period characterized by this evolution of the scale-factor is called a de Sitter stage.

Another relevant aspect of the inflation is the fact that the comoving Hubble Radius decreases. The Hubble Radius, $R_H \equiv \frac{1}{H(t)}$ sets the size of causally connected regions at each time.

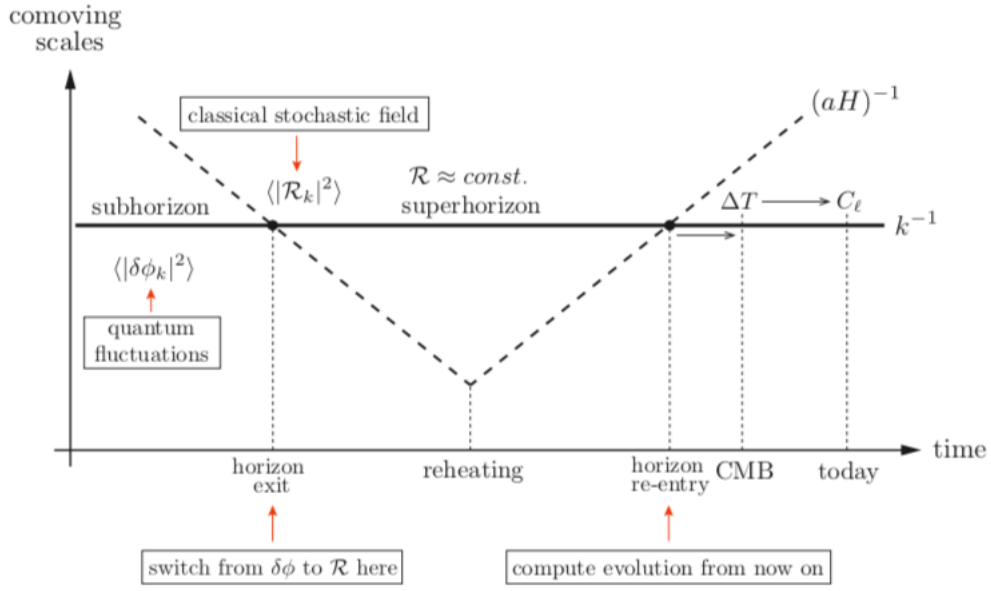

Figure 1. Time evolution of the comoving Hubble Radius during inflation and the following epoch, compared to the evolution of a comoving scale λ.

For ordinary matter we have $RH \propto ct$ which means that the HR increases with time. But, in the Sitter Universe, the HR actually maintains constant through time, while physical lengths continue to grow. This means that these physical lenghts are able to cross, or to exit, the HR at some time. The requirement of sufficiently long inflation corresponds to the requirement that all scales relevant for cosmological observations were able to exit the Hubble Radius during inflation. In a nutshell, the HR is constant during inflation but the comoving HR decreases and the physical wavelength increases much faster than the HR. From here it can be concluded that at early times the fluctuations emerged at micro-physical sub-Hubble scales.

Another requirement for inflation is the so called Slow-Roll conditions:

2

$$\epsilon \equiv \frac{M_{pl}^2}{2}(\frac{V_\phi}{V})^2 = -\frac{\dot{H}}{H^2} = -\frac{d\,ln\,H}{dN} \ll 1 \tag{16}$$

$$\eta \equiv M_{pl}^2 \frac{V_{\phi\phi}}{V} = \frac{d\,ln\,\epsilon}{d\,N} = \frac{\dot{\epsilon}}{H\epsilon} \ll 1 \tag{17}$$

where ϵ and η are the slow-roll parameters. In a regime where $\epsilon, \eta << 1$, inflation occurs and persists and this is called the slow-roll approximation. There are other important requirments for the existence of inflation but won't be discussed here due to lack of necessity to the further discussion.

3.1. Quantum fluctuations: origin of cosmological perturbations

In the introduction it was mentioned fluctuations due to quantum mechanics. These quantum fluctuations oscillate maintaining zero average on a macroscopic time. The accelerated expansion provided by inflation can stretch the wavelength of these fluctuations to scales that go beyond the HR, $k >> aH = \frac{1}{RH}$, where k is the comoving wave number of a fluctuation.

It is known that the inflation provides a solution to the horizon problem, and this is how it goes: after inflation, the radiation and matter eras develop and the perturbations originated quantumlly are surpassed by the HR (that starts increasing after the end of inflation). So, physically speaking, the perturbations are now in a region causally connected and when this happens in a large scale with a non-zero amplitude, combined with the action of gravity, we have the present large-scales structure and the non-isotrope CMB pattern. It is important to refer that the amplitude of the fluctuations do not change in time, constrasting with its wavelengths that increase exponentially.

3.2. Dynamics

Regarding inflation, the fields involved in the dynamics are two: the inflation and the metric tensor, which describes the gravitational degrees of freedom. Now I'm going to consider the fluctuations of these fields and their dynamics. Considering the dynamics of the inflationary perturbations at linear order, beginning with the Einstein-Hilbert action for gravity and the action of a scalar matter field:

$$S = \int d^4x\sqrt{-g}[\frac{1}{2}M_{pl}^2 R - \frac{1}{2}g^{\mu\nu}\partial_\mu\phi\partial_\nu\phi - V(\phi)] \tag{18}$$

where R is the Ricci scalar.

3.3. The power-spectrum

We can characterize the properties of a field perturbations by its power-spectrum. For a generic random field $g(x,t)$, expanding in Fourier space:

$$g(x,t) = \int \frac{d^3k}{(2\pi)^{3/2}} e^{ik.x} g_k(t) \tag{19}$$

The power-spectrum measures the amplitude of the fluctuation at a given mode k. This definition leads to the usual relation:

$$\langle g^2(x,t)\rangle = \int \frac{dk}{k}\Delta_g^2 \tag{20}$$

Where Δ_g^2 is the power-spectrum.

To describe the slope of the power-spectrum a (general) spectral index is also defined as:

$$n_g(k) - 1 \equiv \frac{dln\,\Delta_g^2}{dln(k)} \tag{21}$$

Later we will deal with *scalar* and *tensor* spectral index.

We want to specify the form that the power-spectrum gets when the random field is a canonically quantized scalar field . The quantum-mechanic details regarding this are not relevant here, so I'll just drop the definition of a (dimensionless) power spectrum:

$$\Delta_f(k,\tau) \equiv \frac{k^3}{2\pi^2}|f_k(\tau)|^2 \tag{22}$$

The square of the classical solution determines the variance of quantum fluctuations. Again, the demonstration won't be shown here, but it's important to note that:

$$\Delta^2_{\delta\phi}(k,\tau) = a^{-2}\Delta^2_f(k,\tau) \approx (\frac{H}{2\pi})^2 \tag{23}$$

for $k = aH$, at horizon crossing.

3.4. Curvature Perturbations

At horizon crossing ($k = aH$) we switch from the inflation field to the conserved curvature perturbation R. Through equation 12, these two are related as: $\Delta^2_R = (\frac{H}{\dot{\phi}'})^2\Delta^2_{\delta\phi}$. Noting that $\epsilon = \frac{1}{2}\frac{\dot{\phi}^2}{M^2_{pl}H^2}$, we get: $\Delta^2_R = \frac{1}{2\epsilon}\frac{\Delta^2_{\delta\phi}}{M^2_{pl}}$. Noting that $\Delta^2_{\delta\phi} \approx (\frac{H}{2\pi})^2$ (at horizon crossing), we get:

$$\Delta^2_R(k) = \frac{1}{8\pi^2}\frac{1}{\epsilon}\frac{H^2}{M^2_{pl}} \tag{24}$$

So the power-spectrum is just a function of k. However, if $\Delta^2_R(k)$ is independent of k, we say that the spectrum is *scale-invariant*. But, because H and ϵ can depend on time, it is predicted that the power spectrum will deviate slightly from the scale-invariant form $\Delta^2_R \sim k^0$. Near a reference scale k_*, the k-dependence of the spectrum takes a power-law form:

$$\Delta^2_R(k) \equiv A_s(\frac{k}{k_*})^{n_s-1} \tag{25}$$

where A_s is the amplitude of the scalar spectrum at $K_* = 0.05Mpc^{-1}$ and $n_s - 1$ is the *scalar spectral index*:

$$n_S - 1 \equiv \frac{d\,ln\,\Delta^2_R}{d\,ln\,k} \tag{26}$$

that measures the deviation from the scale-invariance, at $k = k_*$.

Spliting equation 26 and taking the derivative with respect to e-folds:

$$\frac{d\,ln\,\Delta^2_R}{dN} = 2\frac{d\,ln\,H}{dN} - \frac{d\,ln\,\epsilon}{d\,N} \tag{27}$$

Recalling equaitions 17 and 16, we see that the first term is -2ϵ and the second is $-\eta$. Therefore we have that:

$$n_s - 1 = -2\epsilon - \eta \tag{28}$$

The parameter n_s also measures the deviations from the perfect de Sitter limit. Observations have recently detected the small deviation from scale-invariance predicted by inflation: $n_s = 0.9603 \pm 0.0073$.

4. Gravitational Waves from Inflation

Introducing equation 4 in equation 18 and perturbing it at second order:

$$S_T = \frac{M^2_{pl}}{8}\int d^4x a^2(t)[\dot{h}_{ij}\dot{h}_{ij} - \frac{1}{a^2}(\nabla h_{ij})^2] \tag{29}$$

where h_{ij} is a gauge-invariant object. Varying the action with respect to this quantity, we get the equation of motion:

$$\nabla^2 h_{ij} - a^2 \ddot{h}_{ij} - 3a\dot{a}\dot{h}_{ij} = 0 \tag{30}$$

we know that a wave equation takes the form $\ddot{u} = c^2 \nabla^2 u$ so we conclude that tensor perturbations solve a wave equation, and that's why we call them *gravitational waves*!

Because h_{ij} is symmetric, transverse and trace-free, the solutions of that equation are:

$$h_{ij}(x,t) = h(t) e_{ij}^{(+,\times)}(x) \tag{31}$$

with the general solution being:

$$h_{ij}(x,t) = \sum h^{(\lambda)}(t) e_{ij}^{(\lambda)}(x) \tag{32}$$

where $e_{ij}^{(+,\times)}$ is a polarization tensor that satisfies $e_{ij} = e_{ji}, k^i e_{ij} = 0, e_{ii} = 0$ and $+, \times$ being the two polarization states. Equation 31 tell us that tensor modes has two physical degrees of freedom, because of the 4 constraints of being trace-free and transverse (starting from 6 degrees of freedom).

Doing the transformation:

$$v_{ij} \equiv \frac{a M_{pl}}{\sqrt{2}} h_{ij} \tag{33}$$

And defining:

$$\frac{M_{pl}}{2} a h_{ij} \equiv \frac{1}{\sqrt{2}} \begin{pmatrix} f_+ & f_\times & 0 \\ f_\times & -f_+ & 0 \\ 0 & 0 & 0 \end{pmatrix} \tag{34}$$

where $f_{+,\times}$ represents the polarization modes of the gravitational wave. Then we get:

$$S_T = \frac{M_{pl}^2}{8} \int d^4x [v'_{ij} v'_{ij} - (\nabla v_{ij})^2 + \frac{a''}{a} v_{ij} v_{ij}] \tag{35}$$

After moving to Fourier Space and making some tricks, one gets:

$$v_k''^{(\lambda)} + (k^2 - \frac{a''}{a}) v_k^{(\lambda)} = 0 \tag{36}$$

which is a wave equation as well. From here, we can identify two regimes: When $k^2 >> \frac{a''}{a}$, we can ignore the term $\frac{a''}{a}$ and we get $v''_{(k)}{}^{(\lambda)} + k^2 v_{(k)} = 0$ which is a equation of a free harmonic oscillator, so that the tensor perturbations h_{ij} oscillate with a damping factor $1/a$ with frequency $\omega_k = k$. Quantum zero-point fluctuations of these oscillators provide the origin of structure in the Universe. This regime is also analogous of ignoring the effect of the expansion of the Universe. Because $a''/a \sim (a'/a)^2$, we get $k >> aH$, so we're dealing with sub-horizon behaviour. The solution for this regime is:

$$v_k(\tau) = A e^{ikr} \tag{37}$$

which means that the amplitude of the modes of the original field h_{ij} decrease in time with the inverse of the scale-factor as an effect of the Universe expansion.

The second regime, when $k^2 << \frac{a''}{a}$, we neglect k^2 so that: $v_k''^{(\lambda)} - \frac{a''}{a} v_k^{(\lambda)} = 0$ which has two solutions:

$$v_k(\tau) \propto a \tag{38}$$

and

$$v_k(\tau) \propto 1/a^2 \tag{39}$$

Recalling that $v_k \propto h_{ij}$, for the first case we have that $h \propto const$ and for the second a decreasing in time solution. This regime corresponds to the super-horizon regime.

We want to calculate more accurately the power-spectrum of tensor perturbations, solving equation 36. After performing the standard quantization of the field we have to assume that the Universe is in a "Bunch-Davies vacuum state". This is because for inflation there is a prefered choice: At sufficiently early times all modes of cosmological interest were inside the horizon, $\frac{k}{H} \sim |k\tau| >> 1$. This means that in the remote past all observable modes had time-independent frequencies. Dealing with Bessel's equations,the asymptotic form Hankel functions and matching the asymptotic solution to a plane wave, the exact solution for the super-horizon wavelength behaviour is[1]:

$$v_k = e^{i(\nu-1/2)\pi/2} 2^{(\nu-3/2)} \frac{\Gamma(\nu)}{\Gamma(3/2)} \frac{1}{\sqrt{2k}} (-k\tau)^{1/2-\nu} \tag{40}$$

where Γ is the Euler function.

We can now write the tensor power-spectrum. Employing the expression 22 and considering that here we deal with two polarization states, we have:

$$\Delta_t^2(k) = \frac{k^3}{2\pi^2} \sum |h_k^{(\lambda)}|^2 \tag{41}$$

which for super-horizon scales leads to:

$$\Delta_t^2(k) = \frac{8}{M_{pl}^2} (\frac{H}{2\pi})^2 (\frac{k}{aH})^{-2\epsilon} \tag{42}$$

Notice that the *tensor* amplitude is a direct measure of the expansion rate H during inflation. This is in contrast to the *scalar* amplitude which depends on both H and ϵ. We conclude that these GW are almost frozen on super-horizon scales because they all have the same amplitude, due to being almost scale-invariant. For $k = aH$,

$$\Delta_t^2(k) \approx \frac{2}{\pi^2} (\frac{H}{M_{pl}})^2 \tag{43}$$

The scale-dependence of the tensor spectrum is defined in analogy to equation 25 as:

$$\Delta_t^2(k) \equiv A_t (\frac{k}{k_*})^{n_t} \tag{44}$$

where n_t is the tensor spectral index. Scale-invariance then corresponds to $n_t = 0$.

These quantities are usually expressed by the "Hubble flow-functions" ϵ_i , which express the conditions of slow-roll in terms of deviations with respect to an exact exponential expansion: $\epsilon_1 = -\dot{H}/H^2$, $\epsilon_{i+1} \equiv \dot{\epsilon}_i/(H\epsilon_i)$. These parameters are linked to those in equations 17 e 16 by: $\epsilon_1 \simeq \epsilon$ and $\epsilon_2 \simeq -2\eta + 4\epsilon$.

Rewriting these quantities in terms of the Hubble parameter and its derivatives, up to second order:

$$n_t = -2\epsilon_1 - 2\epsilon_1^2 - 2(C+1)\epsilon_1\epsilon_2 \tag{45}$$

$$\frac{dn_t}{d\,ln\,k} = -2\epsilon_1\epsilon_2 \tag{46}$$

with $C = ln2 + \gamma_E - 2 - 0.7296$

4.1. Consistency relation

There is a consistency relation that holds between quantities which involve tensor perturbations in the present inflationary scenario. Often the amplitude of tensors is normalised with respect to the measured scalar amplitude. Introducing the tensor-to-scalar ratio r:

$$r(k^*) \equiv \frac{A_t(k^*)}{A_s(k^*)} \tag{47}$$

This yields the amplitude of the GW with respect to that of the scalar perturbations at some fixed pivot scale k^*. Tensors have not been observed yet, so we only have an upper limit on their amplitude, $r0.17$. This quantity depends on the time-evolution of the inflaton field as:

$$r = \frac{8}{M_{pl}^2}(\frac{\dot{\phi}}{H})^2 \tag{48}$$

From equation 16, we conclude that $r = 16\epsilon$. We also conclude that $n_t \approx \frac{ln\,V}{d\,ln\,k} = -2\epsilon$. Therefore at the lowest order in slow-roll parameters, one finds the following consistency relation:

$$r = -8n_T \tag{49}$$

If this relation really holds true it means that it will be very hard to measure any scale dependence of the tensors, since a large spectral index would invalidate the consistency relation. At present we have only an upper bound on the tensor-to- scalar ratio: $r_{0.05} \in [0.05 < 0.07]$ [1] (the subscript indicates the pivot scale in Mpc^{-1} units).

Inflationary models can be classified according to their predictions for the parameters n_s and r. The figure below shows the predictions of various slow-roll models as well as the latest constraints from measurements of the Planck satellite.

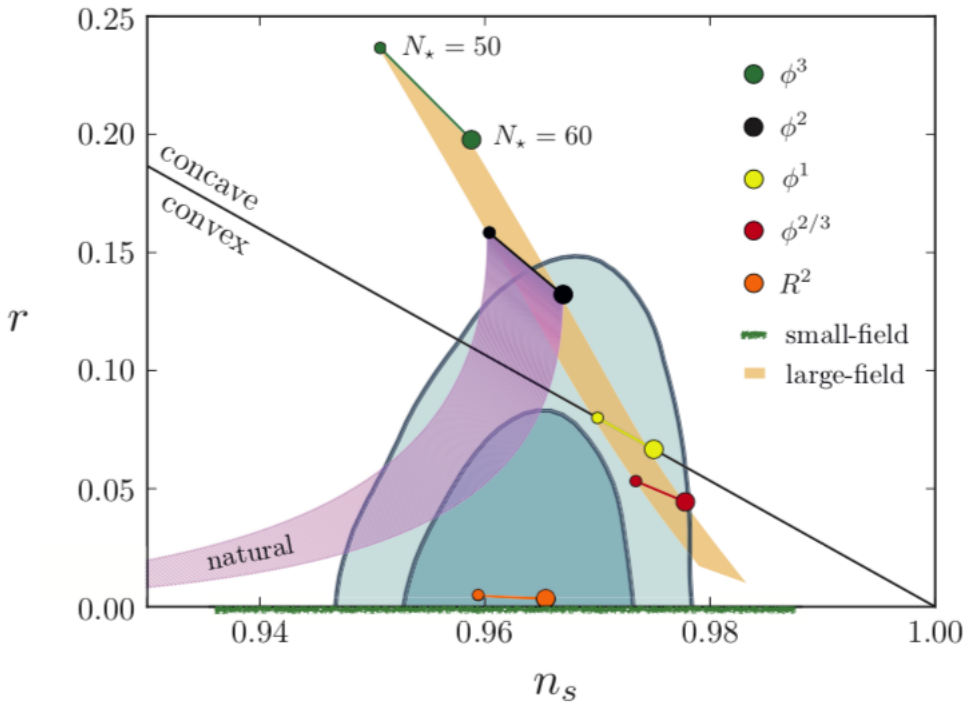

Figure 2. Constraints on the scalar spectral index (n_s) and the tensor amplitude r from measurements of the Planck satellite.[2]

5. Conclusion

The theory of cosmological perturbations is what allows us to connect theories of the very early Universe with the data on the large-scale structure of the Universe at late times and is thus of central importance in modern cosmology. As observed, that the inflationary scenario predicts the production of a background of stochastic GW. One can conclude that the inflation fluctuations are coupled to scalar perturbations of the metric while tensor perturbations constitute the real degrees of freedom of the gravitational field: gravitational waves. There are no constraint equations coming from the stress-energy continuity equation for these modes (in the case of a perfect fluid). Their evolution is only regulated by the traceless spatial part of the Einstein equation, which does not contain direct influence from the energy

content of the Universe. It can be shown that a coupling between GW and the content of the Universe grows up only in the presence of anisotropic stress tensor.

One can also conclude that the scalar (when expressed in terms of a suitable gauge-invariant potential) and the tensor perturbations remain almost frozen until their wavelengths correspond to super-horizon scales, so that the amplitude at the time they re-enter into the causally connected region is the same as the first horizon crossing during inflation (because inflation stretches tensor perturbations wavelengths to super-horizon scales, making their amplitude almost frozen).

The amplitude of the GW signal is usually described by the tensor-to-scalar ratio r. The current best bound on r comes from the joint analysis of Planck, BICEP2, Keck Array and other data, which yields $r < 0.07$ for $k = 0.05 Mpc^{-1}$. Excluding temperature data and assuming a scale-invariant GW power-spectrum, the bound becomes $r < 0.09$ [1]. A crucial point is that, even in the simplest, single-field framework, different inflationary scenarios predict different values of r. The main observational signature of the inflationary GW background would a curl-like pattern (named "B-mode") in the polarization of the Cosmic Microwave Background (CMB). In addition to the B-mode, evidence of primordial GW could come from galaxy and CMB curl-like lensing signatures, induced by tensor modes, or from parameters related to the small modification in the expansion history of the Universe, due to the GW contribution to the overall energy sum.

References

1. M.C.Guzzetti, Gravitational waves from inflation. **2016**, , 1–35.
2. D. Baumann, . In *Cosmology- Part III Mathematical Tripos*; pp 3–40; 111-124
3. Hiranya V. Peiris. In *Cosmology Part II: The Perturbed Universe*, 2016, pp 14-22
4. Robert H. Brandenberger In *Lectures on the Theory of Cosmological Perturbations*, 2003.

Proceedings

A brief review on GUT and Electroweak Baryogenesis, and the Deep Underground Neutrino Experiment

Diogo Calado [1]

[1] Faculdade de Ciências da Universidade de Lisboa; diogombcalado@gmail.com

Received: 27/01/2020; Accepted: date; Published: date

Abstract: Baryogenesis has been a subject of research for many years, and a lot of different theory's emerged to discuss it. In this work, we attend to have a brief discussion on two specific theory's, the GUT Baryogenesis and the Electroweak Baryogenesis, that can be tested in nearby future, and the Deep Underground Neutrino Experiment(DUNE) can make a big impact on restraining this theories. In the first chapters, we will start by making a historical introduction to Baryogenesis, switching to explaining the two major theories of Baryogenesis giving special attention to Baryogenesis via leptogenesis, both in GUT models and Electroweak models. Then we will see what is the DUNE, and how it might contribute to restraining this theories.

Keywords: Electroweak Baryogenesis; GUT Baryogenesis; Deep Underground Neutrino Experiment.

---

1. Introduction

1.1. Historical Introduction

I will start by humbly say that this review is a brief one, not going to mathematical details about the theories since it requires quantum field theory and group theory to go deeper on this subject, and I didn't had classes on neither till the moment.

To start talking about Baryogenesis, we should first start with a historical review on how this theories emerged. We start in 1926, when the Schrödinger's equation was published. Schrödinger's equation was a good way to study quantum mechanics, but soon enough, some problems were revealed in this theory, and the biggest one was that it wasn't invariant at Lorentz transformations. This means, the equation failed with systems with high momentum (relativistic). The search for a Lorentz invariant equation began shortly after, and in the same year, Oskar Klein and Walter Gordon came up with the Klein-Gordon equation, that although could describe relativistic particles, the particles had to have spin s equals to zero.

In 1928, Paul Dirac derived a beautiful equation (1) that was able to describe relativistic particles with spin $s = \frac{1}{2}$ such as leptons, quarks, etc.

$$(i\hbar\gamma^{\mu}\partial_{\mu} - m)\psi = 0 \tag{1}$$

And the solutions to this equation where four distinctive spinor wave equations ψ, where a familiar multiplying term $exp(-imc^2t/\hbar)$ appears in first two solutions, corresponding to the particle with spin $m_s = \pm\frac{1}{2}$. However, the other two solutions had $exp(+imc^2t/\hbar)$ as the multiplying term. Paul Dirac, inspired by the concept of *holes* in condensed matter states, tried to explain this by assuming that $exp(-i(-m)c^2t/\hbar)$ happens, that is, there are states of negative energy, by then proposing the "sea -theory", where vacuum should correspond to a state where all the negative energy states were filled. The absence of a negative energy state (a "hole in the sea") should then be interpreted as an anti-particle. Nowadays, the physics community consider that the minus comes from the time factor, that is $exp(-imc^2(-t)/\hbar)$, and actually the "time arrow" goes in the same direction, however the charges are opposite, so it seems the time goes backwards.

But the important part is, the Dirac's equation opened a whole new chapter in physics, since the anti-particles had emerged from obscurity. In Cosmology, there was no reason to believe that matter and anti-matter weren't created in same amounts in the beginning of the universe. But a big question started to gain weight: ***"Where's the anti-matter in our universe?"***

This question lead to a lot of theories, and even Paul Dirac himself in a lecture given in 1933 tried to answer it, by saying that:
"Although the Earth is composed by matter, and the Sun and solar system is composed by matter, maybe there's some regions in the universe that are identical but made of anti-matter, and globally, have the same density in our universe".
For the time, Dirac's idea was consistent to what we knew about anti-matter: not much. However, nowadays we know this theory is wrong, for two major reasons:

- As far as we know, anti-matter does not form such high density structures as matter, that is, does not form Anti-Helium, Anti-Carbon, etc. so the symmetry between matter and anti-matter is broken.
- The frontiers between the regions of matter and anti-matter would produce a significant γ emission that we do not observe.

There was searches for large anti-matter structures, but none were find. we concluded our universe is dominantly matter. Another theories emerged, like:
"What if the universe evolved in a way that separated matter from anti-matter by void?"
And the reason this theories are not valid is that no model made so far can reproduce such uniform Cosmic Microwave Background (CMB) as we see today. The perturbations in the mean value are only visible in orders below of 10^{-5}, and are homogeneous and isotropically random.
"The Universe just started that way."
This argument has a lot of flaws, since it's a sterile hypothesis, and raises philosophical questions, as, "if the universe had already more matter then anti-matter, then the beginning of the universe that we assume, is really the beginning? Why would the universe evolve from an already determined state? etc."

1.2. Baryogenesis

So no theory could predict the dominance of matter of anti-matter consistently. And only in 1967 Sakharov enumerated three conditions that a baryon-generating interaction must satisfy to produce matter and anti-matter at different rates, there is, to have **Baryogenesis**:

- Baryon number violation B.
- C and CP violation.
- Thermodynamic Non-equilibrium.

The first condition is quite obvious, since the baryons have $B = 1$ and anti-baryons $B = -1$, so from an asymmetry between matter and anti-matter results spontaneously that B is not conserved. The second condition, C and CP violations, were less intuitive, however, C was proven to not be a symmetry. CP however, was though to be a symmetry, but in 1964 (only 3 years sooner) James Cronin and Val Fitch proved to be broken, as they observed that neutral kaons (K^0) had a very weak interaction that was not invariant under CP. that is, K^0 would have a bigger probability of decaying in particles then in anti-particles, by a small fraction. But still this was still a new discovery. Nowadays CP is no longer considered a symmetry however, CPT is. Finally, the last condition, the thermodynamics non-equilibrium is crucial to create a baryon asymmetry since in equilibrium, the interactions would annihilate this asymmetry, since in equilibrium the behavior of an individual particle is not distinguishable this asymmetry wouldn't pronounce itself, leaving the Barion number $B = 0$.

For decades, numerous theories tried to explain this baryonic asymmetry, have tried to answer how this mechanism of symmetry breaking worked. For this to happen, baryons and anti-baryons must have/had a different type of interaction, and they must manifest different properties.
Also very important, the theories must provide a detailed prediction of the baryon to photon ratio:

$$\eta = \frac{n_B - n_{\bar{B}}}{n_\gamma} \tag{2}$$

Where n_B is the number density of baryons, $n_{\bar{B}}$ is the number density of anti-baryons and n_γ the number density of photons in the universe.

Let's start by a very brief and simplistic explanation of GUT Baryogenesis, and then we follow to Electroweak Baryogenesis.

2. GUT Baryogenesis

As the name suggests, GUT Baryogenesis are theories that predict the baryonic asymmetry of the universe (BAU) was a process that occurred in the Grand Unification Theory scale (10^{16} GeV), that corresponds to the first 10^{-36} seconds of the Universe. At this stage of the Universe, this theories predict that the three gauge interactions (the weak, strong and electromagnetic interactions) we observe today are merged into a single interaction. That is, the behavior of Electromagnetic, Weak and Strong Nuclear forces would have the same behavior, as one force only, with one strength of force, mediated by very heavy bosons. This concept of course is different then what we observe with everyday low energies experiments, but we are talking about massively high energies, (10^{16} GeV) and such high energies we're only achieved in the very beginnings of the Universe.

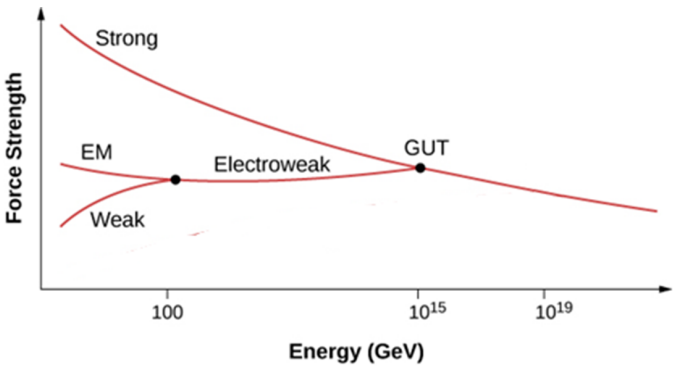

Figure 1. Illustration of how GUT theories predict to be the behavior of the forces strength at high energies. [F.1]

In the Grand Unified Theories (GUT), at such high energies, there are heavy gauge and Higgs bosons whose interactions violates baryon number. Let's see a simple example to better capture the essence of this. Let's consider that existed such a heavy boson X which had two decay channels:

$$X \to qq \quad (A)$$
$$X \to q\bar{l} \quad (B)$$

respectively with decay rates, λ_A λ_B. Let q and l be quarks and leptons which carry baryon number $B = 1/3$ and $B = 0$, and lepton number $L = 0$ and $L = 1$ respectively. The anti-particle would correspond of course to $\bar{B} = -1/3, 0$ and $\bar{L} = 0, -1$ respectively.
Now looking closer to those decay modes we can conclude that if one mode assigns the baryon and lepton number of X based on one decay products, then the other decay mode violates baryon number. Thus, one has B violation. As we mentioned earlier, the next requirement of the Sakharov conditions is CP violation. This requires that the decay rate λ_A of X to quarks, is not equal to the decay rate λ_B of $\bar{X}$ to anti-quarks, which ultimately would arise to the asymmetry in baryon number Ultimately to fulfill all Sakharov conditions one also needs B violating interactions to be out of thermal equilibrium, since in equilibrium the interactions would annihilate this asymmetry. As we mentioned earlier, this step is crucial to create the baryonic asymmetry. This might be achieved in GUT theories, as we will see soon.
Although this theories are appealing, there are some problems with GUT baryogenesis models.

- Typically the mass of the X particle is about 10^{16} GeV, and from measurements of the cosmic microwave background radiation (CMBR) anisotropy the mass of the inflaton, most energetic particle (theorized) during *reheating* [A.1], is of the order of 10^{13} GeV (from measurements of the cosmic microwave background radiation (CMBR) anisotropy) and it is difficult to create particles during reheating either via direct inflaton decays or in the thermal bath.
- If we choose the X mass to be less than 10^{13} GeV, then wee have problems with proton decay, giving a half-life of the proton that we haven't observed. This gets even worse for supersymmetric GUTs.
- In supergravity and superstring theories there are a number of massive scalars which decay after the GUT phase transition releasing a large amount of energy into the Universe. This dilutes the baryon-to-entropy ratio.

GUT Baryogenesis lost the heat, and for many years was a low working subject of investigation. However recently, the understanding of the reheating phase in the Universe after inflation has gone through a radical change. Studying the

equations for the inflaton decay, it's noticeable that for certain values of the momenta of the daughter particles that hits a resonance. The inflaton can then decay very quickly and explosively via "parametric resonance" []. In this case, it is possible for the inflaton field to create X particles during reheating, even if they are heavier than the inflaton, and obtain a baryon asymmetry through their decays.

Some GUT imply that protons decay, via the Higgs particle, magnetic monopoles, or new X bosons, with a half-life of 10^{31} to 10^{36} years. To date, all attempts to observe new phenomena predicted by GUTs (like proton decay or the existence of magnetic monopoles) have failed.

2.1. GUT Baryogenesis via Leptogenesis

Baryogenesis via leptogenesis is a very seducing way to take the baryonic and leptonic asymmetry problems simultaneously. Also, these models do not require big modifications to the Standard Model. Primarily, this kind of mechanisms work by creating a lepton number (L) asymmetry in a manner similar to that in GUT Baryogenesis, but by the out-of-equilibrium decays of heavy right-handed Majorana neutrinos [A.2] in the inflation epoch. Models with heavy right-handed Majorana neutrinos are often invoked to provide mass to the light neutrinos via the *seesaw mechanism* [A.3]. When this heavy neutrinos decay, $B + L$ is violated via *sphaleron processes*[A.4], to convert the lepton asymmetry into a baryonic asymmetry. We can see how this works by supposing that we create a lepton asymmetry of 10 from heavy neutrino decays. Rewriting this in terms of $B + L$ and $B - L$, in the beginning there was no baryonic asymmetry, so $B + L = 10$, and $B - L = -10$. Now, if we have $B + L$ violating processes in thermal equilibrium they will reduce the $B + L$ to 0 while keeping $B - L$ constant. This process will happen naturally, since due to the fact that $B + L$ must be vanishing, the conversion via the sphaleron process results in the final baryonic asymmetry $B \simeq -L$. This type of models are far more complicated than what is explained in this section, but as I said in the beggining this topics require mathematical and physical that goes way beyond my understandings. However, this section was based on [3] and [4] and can be found more details in this subject on those articles.

3. Electroweak Baryogenesis

This theories might be seen as quite similar to the ones discussed on chapter 2.1, however, the main difference can be seen as at what phase the two different branch's of theories propose that baryogenesis occurred. As mentioned before, GUT Baryogenesis are based on very high energies, $\sim 10^{16}$ GeV, near the inflationary epoch. On the other hand, the Electroweak Baryogenesis predicts a production of the baryonic asymmetry in much lower energies, $\sim 10^2$ GeV, during the electroweak phase transition.

It is important to notice that even though it wasn't mentioned before, the standard model of the electroweak interactions has in itself a mechanism capable of producing a baryon number dynamically, it does so while conserving the combination $B - L$. This implies that the sphaleron can also act in the opposite way: if an arbitrary $B - L$ conserving phenomenon produces a baryon number prior to the electroweak transition, then, due to the sphaleron, this transition will automatically wash out such a primordial contribution.[3]

This fact gave rise to the Electroweak Baryogenesis theories, where has the name suggests, the baryonic number asymmetry comes from the electroweak transition

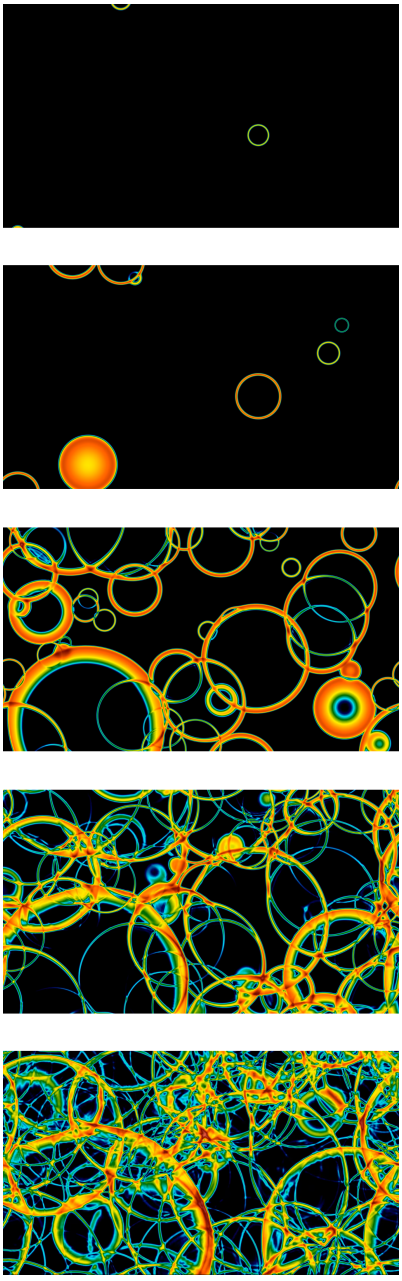

Figure 2. Illustration of how the 1^{st} order of Higgs transition propagated in space, via spontaneous bubbly formations, expanding the perturbation to the minimum value for the potential for nearby regions, so inside the bubble Higgs field as lost his potential. Now particles have a mass associated. It's thought that also the inflaton field decayed in a similar way. [F.2]

itself. In order for the production of baryons to simply be possible, as we discussed before, the transition should be out of equilibrium. Then, the Higgs field would had to vary rapidly. To compensate the weak CP violation, the transition should be as far from equilibrium as possible, so we consider a first-order transition of the Higgs field. [3][4][6] Such a transition proceeds with bubbles formation, between the the broken phase nucleate within the surrounding plasma in the symmetric phase as seen in Figure 3. These bubbles expand, collide, and coalesce until only the broken phase remains, as demonstrated in Figure 2.

With that so, baryon in EWBG takes place in the vicinity of the expanding bubble walls. The process can be divided into three steps:

Step 1: Particles in the plasma scatter with the bubble walls. If the underlying theory contains CP violation, this scattering can generate CP (and C) asymmetries in particle number densities in front of the bubble wall.

Step 2: These asymmetries diffuse into the symmetric phase ahead of the bubble wall, where they bias with the electroweak sphaleron transitions to produce more baryons than anti-baryons.

Step 3: Some of the net baryon charge created outside the bubble wall is swept up by the expanding wall into the broken phase. In this phase, the rate of sphaleron transitions is strongly suppressed, and can be small enough to avoid washing out the baryons created in first two steps.

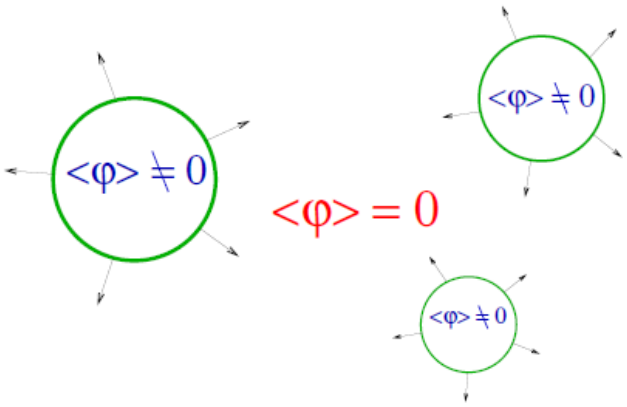

Figure 3. Expanding bubbles of electroweak-broken phase within the surrounding plasma in the electroweak-symmetric phase. The $< \phi >$ represents the expected value of the Higgs field.[F.3]

Creating the required conditions for baryogenesis, we need to take into account that in order for the $B - L$ violation to be weak in the true vacuum after the transition, the energy of the sphaleron should be very large compared to the temperature right after the bubble surface, i.e. the intermediate bosons should have significant masses, and the expectation value of the Higgs field should grow very rapidly.[9]

4. Deep Underground Experiment

4.1. Why neutrinos?

The observation that neutrinos have mass and oscillate between flavors are some recent demonstrations that the Standard Model is incomplete. We know now that each of the three flavors of neutrinos, ν_e , ν_μ and ν_τ , is known to be a different mix of three mass eigenstates ν_1, ν_2 and ν_3. But a big question is how does the neutrinos help in this questions? As we saw in the Chapter 2 and 3, neutrinos can be the key to understand better this subject. DUNE will be able to better understand how this asymmetry of baryonic number was created, by the

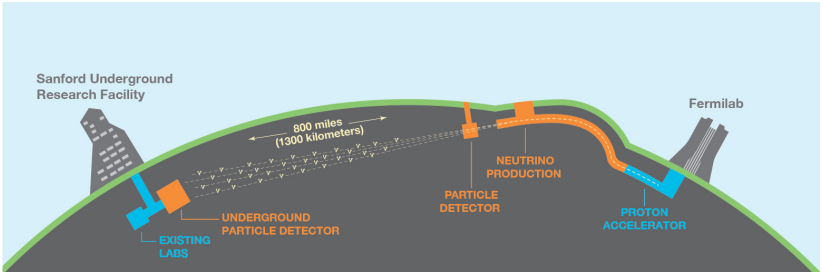

Figure 4. Illustration of the DUNE setup. The neutrino beam is emitted in the Fermilab underground proton accelerator facilities separated by 1300 kilometers of the earth's crust, and later on received in the Sanford Underground R.F.[F.4]

following actions:

- By studying the properties of neutrino and anti-neutrino oscillations, DUNE is pursuing the most promising avenue for understanding this asymmetry.
- Resolution by DUNE of the detailed mixing patterns and ordering of neutrino mass states, and comparisons to the corresponding phenomena in the quark sector could reveal underlying symmetries that are as yet unknown.
- Experimental evidence hints that the physical forces observed today were unified into one force at the birth of the Universe. A lot of the GUTs predict that protons should decay, a process that has never been observed, and the DUNE will be able to test some possible decay modes.

DUNE has also been designed to address a wide range of scientific topics besides Baryogenesis and neutrinos oscillations, such as supernova neutrino bursts, that we will not address in this essay.

4.2. How will DUNE contribute to all this topics?

DUNE will make precision measurements of the parameters that govern $\nu_\mu \to \nu_e$ and $\bar{\nu_\mu} \to \bar{\nu_e}$ oscillations. The intrinsic challenges of producing and detecting ν_τ's is hard to overcome, being the oscillation modes $\nu_{e,\mu} \to \nu_{\mu,e}$ and $\bar{\nu_{e,\mu}} \to \bar{\nu_{\mu,e}}$ provide the most promising experimental signatures of leptonic CP violation.
This measurements will be able to determine the *"mass hierarchy"*[A.5], the mixing angles θ_{13} and θ_{23} with considerable accuracy, and measurement of the charge-parity (CP) violating phase δ_{CP}. That is, looking at Figure 3 we can observe that that the Pontecorvo–Maki–Nakagawa–Sakata (PMNS) matrix makes the matricial connection of the flavors to the mass eigenstates. Going deeper on what are the values of the elements of the PMNS matrix, we see that in Figure 4, the relation between the the mixing angles and the δ_{CP}, with the PMNS matrix elements.

$$\begin{bmatrix} \nu_e \\ \nu_\mu \\ \nu_\tau \end{bmatrix} = \underbrace{\begin{bmatrix} U_{e1} & U_{e2} & U_{e3} \\ U_{\mu 1} & U_{\mu 2} & U_{\mu 3} \\ U_{\tau 1} & U_{\tau 2} & U_{\tau 3} \end{bmatrix}}_{= U \longrightarrow \text{Pontecorvo–Maki–Nakagawa–Sakata (PMNS) matrix}} \begin{bmatrix} \nu_1 \\ \nu_2 \\ \nu_3 \end{bmatrix}$$

Figure 5. Relationship between the eigenvalues of the flavor to the eigenvalues of mass.

$$U = \begin{bmatrix} U_{e1} & U_{e2} & U_{e3} \\ U_{\mu 1} & U_{\mu 2} & U_{\mu 3} \\ U_{\tau 1} & U_{\tau 2} & U_{\tau 3} \end{bmatrix} = \begin{bmatrix} c_{12}c_{13} & s_{12}c_{13} & s_{13}e^{-i\delta_{CP}} \\ -s_{12}c_{23} - c_{12}s_{23}s_{13}e^{i\delta_{CP}} & c_{12}c_{23} - s_{12}s_{23}s_{13}e^{i\delta_{CP}} & s_{23}c_{13} \\ s_{12}s_{23} - c_{12}c_{23}s_{13}e^{i\delta_{CP}} & -c_{12}s_{23} - s_{12}c_{23}s_{13}e^{i\delta_{CP}} & c_{23}c_{13} \end{bmatrix}$$

$$\boxed{\text{sen}\theta_{ij} = s_{ij} \;\; ; \;\; \cos\theta_{ij} = c_{ij}}$$

Figure 6. Pontecorvo–Maki–Nakagawa–Sakata (PMNS) matrix. AS we can see there's a strong dependence of the matrix values and the mixing angles. also, δ_{CP} as we can see corresponds to a phase transition of the matrix. There are other forms to write the PMNS, that are more clear to see the phase transition mediated by δ_{CP}.

4.2.1. Measurement of the mixing-angles and the CP violating phase

By determining with more accuracy the values of the mixing angles θ_{13} and θ_{23} and the δ_{CP}, the DUNE is making a big step on understanding new symmetries, and understanding if the neutrinos could have been a big protagonist on Baryogenesis. For instance, a nonzero value of the CP-violating phase implies that neutrinos and anti-neutrinos oscillate differently. We will go back to this soon.

The magnitude of the CP-violating terms in the oscillation depends most directly on the size of the Jarlskog Invariant, a function that was introduced to provide a measure of CP violation independent of mixing-matrix parameterization. The Jarlskog Invariant is given by:

$$J_{CP}^{PMNS} = \frac{1}{8} \cdot sin(2\theta_{12})sin(2\theta_{13})sin(2\theta_{23})cos(2\theta_{13})sin(\delta_{CP}) \tag{3}$$

Giving the current accepted values, we have:

$$J_{CP}^{PMNS} \approx 0.3sin(\delta_{CP}) \tag{4}$$

Comparing to the the quark sector, that has small mixing between families, and for which Jarlskog Invariant is given by $J_{CP}^{CKM} \approx 3 \cdot 10^{-5}$, This might lead to a much bigger value [10]. The DUNE experiment will be able to calculate the Jarlskog Invariant for the neutrinos, since it will be able to measure with a good precision the δ_{CP} parameter.

4.2.2. Measurement of the proton decay life-time

The proton decay mode $p \rightarrow e^+ + \pi^0$ is often predicted to have a high branching ratio and if exists, will definitely give a distinct signature in DUNE, although is unlikely to compete on a reasonable time-scale with water Cherenkov experiments, such as Super-Kamiokande and Hyper-Kamiokande. Another key mode is $p \rightarrow K^+\bar{\nu}$. This mode is dominant in most supersymmetric GUTs, many of which also favor other modes involving kaons in the final state.
The key signature for $p \rightarrow K^+\bar{\nu}$ is the presence of an isolated charged kaon (which would also be monochromatic for the case of free protons, with the momentum $p \simeq 340$ MeV). Unlike the case of $p \rightarrow e^+ + \pi^0$, where the maximum detection efficiency is limited to 40–45% due to the inelastic intra-nuclear scattering of the π^0, the kaon emerges intact from the nucleus with 97% probability. DUNE will be able to distinguish this kind of events from the background, since it will be able to detect the electro magnetic shower produced after the decays of this elements. Mainly, the background for this reactions (and also the neutrino's oscillations) is the cosmic radiation, and the DUNE will be situated very deeply underground [12].

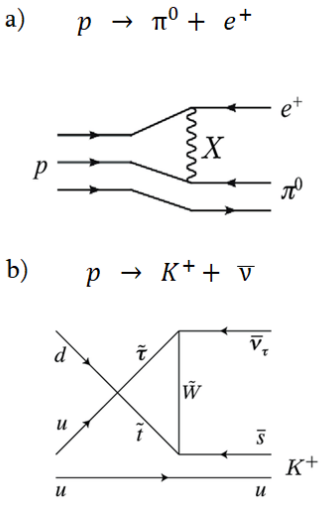

Figure 7. The two most probable decay modes for the proton[F.7].

4.3. Methods applied for this measurements

The frequency of neutrino oscillation among the weak-interaction (flavor) eigenstates depends on the difference in the squares of the neutrino masses:

$$\Delta m_{ij}^2 = m_i^2 + m_j^2 \tag{5}$$

a set of three neutrino mass states implies two independent mass-squared differences (Δm_{21}^2 and Δm_{32}^2). The ordering of the mass states is also a good method to known the neutrino mass hierarchy.
Whereas the Standard Model allows for violation of charge-parity (CP) symmetries in weak interactions, CP transformations followed by time-reversal transformations (CPT) are invariant. Under CPT invariance, the probabilities of neutrino oscillation and antineutrino oscillation are equivalent, that is, $P(\nu_x \rightarrow \nu_x) = P(\bar{\nu_x} \rightarrow \bar{\nu_x})$ where $x = e, \mu, \tau$. CPT invariance in neutrino oscillations was recently tested by measurements of $P(\nu_\mu \rightarrow \nu_\mu)$ and $P(\bar{\nu_\mu} \rightarrow \bar{\nu_\mu})$ oscillations and no evidence for CPT violation was found.
The oscillation probability of $\nu_{\mu,e} \rightarrow \nu_{e,\mu}$ through matter, in a constant density approximation, keeping terms up to second order in $\alpha \equiv |\Delta m_{21}^2|/|\Delta m_{32}^2|$ is given by:

$$P(\nu_\mu \rightarrow \nu_e P_0 + P_{sin\delta(CP)} + P_{cos\delta(CP)} + P_3 \tag{6}$$

where:

$$P_0 = sin^2\theta_{23}\frac{sin^2 2\theta_{13}}{(A-1)^2}sin^2[(A-1)\Delta] \tag{7}$$

$$P_3 = \alpha^2 cos^2\theta_{23}\frac{sin^2 2\theta_{12}}{A^2}sin^2[A\Delta] \tag{8}$$

$$P_{sin\delta(CP)} = \alpha\frac{8J_{CP}^{PMNS}}{A(1-A)}sin\Delta sin(A\Delta)sin[(1-A)\Delta] \tag{9}$$

$$P_{cos\delta(CP)} = \alpha\frac{8J_{CP}^{PMNS}cot\delta_{CP}}{A(1-A)}cos\Delta sin(A\Delta)sin[(1-A)\Delta] \tag{10}$$

where $\Delta = \Delta m^2_{31}L/4E$, and $A = \sqrt{3}G_F N_e 2E/\Delta m^2_{31}$ [10].
The physical characteristics of an appearance experiment are therefore determined by the baseline and neutrino energy at which the mixing between the ν_1 and ν_3 states is maximal, as follows:

$$\frac{L(km)}{E_\nu(GeV)} = (2n-1)\frac{\pi}{2}\frac{1}{1.27\cdot\Delta^2_{31}(eV^2)} \tag{11}$$

Which gives approximately:

$$\frac{L(km)}{E_\nu(GeV)} \approx (2n-1)\cdot 510km/GeV \tag{12}$$

The dependences on E_ν of the oscillation probability for the DUNE baseline of $L = 1,300km$ are plotted on the right in Figures 8.

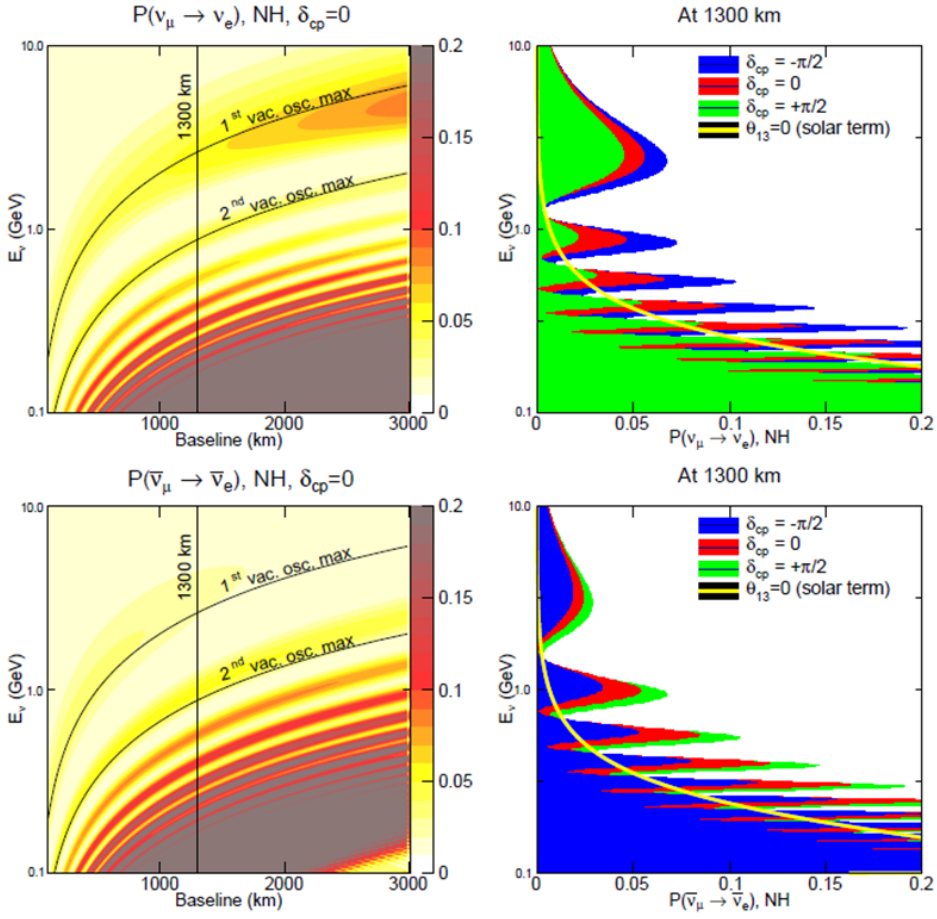

Figure 8. The top figures correspond to $\nu_\mu \to \nu e$ transition, while the figures in the bottom to $\bar{\nu_\mu} \to \bar{\nu_e}$. [F.8].

As we can see in Figure 8, in the left figures there is a clear dependency on the relation between E_ν and the Baseline distance, to the probability of detecting the oscillation between the μ and e flavor. As we can see in the right figures, the amplitude of the probability of detecting the oscillation between the μ and e flavor varies with the variation of the parameter $\delta(CP)$, being the different colors the corresponding to different values.
We can also see that in order to measure the value of $\delta(CP)$ with a good precision, it is required very rigorous assemble and calculations, since the variations in the probability is at the order of $\sim 10^{-2}$. We also see a big difference in the amplitudes of the probabilities between matter and anti-matter, that is do to the interaction with matter. We will discuss this in the next sub chapter.

4.4. Matter effects and Mass Hierarchy

As we know, the matter effect has a huge impact on the difference of the probability of detecting $\nu_\mu \to \nu_e$ and $\bar{\nu_\mu} \to \bar{\nu_e}$, since the anti-neutrino has more chances of interacting with matter then the neutrino. This means that as we can see in Figure 8, if we look closely, the probability of detecting the two different oscilations is quite signifficant. In the figure on the left, we can see that this difference is even more for higher energies, The significant impact of the matter effect on the $\nu_\mu \to \nu_e$ and $\bar{\nu_\mu} \to \bar{\nu_e}$ oscillation probabilities at the distance of 1300 km implies that the measurements over long distances through the Earth provide a powerful probe into the neutrino mass hierarchy.

- For normal hierarchy, $P(\nu_\mu \to \nu_e)$ is enhanced and $P(\bar{\nu_\mu} \to \bar{\nu_e})$ is suppressed. The effect increases with baseline at a fixed L/E.
- For inverted hierarchy, $P(\nu_\mu \to \nu_e)$ is suppressed and $P(\bar{\nu_\mu} \to \bar{\nu_e})$ is enhanced. The effect increases with baseline at a fixed L/E.

In Fig 9 we can see the the same plots as before with same analysis, but with normal and inverted hierarchy.

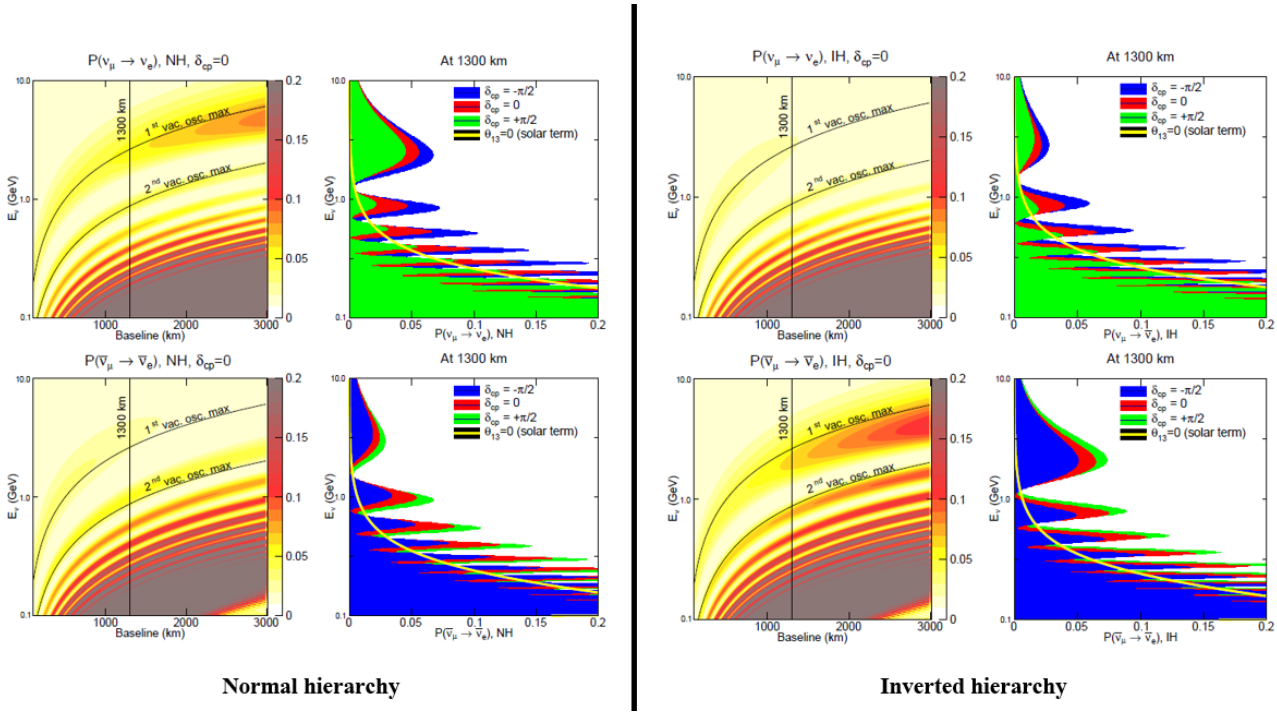

Figure 9. The left figures correspond to the same plot as before, and as we think that the neutrino mass hierarchy is (normal), and in the right figures we can see how the same experience will change their results if the mass hierarchy is inverted.[F.9]

A good way of seeing really how much the probabilities are change is by introducing the variable ζ:

$$\zeta = (P - \bar{P})/(P + \bar{P}) \tag{13}$$

So as we can see, now we have a variable that varies in the range $-1 < \zeta < 1$, and in the frontiers:

- -1: Corresponds to having zero probability of having $\nu_\mu \to \nu_e$ is 0, and for $\bar{\nu_\mu} \to \bar{\nu_e}$ 1.
- 0: Corresponds to having zero the same probability for both oscilations.
- 1: Corresponds to having zero probability of having $\nu_\mu \to \nu_e$ is 1, and for $\bar{\nu_\mu} \to \bar{\nu_e}$ 0.

So having the matter effect into account, we can plot the ζ as a function of the distance of detection and neutrino energy E_ν, for normal and inverted mass hierarchies, and for two values of $\delta(CP)$. Performing this steps, we get Figure 10.

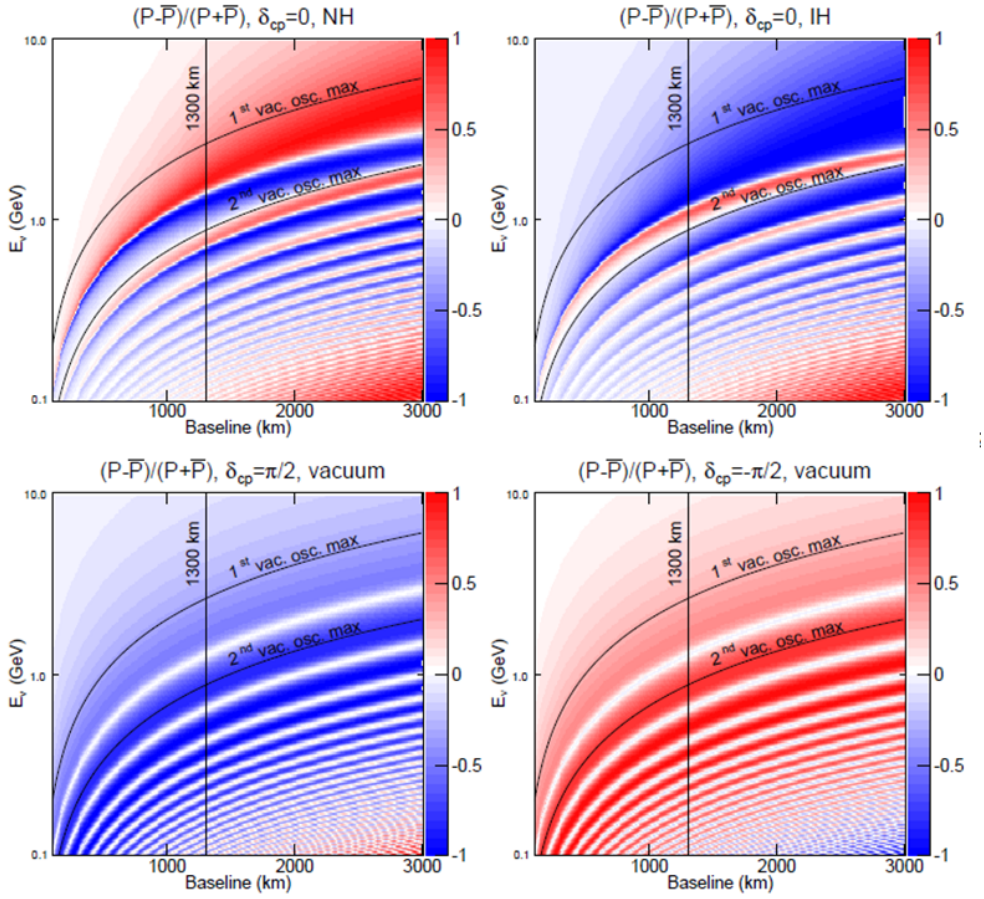

Figure 10. On the top: The left figure corresponds to the plot of ζ as a function of the baseline distance and the energy of the neutrino, having $\delta(CP) = 0$. The right figure also contains ζ as a function of the baseline distance and the energy of the neutrino and $\delta(CP) = 0$, but now is considering an inverted hierarchy.
On the bottom we see how the $\delta(CP)$ will vary the ζ assuming vacuum, that is, with no interaction of matter, considering on the left $\delta(CP) = \pi/2$ and on the right $\delta(CP) = -\pi/2$. [F.10]

As we can see in the Figure 10, DUNE will be able to destinguish if we have for example $\zeta > 0$ and $\delta(CP) = \pi/2$ or $\zeta < 0$ and $\delta(CP) = \pi/2$, since at the maximum of oscillations at that distance occurs in disntint values for ζ in each case.
So DUNE will be able to both discover the mass hierarchy and the $\delta(CP)$ value, via the interaction of the neutrinos with matter.

5. Conclusions

In this work we were able to get a good picture on how the two currently more accepted theories for Baryogenesis try to describe this phenomena that we observe that is baryon and lepton number asymmetry. We saw oh GUT theories try to describe the phenomena, via heavy bosons, and via right-handed Majorana neutrinos. We saw how the electroweak attempts to describe the same asymmetry via a first-order transition on Higgs field, by the sphaleron process. We weren't able to go fully on the mathematics of the theories, but we rather had a nice view on how the mechanisms work.
Also, we had a quick view on how DUNE can become a great tester on some of this theories, will studying deeply the nature of the neutrinos oscillations, and being able to not only measure the δ_{CP} parameter (that is still unmeasured) but also give a more precise value of θ_{12} and θ_{23}.
We also saw that by the perturbation of the matter in the ν_μ and ν_μ beam, they will be able to discover the mass hierarchy, that may reveal new contributes to an incremented neutrino physics standard model.
Combining the ν_μ disappearance signal with the ν_e appearance signal can help determine the θ_{23} octant and constrain some of the theoretical models of quark-lepton universality.

Sincerely hope you have enjoyed reading this essay as much as I did composing it.
The End.

Appendix A

Appendix A.1 - Inflaton Field and Reheating

The horizon and flatness problems of the Standard Big Bang Cosmology are beautifully solved if, in the first moments of the Universe ($\sim 10^{-34}$ to 10^{-32} s), the energy density was dominated by some form of "vacuum energy", causing comoving scales grow quasi-exponentially. This "vacuum energy" is generally associated with the potential V(ϕ) of some scalar field ϕ, the *inflaton*, which is displaced from it's initial local minimum of it's potential. As a by-product, quantum fluctuations of the inflaton field may be the seeds for the generation of structure and the fluctuations observed in the cosmic microwave background radiation.
Inflation ended when the potential energy associated with the inflaton field became smaller than the kinetic energy of the field. At this stage we have a super fast expanded and cold universe, and we know that somehow this low-entropy universe has to be transformed into a high-entropy hot universe dominated by radiation. The process by which the energy of the inflaton field is transferred from the inflaton field to radiation has been called reheating. [2] The theories of inflation nowadays count for many details in this processes, but summing up, the reheating occurs because when the potential energy V(ϕ) is converted to kinetic energy is in the formation of very brief particles, the inflaton particles, as the Figure A1 suggests. The more the potential gets closer to the minimum, the more inflatons there are. Inflaton particles are unstable and quickly decay, dispersing their energy to the other quantum fields, and thus reheating the Universe to about 10^{13} GeV, leaving the primordial "soup" of particles in thermal equilibrium, as theorized in Standard Big Bang Cosmology.

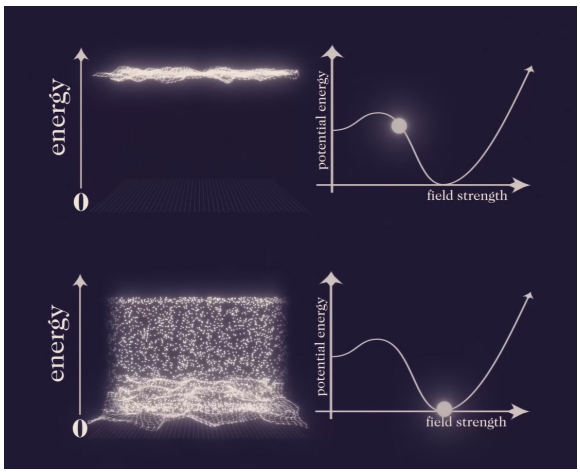

Figure A1. Illustration of how inflation theories predict how the inflaton field to decaying to the minimum of the potential energy to be the behavior of the forces strength at high energies.

Appendix A.2 - Majorana Neutrinos

Majorana particles are particles with charge zero that are indistinguishable from they're anti-particles. No Majorana particles were found yet, however, one huge question that we still face nowadays with modern physics is if the neutrinos are Majorana particles, or they're theorized right-handed brothers. But now, we are talking about this high mass and right-handed neutrinos, that could be the answer for how the mechanism of baryogenesis via leptogenesis happened.[6]

Appendix A.3 - Seesaw Mechanism

The electroweak symmetry is broken by the vacuum expectation of the Higgs doublet $< H_0 > \cong 246$ GeV, which gives mass to the gauge bosons and the fermions, all fermions except the neutrino. The model had been a complete success in describing all known low energy phenomena, until the evidence for neutrino masses appeared. Note that there is no right handed neutrino in the Standard Model(SM) and this directly leads to the fact that neutrinos are massless at the tree level. This results can be taken into account, due to the existence of an exact $B - L$ symmetry of the SM. It would therefore appear that non-zero neutrino mass ought to be connected to breaking of $B - L$ symmetry. The seesaw mechanism provides a very natural and attractive explanation of the smallness of the neutrino masses compared to the masses of the charged fermions of the same generation through the existence of heavy right-handed neutrinos. This annex was based on references [7] and [8], and more can be discovered about this subject at those papers.

Appendix A.4 - Sphaleron Processes

The sphaleron process is basically the $(B + L)$ violating process at the quantum level. The sphaleron is crated by the transition between false vacuum (vacuum with the Higgs field coupled) and the true vacuum (with electroweak symmetry broken). Since this process only occurs at such high energies, and drastic transitions, it's highly suppressed at low energies. In the unbroken phase (outside of the bubble), the rate for baryon number violation is:

$$\Gamma \sim \alpha_W^4 T^4 \tag{A1}$$

Where α_W it's the weak coupling and T the temperature in Kelvins. In the broken phase (inside the bubble) the rate of baryon number violation is given by:

$$\Gamma \sim exp(-\frac{a < \phi >}{T}) \tag{A2}$$

Where a is a parameter to determine and $< \phi >$ the expected value of the Higgs field.
So the sphaleron process is in equilibrium outside of the bubble wall, and is out of equilibrium inside, being the walls the responsible for the out of equilibrium for the sphaleron process.[6][3]

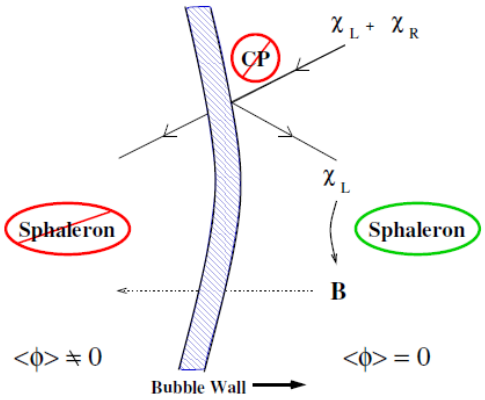

Figure A2. Sketch of the electroweak baryogenesis mechanism: The Higgs bubble walls separate the symmetric phase from the broken phase. If the reflection of left-handed electroweak particles contains CP violation, the sphaleron process (that only is active in the symmetric phase) generates a net baryon number.

Appendix A.5 - Mass Hierarchy (Neutrinos)

The neutrino mass hierarchy, that is, if whether the ν_3 mass eigenstate is heavier or lighter than the ν_1 and ν_2 mass eigenstates, is one of the remaining undetermined fundamental features of the neutrino Standard Model. Despite the obvious difficulty of experiments involving neutrinos, it is now clear beyond any doubt that neutrinos have masses, although tiny, and that they mix, unlike the assumptions of the standard model. Thanks to the discoveries of the last twenty years, we now have a simple three-flavor description of these new phenomena that explains most of the

data. Despite the success, this is not the end of the story. Further experimental and theoretical efforts is needed so that the next step, formulation of a new theory that encompasses the new insight into the neutrino physics, can be accomplished.[11]

References

1. António Silva (my Prof.), Lectures provided on the "Early Universe".
2. P. Peter Jean-Philippe Uzan, "Primordial Cosmology", chapter 9.3, *Oxford* **2009**.
3. Raghvan Rangarajan, "Baryogenesis in the early Universe", *IAS* **1999**.
4. Mark Trodden, "Baryogenesis and Leptogenesis", *Syracuse University* **2004**.
5. Antonio Riotto, Lectures on "Theories of Baryogenesis", *CERN* **1998**.
6. David E. Morrissey, "Electroweak baryogenesis", *TRIUMF* **2012**.
7. R.N. Mohapatra, "Seesaw Mechanism and it's applications.", *University of Maryland* **2004**.
8. E. Kh. Akhmedov, "Seesaw Mechanism and neutrino mass matrix.", *CFIF-IST* **1999**.
9. Kaori Fuyuto, "Electroweak Baryogenesis and Its Phenomenology"(Thesis), section 2.1.1, *Springer Nature Singapore* **2018**.
10. "The Long-Baseline Neutrino Experiment: Exploring Fundamental Symmetries of the Universe", *Fermilab* **2014**.
11. X. Qian, "Neutrino Mass Hierarchy", *Brookhaven National Laboratory* **2015**.
12. Vitaly A. Kudryavtsev, "Underground physics with DUNE", *University of Sheffield* **2016**.

Figures References

F.1. Modified image, taken from http://www.astronomycafe.net/FAQs/q1050x.html
F.2. Frames from a simulation video, made by Mark Hindmarsh. link: http://www.sussex.ac.uk/profiles/7423/research
F.3. Image taken from reference [6].
F.4. Image taken from https://www.dunescience.org/
F.7. Image taken from https://www.sheffield.ac.uk/physics/research/pppa/nugroup/dune/nudune-phys
F.8. Graphics taken from reference [10].
F.9. Graphics taken from reference[10].
F.10. Graphics taken from reference[10].
F. A1. This illustration is obtained by two frames of the video *"What Caused the Big Bang?"* made by PBS Space Time.
F. A2. Image taken from reference [6].

Proceedings

Electroweak Baryogenesis

André G. C. Baptista [1]

[1] Faculdade de Ciências da Universidade de Lisboa; abaptista@oal.ul.pt

Received: date; Accepted: date; Published: date

Abstract: Unless we impose an initial asymmetry to reproduce the observations made in our Local Universe, there must have been some dynamical mechanism at work through which the number of baryons became much larger than that of anti-baryons: this mechanism is called Baryogenesis, and many theories have been conjectured so as to explain the intricacies of this phenomena. In this work, an introduction to the basic concepts needed to formulate these theories will be followed by a more in-depth look at the Electroweak Baryogenesis hypothesis, and why it fails to deliver a working explanation for the unanswered origin of baryon asymmetry.

Keywords: Baryogenesis; Sakharov; Baryons; Anti-Baryons; Asymmetry; Electroweak; Transition; Instantons; Sphalerons;

1. Introduction

Hot Big Bang cosmology is a widely accepted model for the evolution of the Universe, since it is able to reproduce the Hubble expansion of the Universe, the Cosmic Microwave Background and the abundances of both hydrogen and helium observed in the Universe. Still, it fails when trying to explain why matter predominates heavily over anti-matter, since the laws of physics should not distinguish between the two and both should have been produced in an equal manner. This so called *baryon asymmetry* can be quantified by a dimensionless baryon number $\boldsymbol{B}$, which will correspond to the ratio of the baryon number density to the entropy density: [1]

$$B \equiv \frac{n_B}{s} \approx \frac{1}{7}\eta \approx (6-10) \times 10^{-11} \tag{1}$$

where ($n_B \equiv n_b - n_{\bar{b}}$), s is the entropy density and η is the baryon-to-photon ratio and is estimated to be in the range of $(4-7) \times 10^{-10}$. For an isentropic (no significant entropy production) expansion of the Universe, and provided that the baryon number is conserved, this ratio will remain constant. Even though the baryon number value is very small, n_B must not differ from zero, otherwise matter-antimatter annihilations would have devoid the Universe of both. [1]

Another thing to keep in mind is that, even though the baryon asymmetry is large, with ($n_b >> n_{\bar{b}}$), since B is small then at some point in the early stages of the Universe the asymmetry was much smaller than when compared to the present day. This can be explained if we take a step back to the point in time when the temperature of the Universe was greater than the mass of a nucleon. In such conditions, nucleons and anti-nucleons would have been as abundant as photons: [1]

$$n_N \approx n_{\overline{N}} \approx n\gamma \tag{2}$$

During this earlier epoch, the Universe could almost be said to be in baryonic symmetry. For very high temperatures in the standard model, there are interactions that violate the conservation of the baryon number ($t \leq 10^{-34} sec$ Harvey and Turner 2). In a scenario of thermal equilibrium, where the rate of reactions restoring the balance in the Universe is able to keep up with its rapid expansion, the number of baryons minus the number of anti-baryons must vanish - the production of a particle must equal that of its anti-particle. Still, observations in our local Universe indicate a strong asymmetry between baryons and anti-baryons. Models that try to explain these observations by making up a Universe with equal number of baryons and anti-baryons but distributed in an inhomogeneous way are very constrained, and would require regions of contact between matter-dominated and anti-matter-dominated domains which would result in strong emissions of X and Gamma-rays, which have not yet been detected. [3]

Believing that there is an initial asymmetry, there must have been some dynamical mechanism at work through which the number of baryons became much larger than that of anti-baryons: this mechanism is called Baryogenesis.

Some theories are able to achieve this genesis at low energies, and in these cases we expect them to be testable in accelerators, while in other theories the baryon number is produced at high energies and then protected from thermalization by the $B - L$ symmetry. [3]

1.1. Sakharov Conditions

The Dirac equation tells us each particle will have an anti-particle counterpart. The *CPT* Theorem then ensures us that each particle-anti-particle pair will have the same mass and the same lifetime but opposite charge. It is very peculiar then that observational studies yield a large disproportion between matter and anti-matter, with anti-matter reservoirs and/or points of concentration being apparently missing in the observable Universe. [4]

When trying to justify this phenomena, one comes across two simple ideas that might give the answer: [4]

1) Either the Universe, in its beginning, had a preference for matter, meaning it started with a baryon number other than zero;

2) No such predisposition occurred, but rather mechanisms which favoured an imbalance towards matter had an accumulative effect over time.

Andrei Sakharov, in 1967, defined the conditions under which it is possible to produce an asymmetry between baryons and anti-baryons in the Universe. This followed the discovery of the Cosmic Background Radiation discovery and of the $\hat{C}\hat{P}$-violation (the product of charge conjugation and parity) in the neutral kaon K system:

- Violation of the baryon number: This is necessary if we consider the initial condition that the Universe began containing as many baryons as anti-baryons, or whether it started containing none of each. Baryon number violation must occur in the fundamental laws. If baryon number violating interactions were in equilibrium, since the Universe would have begun with a zero baryon number it would ought stay that way and not be able to generate the non-zero asymmetry we observe today; [5]
- C-symmetry violation and $\hat{C}\hat{P}$-symmetry violation: C-symmetry violation would ensure that reactions with a preference for producing baryons would not be counter-balanced by reactions with a preference for producing anti-baryons. If $\hat{C}\hat{P}$ is conserved, every reaction producing a particle would be balanced by a reaction producing its respective anti-particle at the same rate, and so the initial baryon number, which is assumed to be zero, would be conserved; [3] [5]
- Out-of-equilibrium state: For most of the time, the Universe has been in thermal equilibrium. The Cosmic Background Radiation is the closest-to-theory blackbody spectrum observed in nature, and shows us that the Universe was in thermal equilibrium 10^5 years after the Big Bang. The widely accepted theory of Big Bang Nucleosynthesis also provides us with evidence that the Universe was in equilibrium around two-three minutes after the Big Bang. But if that was the case, then even both B and $\hat{C}\hat{P}$-symmetry violating interactions would not produce a net asymmetry, since $\hat{C}\hat{P}\hat{T}$-symmetry would ensure that the production of an arbitrary type of particle via one mechanism is not immediately compensated by the disappearance of this particle through the inverse reaction, which would occur with the same frequency in this equilibrium; [3] [5]

When these conditions are met, it is possible to produce a non-vanishing global baryon number.

We have not yet observed particle interactions which do not conserve the baryon number, meaning all reactions will have an equal baryon number before and after. We can write this mathematically using the commutator of the baryon number quantum operator with respect to the perturbative Standard Model hamiltonian: [4]

$$[\hat{\mathbf{B}}, \hat{\mathbf{H}}] = \hat{\mathbf{B}}\,\hat{\mathbf{H}} - \hat{\mathbf{H}}\,\hat{\mathbf{B}} = 0 \tag{3}$$

The violation of the $\hat{C}\hat{P}$-symmetry was discovered in 1964 and, with regards to the last condition, it can be rewritten as the rate of reaction which creates baryon-asymmetry must be lesser than the rate of expansion of the Universe. For this scenario, particle-anti-particle pairs would not be able to achieve thermal equilibrium since the rapid expansion of space would reduce the rate for pair-annihilation interactions.

1.2. Out-of-Equilibrium Decay

A model which takes all of Sakharov's conditions into consideration and can be seen as a standard scenario for theory-crafting is the *out-of-equilibrium decay scenario*.

If we hypothesize a super heavy ($\geq 10^{14}$ GeV) **X**-boson which interactions violate B conservation, with a coupling strength to fermions of $\alpha^{1/2}$ and mass M, dimensionally, its decay rate $\Gamma_D = \tau^{-1}$ will be: [1]

$$\Gamma_D \approx \alpha M \tag{4}$$

Assuming baryonic symmetry for the Universe at Planck time (10^{-43} s), with all fundamental particle species (fermions, gauge and Higgs bosons) present with equilibrium distributions and a temperature $T \sim 3 \times 10^{18}$ GeV $>> M$, then both X, $\overline{X}$ bosons are relativistic and statistically as abundant as photons: [1]

$$n_X = n_{\overline{X}} \approx n_\gamma \tag{5}$$

For $T < M$, the equilibrium abundance of these bosons with respect to photons will be: [1]

$$X_{EQ} \approx (\frac{M}{T})^{\frac{3}{2}} exp(-\frac{M}{T}) \tag{6}$$

where $X_{EQ} \equiv n_X / n_\gamma$ is the number of X-bosons per co-moving volume.

As T decreases, the reactions preserving the equilibrium for the number of X,$\overline{X}$ bosons must have a much higher rate than the expansion of the Universe: $H = \dot{T}/T$. If at $T = M$ we have $\Gamma_D >> H$ then these bosons are able to adjust their abundance numbers so as to preserve their equilibrium value, and no asymmetry is derived from this. But, if $\Gamma_D < H$ at $T = M$, then the bosons will not decay on the expansion timescale ($\tau > t$) and will remain as abundant as photons for $T \leq M$. This overabundance is the key factor that will reproduce an out-of-equilibrium state. Only much later ($T << M$) do these bosons start decaying with no suppressing inverse decay process (see Figs. 1 and 2). [1]

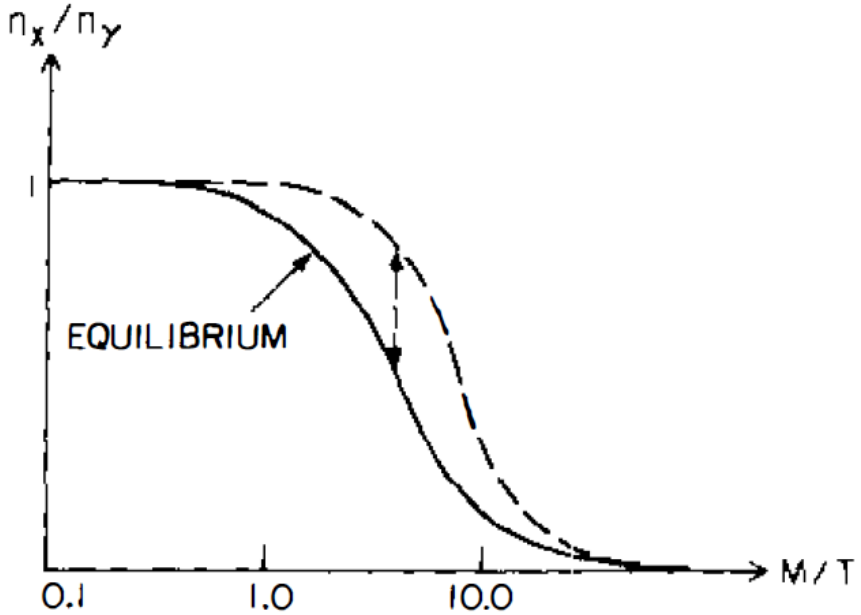

Figure 1. The evolution of the abundance ratio for X-bosons to photons over time (with $z \equiv M/T$). The spaced line represents an out-of-equilibrium abundance, and the arrow denotes the depart from equilibrium. Credit: Kolb and Turner [1].

For a decay of X,$\overline{X}$ bosons into two channels with baryon numbers B_1 and B_2 and branching ratios r and $(1-r)$ (with $\overline{X}$ baryon number values symmetrical to X), the mean net baryon number of the decay products will be: [1]

$$B_X = rB_1 + (1-r)B_2 \tag{7}$$

and, for $\overline{X}$: [1]

$$B_{\overline{X}} = -\bar{r}B_1 - (1-\bar{r})B_2 \tag{8}$$

with the decay of an X,$\overline{X}$ pair producing an average baryon number ϵ: [1]

$$\epsilon \equiv B_X + B_{\overline{X}} = (r-\bar{r})(B_1 - B_2) \tag{9}$$

where, if $B_1 = B_2$, the baryon number would not be violated by these bosons. C-symmetry and $\hat{C}\hat{P}$-symmetry would also be conserved for $r = \bar{r}$, with $\epsilon = 0$ for this occasion as well.

At the time when X-bosons start decaying their abundance is still approximate to that of photons. With this in mind, the net baryon number density produced will be: [1]

$$n_B \approx \epsilon n_\gamma \tag{10}$$

The entropy density is $s \approx g_* n_\gamma$, and so the baryon asymmetry will be: [1]

$$\frac{n_B}{s} \approx \frac{\epsilon}{g_*} \approx 10^{-2}\epsilon \tag{11}$$

If X is a gauge boson, then $\alpha \approx 1/45$ and so $M \geq 10^{16}$ GeV. [1]

If it is a Higgs boson, then α is arbitrary. [1]

If it is in the same representation as the light Higgs boson, then $\alpha \approx (m_f/M_W)^2 \alpha_{gauge} \approx 10^{-3} - 10^{-6}$, with m_f being the fermion mass and $M_W \approx 80$ GeV the mass of the W-boson. [1]

The Higgs boson seems to satisfy this mass condition more than a gauge boson would. For $M > g_*^{-1/2} \alpha m_{pl}$, only a modest C-symmetry, $\hat{C}\hat{P}$-symmetry violation is needed: $\epsilon \approx 10^{-8}$.

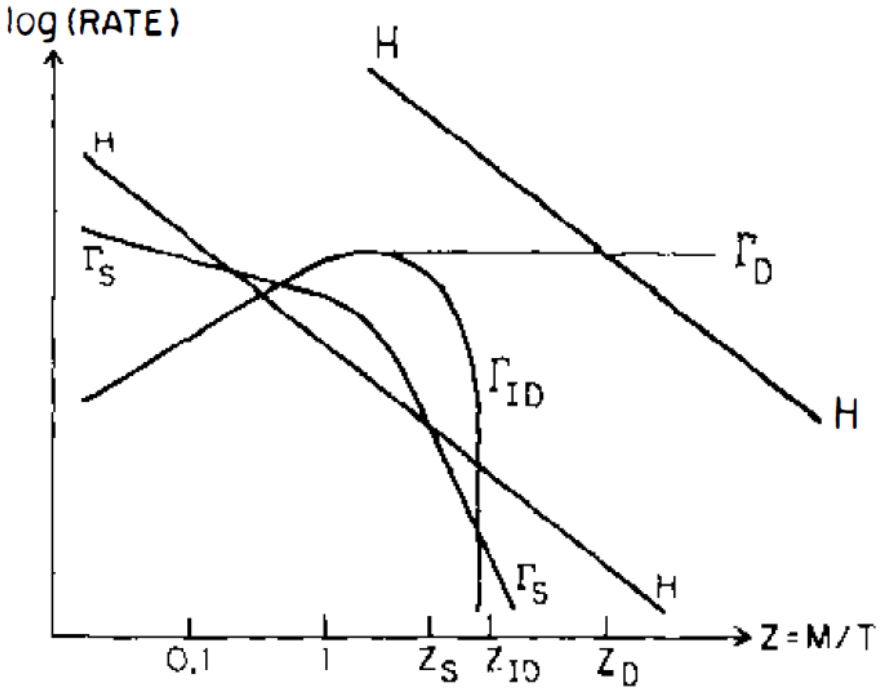

Figure 2. A logarithmic representation of the decay rates as a function of $z \equiv M/T$. H is the expansion rate of the Universe, Γ_D and Γ_{ID} are the decay and inverse decay rate, respectively, and Γ_2 the 2 <-> 2 scattering rate. The upper H line represents the case for $K << 1$, where $K \equiv (\Gamma_D/H)_{T=M}$. At $z \approx 1$ all reactions are below the expansion rate ($\Gamma < H$), and the X-bosons will only decay at $\Gamma_D = H$ ($z \approx z_D$). The lower line corresponds to $K_c > K > 1$. Here, at $z \approx 1$, all reaction rates keep up with H, with inverse decays and 2 <-> 2 scattering freezing out ($\Gamma = H$) at $z \approx z_{ID}$ and z_s, respectively. Credit: Kolb and Turner [1].

1.3. Models for Baryogenesis

The Standard Model is able to explain why the baryon and lepton numbers are conserved to a very good approximation. To understand this, let us consider the modern understanding of Maxwell's equations.

A quantum field theory is characterized by its field content and a Lagrangian density. In the Lagrangian, one distinguishes renormalizable and non-renormalizable terms. Renormalizable terms have coefficients with mass dimension greater than zero; non-renormalizable terms have coefficients (couplings) with mass dimension less than zero. For example, in quantum electrodynamics, the electron mass has dimension one, while the charge of the electron is dimensionless (throughout we use conventions where $\hbar$ and c are dimensionless). [5]

Requiring Lorentz-invariance, gauge-invariance and renormalizability leaves only one possible solution for the Lagrangian of electrodynamics: the Maxwell Lagrangian, whose variation yields Maxwell's equations. Using these symmetry principles, we can write down an infinite number of possible non-renormalizable terms, which would yield non-linear modifications of Maxwell's equation. [5]

With this in mind, at the level of renormalizable terms, there simply are no interactions one can write which violate either baryon number or the conservation of the separate lepton numbers (electron, μ and τ number). It is possible to add dimension-five operators (suppressed by some scale $1/M$) which violate lepton number, and dimension-six operators (suppressed by $1/M^2$), which violate the baryon number (Fig. 3). The discovery of the neutrino mass probably amounts to a measurement of some of these lepton-number-violating operators. The scale of the new physics associated with these operators is theoretically estimated to be between about 10^{11} and 10^{16} GeV. [5]

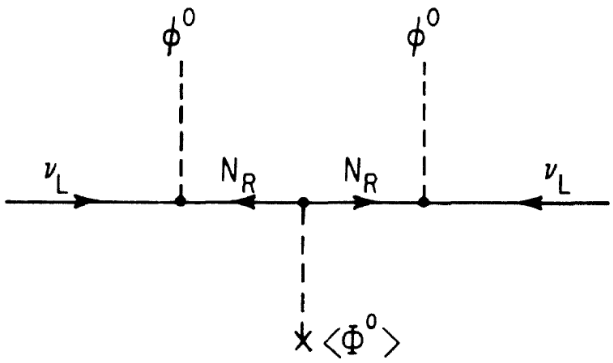

Figure 3. Feynman diagram leading to the dimension-five operator which violates the lepton number. N_R corresponds to the super heavy right-handed neutrino, v_L to the light left-handed neutrino, ϕ^0 is the neutral electroweak Higgs boson and Φ^0 is a super heavy Higgs boson. Credit: Harvey and Turner [2]

What is the scale M_B associated with baryon number violation, then? Quantum effects in gravity are expected to violate all global quantum numbers (e.g. black holes swallow up any quantum numbers not connected with long range fields like the photon and graviton), so $M_B \leq M_P$, where M_P, the Planck mass, is about 10^{19} GeV. [5]

The Universe is thought to have underwent a period of inflation early in its history. During this period, the Universe expanded rapidly by an enormous factor. Inflation should have taken place below the scale of quantum gravity, and thus any baryon number produced in the Planck era was diluted to a totally negligible level. We still do not have an answer for the asymmetry we find in our Local Universe, but several mechanisms have been proposed to try and understand what might have happened: [5]

- Planck Scale Baryogenesis: The idea that Planck scale phenomena is responsible for the asymmetry. We already have advanced cosmological arguments that this is unlikely;
- Baryogenesis in Grand Unified Theories (GUT Baryogenesis): One of the first well-envisioned scenarios proposed to explain the asymmetry. Grand Unified Theories unify the gauge interactions of the strong, weak and electromagnetic interactions in a single gauge group. They violate baryon number and have heavy particles, with masses of the order of MGUT $\approx 10^{16}$ GeV, whose decays can provide a departure from equilibrium. The main flaw of this theory is that the temperature of the Universe just after reheating is well below MGUT. But, even if it were very large, this unification requires supersymmetry - a hypothetical symmetry between fermions

and bosons. This would require the existence of a spin-3/2 partner for the graviton, called the *gravitino*. In most models for supersymmetry breaking, these particles have masses of the order of TeV and are very long lived, and even though they are weakly interacting still too many gravitinos are produced unless the reheating temperature is well below the unification scale [6];

- Electroweak Baryogenesis: This is the subject reviewed in this work. The Standard Model satisfies all of the conditions for baryogenesis. This is quite peculiar, since at low temperatures the model seems to preserve baryon number, but it turns out that baryon and lepton number are badly violated at very high temperatures. The departure from thermal equilibrium can arise at the electroweak phase transition. This transition can be of first order, providing an arrow of time and allowing for the $\hat{C}\hat{P}\hat{T}$-symmetry violation. It turns out, however, that any baryon asymmetry produced by this model is far too small to account for the observations. In certain extensions of the Standard Model, it is possible to obtain an adequate asymmetry but, in most cases, the allowed region of parameter space is very small (for example, the Minimal Supersymmetric Standard Model (MSSM));
- Leptogenesis: The observation that the weak interactions will convert some lepton number to baryon number means that, if one produces a large lepton number at some stage, this will be processed into a net baryon and lepton number. The observation of neutrino masses may be the key to corroborate this theory. Many, but not all, of the relevant parameters can be directly measured;
- Production by coherent motion of scalar fields (the Affleck-Dine mechanism): This mechanism, which can be highly efficient, might be the answer if we find that nature is supersymmetric. This idea proposes that the ordinary quarks and leptons are accompanied by scalar quarks and leptons. We may be able to ascertain the status of supersymmetry in the Universe in the next generation of high energy accelerators. So, it is possible we will uncover the basic underlying physics and measure some (but not all) of the relevant parameters;

The main focus of this work will be the Electroweak Baryogenesis hypothesis, and how it fails to explain the asymmetry in baryons we see in the Local Universe.

2. Electroweak Baryogenesis

2.1. Electroweak Anomalies

Earlier, we stated that the renormalizable interactions of the Standard Model preserve baryon number. This statement is valid classically, but fails to stay true in quantum theory.

At the classical and perturbative levels, the baryon and lepton numbers are conserved separately by the electromagnetic and weak interactions but, at the quantum level, the theory considers what are called *anomalies*, making it so that both baryonic and leptonic currents are not conserved. These effects are expected to be tiny because they are thought to be caused by quantum mechanical tunneling, and are suppressed by a barrier penetration factor. At high temperatures, there is no such suppression, so baryon number violation is a rapid process which can come to thermal equilibrium. These effects are of the order: [5]

$$e^{-(2\pi/\alpha_W)} \approx 10^{-65} \tag{12}$$

where α_W corresponds to the W-boson coupling strength to fermions.At these magnitudes, it is possible to violate the symmetries predicted by the Standard Model. These effects originate from the fact that the baryon number and lepton number are *anomalous*. This is expressed by the following relation, and it shows that the baryon number current j^μ_B is not conserved: [3]

$$\partial_\mu j^\mu_B = \partial_\mu j^\mu_L = \frac{N_F}{8\pi^2} Tr B_{\mu\nu}\tilde{B}_{\mu\nu} \tag{13}$$

with a number $N_F = 3$ of families and with $B_{\mu\nu}$ corresponding to the SU(2) field strengths: [3]

$$\begin{aligned} B_{\mu\nu} &\equiv \frac{1}{2}\sum iB_{i\mu\nu}\sigma^i \\ \tilde{B}^{\mu\nu} &\equiv \frac{1}{2}\epsilon^{\mu\nu\alpha\beta}B_{\alpha\beta} \end{aligned} \tag{14}$$

which generalizes to the case of a group with arbitrary T^i generators by performing the substitution $\frac{1}{2}\sigma^i \to T^i$. It should be highlighted that the B - L current is conserved, since $j^\mu_B - j^\mu_L$ is anomaly-free and is an exact conserved quantity in the Standard Model (as well as SU(5) and SO(10) Grand Unified Theories). [5]

2.2. Chern-Simons Number

A violation of the current conservation does not lead to violations of the symmetry.

The expression on the right-hand side of eq.(13) can be simplified if we notice the identity: [3]

$$TrB_{\mu\nu}\tilde{B}^{\mu\nu} = \partial_\mu\{\epsilon^{\mu\nu\alpha\beta}Tr[(B_{\nu\alpha} + \frac{2}{3}B_\nu B_\alpha)B_\beta]\} \tag{15}$$

where $B_\mu = \frac{1}{2}B_{i\mu}\sigma^i$. This shows that eq.(13) is a total divergence and, in view of this: [5]

$$\tilde{j} = j^\mu_B - \frac{3g^2}{8\pi^2}K^\mu \tag{16}$$

is conserved. In perturbation theory (i.e. in Feynman diagrams), K^μ falls to zero rapidly (typically with a rate of $1/r^6$) at infinity, and so its integral is zero. This insures that the baryon number is conserved and marks the end for abelian gauge theories, but for non-abelian theories there are non-perturbative field configurations which contribute to the right-hand side. These lead to violations of the baryon number and the separate lepton numbers proportional to $(e^{-2\pi/\alpha})$ [5]. These configurations are called *instantons*, which will be discussed in Section 2.3. But, before we can understand that, we must first define the Chern-Simons number parameter.

Denoting by $B = (\int d^3\mathbf{x}\ j^0_B)$ the baryon number associated with the current j^μ_B and using the fact that all configurations of physical interest vanish sufficiently fast at infinity, we find that between the times t_1 and t_2, the variation of the baryon number ΔB is given by: [3]

$$\Delta B = N_F\Delta N_{CS} = N_F[N_{CS}(t_2) - N_{CS}(t_1)] \tag{17}$$

with the Chern-Simons numbers being defined as: [3]

$$N_{CS} = \frac{1}{4\pi^2}\int d^3\mathbf{x}\epsilon^{ijk}Tr[B_i(\partial_j B_k + \frac{4}{3}B_j B_k)] \tag{18}$$

end up being **Integer** numbers as long as the field configuration is pure gauge (i.e. we can write $\boldsymbol{B} = -i\ \mathrm{U}^{-1}\ \nabla\ \mathrm{U}$ where U is a gauge transformation [3]).

2.3. The Instanton and the Sphaleron

Two pure gauge field configurations are indistinguishable at the perturbative level. They both can be used as a vacuum state since they do not have the same Chern-Simons number. [3]

The Euclidean solution is called the *instanton*, which interpolates between these two configurations. If the structure of an *instanton* is known, the probability to tunnel from one vacuum state to another can be computed, and this will go hand-in-hand with the probability of producing a baryon number.

We have, at weak-coupling, an infinite set of states, labeled by integers, separated by barriers from one to another. In the tunneling processes which change the Chern-Simons number due to the anomaly, the baryon and lepton numbers will change. The exponential suppression found in the *instanton* calculation is typical of tunneling processes, and the expected magnitude of this effect is negligible in non-cosmological situations. [3]

We can then assume that the configuration space has an infinity of minima, one for each value of $\mathrm{N}_{CS} \in \mathbb{Z}$ corresponding to the pure gauge vacuum configurations related with the *instantons* (Fig. 4). The height of the potential barrier separating these states can be determined by studying the time-independent configuration which corresponds to the energy maximum. This will be a solution of the static equations of motion with finite energy and it is known as

a "*sphaleron*" [7]. This solution was found by Klinkhamer and Manton, it is necessarily unstable and has an energy of the order of: [3]

$$E_{sphaleron} \propto M_W / g_2^2 \tag{19}$$

where M_W is the W-boson vector mass and g_2 is a gauge transformation of index 2.

The rate for thermal fluctuations to cross the barrier per unit time per unit volume should be of the order of the Boltzmann factor (for this configuration) times a suitable prefactor [8] [9] [10]. It was found that, through the *sphaleron* mode, the transition width per unit volume for a unit Chern-Simons variation [transition of ΔB = 3 in the standard model] is of the order: [3]

$$\frac{\Gamma_{\text{sphaleron}}}{V} \simeq T^4 exp(\frac{E_{\text{sphaleron}}}{T}) \tag{20}$$

when the Universe is at a temperature T, and with $E_{sphaleron}$ being the temperature dependent *sphaleron* mass. The rate becomes large as the temperature approaches the W-boson mass and, when reaching the electroweak transition, the mass of the intermediate boson decreases so that this last result can no longer apply.

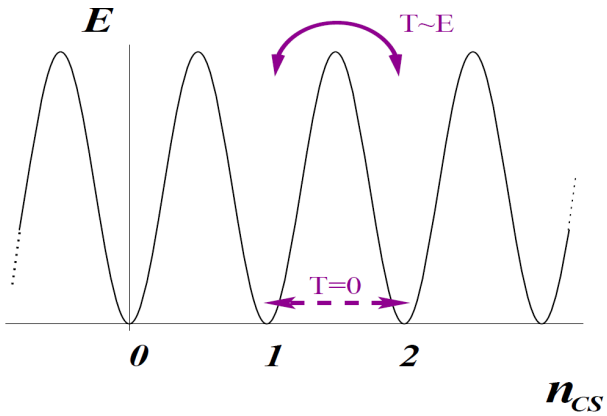

Figure 4. A representation for a Yang-Mills vacuum structure. The *instanton* transitions between vacua with different Chern-Simons numbers are extinguished at zero temperature while, at finite temperature, these are allowed via *sphalerons*. Credit: Dine and Kusenko [5].

2.4. Electroweak Baryogenesis

As we know, the $\hat{C}\hat{P}$ symmetry is not respected by the electroweak interactions due to the non-trivial phase δ_{CKM} of the CKM matrix. The estimation made for this value is: [3]

$$\delta_{CKM} \leq 10^{-25} \tag{21}$$

and, since this value is a pre-factor for the estimate for baryon production based on the *sphaleron*, because $\Delta B = N_F \Delta N_{CS}$ is already weak, this number will be further reduced by the phase factor δ_{CKM}.

Returning to our original expression for the anomaly (eq. 13), we see that, while the separate baryon and lepton numbers are violated in these processes, the combination $B - L$ is conserved. This result leads to three observations: [5]

- If, in the beginning of the Universe, the baryon and lepton numbers are created but the net $B - L = 0$, B and L will subsequently be lost through *sphaleron* processes;
- For the case when a net $B - L$ (e.g. creates a lepton number) is created, the *sphaleron* process will leave both baryon and lepton numbers comparable to the original $B - L$;
- As it was already mentioned, the Standard Model satisfies, by itself, all of the conditions for baryogenesis;

The standard model of the electroweak interactions has, in itself, a mechanism capable of producing a baryon number dynamically while conserving the combination $B - L$, implying that the *sphaleron* can act in the opposite way: if an arbitrary $B - L$ conserving phenomenon produces a baryon number prior to the electroweak transition then, due to the *sphaleron*, this transition will automatically wash out such a primordial contribution.

It has been discussed that the Standard Model satisfies the first and second Sakharov conditions, but the departure from equilibrium is harder to reproduce. I alluded to the fact that in the electroweak theory there is a phase transition to a phase with massless gauge bosons. For a sufficiently light Higgs, this transition is of first order. At zero temperature, in the simplest version of the Standard Model with a single Higgs field, Φ, the Higgs potential is given by: [5] [11]

$$V(\Phi) = -\mu^2|\Phi|^2 + \frac{\lambda}{2}|\Phi|^4 \tag{22}$$

where $M_H^2 = 2\lambda v^2 = -2\mu^2$ is the Higgs-boson mass. The potential has a minimum at $\Phi = \frac{1}{\sqrt{2}}v_0$, breaking the gauge symmetry and giving mass to the gauge bosons by the Higgs mechanism. For the case of a finite temperature T, the potential is given by: [5]

$$V(\Phi, T) = D(T^2 - T_0^2)\Phi^2 - ET\Phi^3 + \frac{\lambda}{4}\Phi^4 + ... \tag{23}$$

with: [5]

$$\begin{aligned} T_0^2 &= \frac{1}{4D}(m_H^2 - 8Bv_0^2) \\ B &= \frac{3}{64\pi^2 v_0^2}(2M_W^2 + M_Z^4 - 4m_t^4) \\ D &= \frac{1}{8v_0^2}(2M_W^2 + m_Z^2 + 2m_t^2) \\ E &= \frac{1}{4\pi v_0^3}(2M_W^3 + m_Z^3) \sim 10^{-2} \end{aligned} \tag{24}$$

E turns out to be a rather small, dimensionless number of order 10^{-2} . If we ignore the Φ^3 term, we have a second order transition, at temperature T_0, between a phase with $\Phi \neq 0$ and a phase with $\Phi = 0$. Because the W and Z masses are proportional to Φ, this is a transition between a state with massive and massless gauge bosons. [3] [5] [11]

The electroweak transition in itself then also poses an obstacle since it should be out of equilibrium in order to produce a baryon which compensates the $\hat{C}\hat{P}$-symmetry violation. Because of the Φ^3 term in the potential, the phase transition is potentially at least weakly first order, producing only a small coefficient of the order of 10^{-2}. This is indicated in Figs. 5 and 6.

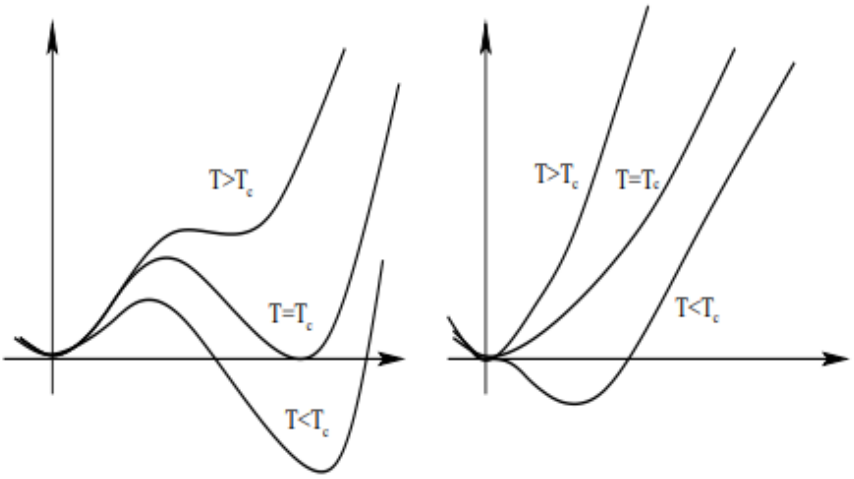

Figure 5. First and second order phase transitions. Credit: Dine and Kusenko [5].

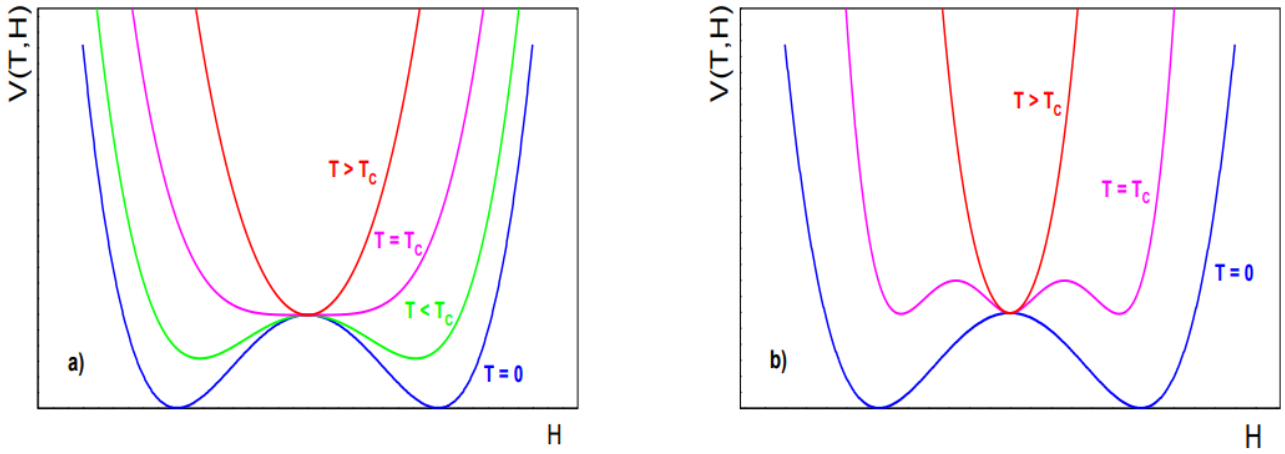

Figure 6. Higgs potential for several temperatures compared with the critical temperature T_c for: a) second order phase transition; b) first order phase transition. Credit: Melo [11]

The appearance of a second, distinct minimum at a critical temperature is visible. A first order transition is not, in general, an adiabatic process. As we lower the temperature to the transition temperature, the transition proceeds by the formation of bubbles. Keeping in mind that the transition is weakly first order, and hence happens by nucleation, the bubbles of true vacuum will be expanding in the space otherwise still in the false vacuum. Inside the bubble, the system is in the true equilibrium state (the state which minimizes the free energy), while outside it tends to the original state. The Higgs fields will vary rapidly on the surface of these bubbles, reproducing the conditions needed for baryogenesis. These bubbles form through thermal fluctuations at different points in the system and grow until they collide, completing the phase transition. It has been shown that various non-equilibrium processes near the wall can produce baryon and lepton numbers [12] [13]. It would then be necessary that the production process stops rapidly in the true vacuum after the bubble passage, so as to free the number of baryons produced. If these processes were to happen in the true vacuum, which is in thermodynamical equilibrium, the anti-baryons would be rapidly produced inside this space in order to compensate the asymmetry created. [3] [5]

In order for the B - L to be weak, the intermediate bosons should have significant masses and the expectation value of the Higgs field should grow very rapidly, so as to make the energy of the *sphaleron* very large when compared to the temperature right after the bubble surface. This would depend on the coefficients obtained in the effective potential and on the Higgs mass at zero temperature. Given the constraints on the latter ($M_H \geq 115$ GeV), the *sphaleron* transition, which is the mechanism that produces the required baryon number across the bubble surface, reduces it drastically in the subsequent true vacuum phase. The electroweak theory is therefore not sufficient for baryogenesis, and the standard model must be extended. [3]

References

1. Kolb, E.W.; Turner, M.S. Grand unified theories and the origin of the baryon asymmetry. *Annual Review of Nuclear and Particle Science* **1983**, *33*, 645–696. doi:10.1146/annurev.ns.33.120183.003241.
2. Harvey, J.A.; Turner, M.S. Cosmological baryon and lepton number in the presence of electroweak fermion-number violation. Technical report, 1990.
3. Peter, P.; Uzan, J.P. *Primordial Cosmology*; Oxford Graduate Texts, Oxford University Press, 2013.
4. Sakharov, A.D. Violation of CP Invariance, C asymmetry, and baryon asymmetry of the universe. *Pisma Zh. Eksp. Teor. Fiz.* **1967**, *5*, 32–35. [JETP Lett.5,24(1967); Sov. Phys. Usp.34,no.5,392(1991); Usp. Fiz. Nauk161,no.5,61(1991)], doi:10.1070/PU1991v034n05ABEH002497.
5. Dine, M.; Kusenko, A. Origin of the matter-antimatter asymmetry. *Reviews of Modern Physics* **2003**, *76*, 1–30, [arXiv:astro-ph/hep-ph/0303065]. doi:10.1103/RevModPhys.76.1.
6. Kallosh, R.; Kofman, L.; Linde, A.; van Proeyen, A. Gravitino production after inflation. **2000**, *61*, 103503, [arXiv:hep-th/hep-th/9907124]. doi:10.1103/PhysRevD.61.103503.
7. Manton, N.S. Topology in the Weinberg-Salam theory. *Phys. Rev. D* **1983**, *28*, 2019–2026. doi:10.1103/PhysRevD.28.2019.

8. Arnold, P.; McLerran, L. The sphaleron strikes back: A response to objections to the sphaleron approximation. **1988**, *37*, 1020–1029. doi:10.1103/PhysRevD.37.1020.
9. Dine, M.; Lechtenfeld, O.; Sakita, B.; Fischler, W.; Polchinski, J. Baryon number violation at high temperature in the standard model. *Nuclear Physics B* **1990**, *342*, 381–408. doi:10.1016/0550-3213(90)90195-J.
10. Kuzmin, V.A.; Rubakov, V.A.; Shaposhnikov, M.E. On anomalous electroweak baryon-number non-conservation in the early universe. *Physics Letters B* **1985**, *155*, 36–42. doi:10.1016/0370-2693(85)91028-7.
11. Melo, I. Higgs potential and fundamental physics, 2019, [arXiv:physics.gen-ph/1911.08893].
12. Cohen, A.G.; Kaplan, D.B.; Nelson, A.E. Progress in Electroweak Baryogenesis, 1993, [arXiv:hep-ph/hep-ph/9302210].
13. Rubakov, V.A.; Shaposhnikov, M.E. Electroweak Baryon Number Non-Conservation in the Early Universe and in High Energy Collisions, 1996, [arXiv:hep-ph/hep-ph/9603208].

Proceedings

DARK MATTER - OBSERVATIONAL OVERVIEW AND POSSIBLE CANDIDATES

Afonso do Vale [1]

[1] Faculdade de Ciências; fc47932@alunos.fc.ul.pt

Abstract: It has become clear, from different arguments made on a wide range of observational data, that the luminous matter we can detect in the observable universe cannot account for large scale gravitational effects. This suggest that there needs some sort of non luminous matter that accounts for a majority of the matter in the universe. **dark matter** First hypothesis suggested some sort of non luminous baryonic matter, such as brown dwarf clusters or a bigger density of very compact objects (black holes and neutron stars) - MACHOs. I has been found that this non luminous baryonic matter composes around 20% of dark matter. Other studies find that barionic matter should account for 5% of the current universe, thus further discrediting MACHOs. Dark matter should then have a non baryonic origin which can be explained by neutrinos, for **hot dark matter**, or axions/WIMPS, for **cold dark matter**. In this proceedings essay we shall review observational evidence regarding the subjects of dark matter - exposing their reliability and scientific consensus, characterize the different types of possible dark matter candidates and finally have some in depth discussion regarding state of the art theories.

1. Introduction

Science has relied on photometric analysis of light sources in order to estimate the masses of said sources since the earliest detections. Mass-Luminosity relations permitted researchers to calculate the needed mass for the source to have a certain luminosity profile. This relation, first though of by Jakob Karl Ernst Halm, would state that luminosity would follow a power law proportion with the mass that, in theory, was needed to produce said luminosity[1]. This can be expressed as follows:

$$\left(\frac{L}{L_\odot}\right) = \left(\frac{M}{M_\odot}\right)^a \tag{1}$$

Where the power a is between $1 < a < 6$, with 3.5 being a value widely used for main sequence and 1 being the end value as the star reaches the Eddington Limit - radiation pressure due to high luminosity higher than the gravitational force that keeps gas layers bound.

Using this concept we were able to model precise relations for many different types astronomical sources, from stars to galaxies and clusters. Mass determination through the luminosity-mass relations thus became a standard in how we measured mass of distant sources. In the early parts of the 20th century people starting developing another techniques to measure mass as astrophysical knowledge grew and large variations from theory started being hinted at by several studies .

The study of galaxies and cluster, in other words the largest scale of cosmological configurations thought possible at the time, was key into this scientific pursuit. First, Oort was measuring the velocity of stars in the plane of the milky way through the Doppler shift in their spectra and found out that their velocities hinted at a central mass of the galaxy roughly 7 times higher than photometric results previewed [2]. Oort acknowledges this, writing a section titled *On dark matter*. He explained that the data presented evidence on the obscuration of the milky way; in fact, so much that 85% of our galaxy had to be obscured in order for the photometric results to match the gravitationally derived ones. Around the same time[1], Zwicky found the same conclusion for the Coma cluster[3]! The Coma cluster (A1656) is one of two main clusters of galaxies belonging to the Coma supercluster; it is also very rich in different galaxy types and doesn't lie on the galactic plane, thus is less obscured by gas and contaminated with galactic stars. Zwicky

[1] First work from 1933. Cited source is a re-print

was analyzing the spectra from 800 galaxies in the Coma cluster; using Doppler shift analysis he was able to get the velocity dispersions of these galaxies and thus their kinetic energies. He then applied the Virial theorem to this system:

Theorem 1. *For a relaxed system em LTE*

$$\langle U \rangle = -2\langle K \rangle \tag{2}$$

Assuming that the clusters only interacted through gravitation he employed Newtonian gravity , using mass derived from Luminosity/Mass relations, in order to obtain the clusters average kinetic energy. Comparing the observed velocities dispersion, which were on the order of thousands (1500-2000) of kilometers per second, to the derived average velocity using luminous mass, which is around $80 kms^{-1}$, Zwicky concluded that non-luminous (cold) matter, or **dark matter**, definitely accounted for the majority of the mass of the Coma cluster. As Oort, Zwicky also pointed to a definitely cold baryonic origin for dark matter. Both researchers couldn't,at the time, have the required particle physics knowledge to reach more complex conclusions.

Indeed the dark matter - in this case we refer to the classical non-luminous barionic matter definition - which these two researchers hinted at has now been efficiently excluded from the main component of dark matter, either by lensing effects (see Section 2.1) and cosmological evidence (see Section 2.2) mainly from the Cosmic Microwave Background (CMB) and Primordial Nucleosynthesis. We will give a thorough review on why baryonic sources for dark matter can only account for a small percentage on our MACHOs -MAssive COmpact Halo Objects- section.

Following these two researchers, another substantially important work was published years later by Vera Rubin [4] which cemented dark matter as one of the most important topics of discussion of todays age. We will review her work first on the observational evidence section, followed by reviews on microlensing dark matter related studies and finally we review the cosmological importance of dark matter and how it holds up against recent observations. We conclude this essay with an analysis into different possible mechanisms to account for dark matter. First we review the possibility of non luminous baryonic matter such as brown dwarfs or cold compact objects, which would be the classic view. Afterwards we head into the possibility of non baryonic dark matter, which could first be explained by neutrinos, the only weakly interacting particle with neutral charge within the Standard Model (SM) of particle physics and thus its best candidate for dark matter. If we go out of the SM we will be looking at a new type of particle yet undiscovered. This particle should be massive and weakly interacting in order for to produce the effects we know happen at larger scales (clusters, galaxies) which drives the nomenclature of state of the art dark matter candidates as WIMPs. The most promising WIMP is the neutralino, which arises from a supersymmetrical extension to the standard model. We will talk mainly about this promising candidate particle but we will also mention exotic candidates such as the axino and Kaluza-Klein particles.

2. Observational evidence and concept review

2.1. How to observe dark matter: early rotational velocity measurements

On the introduction we reviewed the early works of Oort and Zwicky, which were working amidst the creation of modern cosmology and particle physics, as so their scientific tool was indeed limited. By 1983 the scientific paradigm had changed quite a bit, which made Vera Rubin's work on dark matter in every way more influential since it ignited a flame into dark matter research right as new tools were being developed in the already well established fields of modern cosmology and particle physics.

In the work by Vera Rubin and collaborators studied spectra from around 60 individual galaxies aiming at analyzing their rotation curves. They chose their galaxies so that their orientation enabled them to study their rotation. That is, the disk, if the galaxy were to have a disk like shape, would have to be observed somewhat edge on in order for a part of the gas to be receding from the observer and another part to be approaching. This rotation Doppler shifts the light emitted by the gas, so if we look at certain emission lines -such as the H_α line of the spin inversion of the hydrogen atom- we can measure this Doppler displacement after all other sources of reddening have been taken account of. This Doppler shift can then determine the rotation curves of galaxies; Rubin and collaborators not only did this, they mapped the rotation curves along different radii and were able to obtain the velocity profile of these gases as their distance from the galactic nucleus grew. How could we compare this rotation profile with distance? Well,

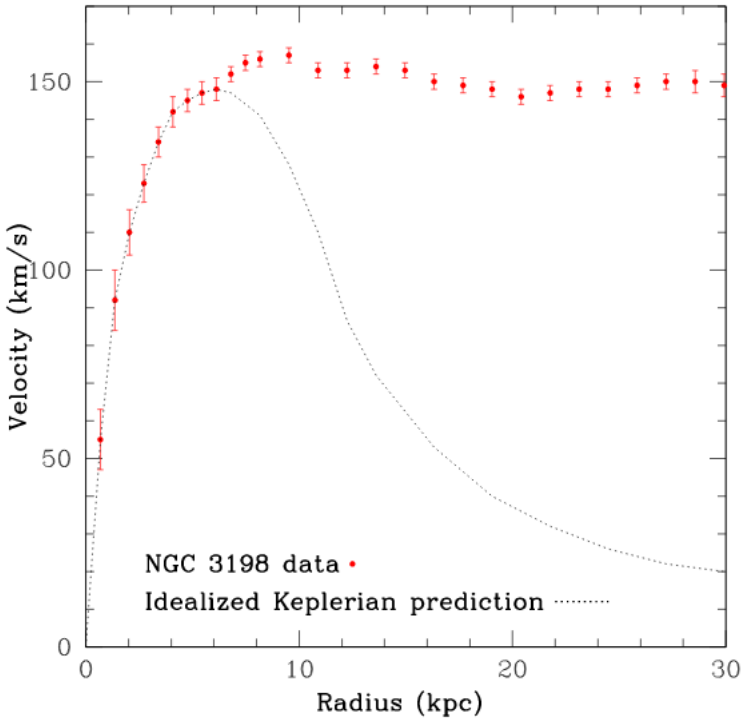

Figure 1. Rotation curve of HI regions in NGC 3198 [5]. Keplerian behavior is plotted against observations in order to better understand the deviation. As explained in Section 2.1 the absence of a drop off in the orbital velocities of theses gases implies that the mass should be increasing with the radius. Since luminous matter is known to be most located around the central regions, dark matter has to be responsible for this extra needed gravitational pull.

for our own solar system we know that keplerian behavior applies, that is, newtonian gravity. So if we compute the centripetal acceleration of a body orbiting another central massive object using newtons second law we can obtain a relation for the orbital velocity as follows:

Theorem 2. *Newton's second law*

$$F = ma \tag{3}$$

Assuming newtonian gravity acting as a centripetal force and knowing $a_c = \frac{v^2}{r}$ *- where v is the orbital velocity:*

$$\frac{GM(r)}{r^2} = \frac{v^2}{r} \tag{4}$$

$$v = \sqrt{\frac{GM(r)}{r}} \tag{5}$$

From this expression we get the Newtonian dependence of the orbital velocity on the radius:

$$v \propto r^{-\frac{1}{2}} \tag{6}$$

This last relation was found to not be true in the case of the observed gas in galaxies by Rubin. They found no fell off in the velocities, indicating that most mass should not be contained in the central regions, where most visible light is observed. Additionally this flatten of the velocity - sometimes even a slight increase - as r increases implies that the matter should be increasing linearly with r at least. To better understand this we now follow an approach using Gauss's law for a uniform sphere sphere of mass M[6].

Theorem 3. *Using Gauss's theorem we can relate the flux of the gravitational field through a surface of uniform mass as being proportional to the whole mass within the surface*

$$\int_S \vec{g}\vec{A} = 4\pi G M_{cluster}(r) \tag{7}$$

$$\vec{g} = \frac{G M_{cluster}(r)}{r^2} \tag{8}$$

Analyzing this last expression - equation 8 - we can see that if we expect the mass to decrease or even stay constant as the radius increases, the gravitational field should decrease and thus velocities should too. When the total mass is increasing with radius the field can remain constant or grow! This is the behavior though to happen for small radius where most luminous matter is concentrated because the total mass is increasing as the radius increases - this cannot be said for luminous matter after we leave the nuclear regions of the galaxy. What really happens is illustrate in figure 1: velocities first grow somewhat linearly with the radius and stay constant from a certain point onward. With data such as the one illustrated on figure 1 for 60 individual galaxies, Rubin came to the conclusion that indeed most matter in the universe was non-luminous - around 90% - and located in halo like shapes around individual galaxies. She found that dark matter had to be responsible for the high rotational velocities of stars and gases in the galaxy disk and thus a new scientific drive was introduced to the community: what exactly could dark matter be? Rubin pointed out in her work how the answer was still far from being discovered as the possible candidates ranged roughly 70 orders of magnitude in mass, from neutrinos to massive black holes. This drove a wide search for dark matter candidates that could be explained by existing physical theories. The Standard model could offer the neutrino, which although earlier on was not though of possessing a mass, later studies showed how massive neutrinos could solve some unexplained problems such as the solar neutrinos problem. We will talk more about neutrinos in our possible candidates section. Other possible particle candidates that derive from extensions to accepted theories or some that are postulated by exotic theories not yet falsified by any observational means - such as multiverse theory - are also explained.

Before new particle candidates were being seriously considered, baryonic matter was still a possibility. Some baryonic objects are known to not produce visible radiation. Brown dwarfs are one of these bodies; they usually have very low temperatures, which means they emit a very low amount of visible light. Although these temperatures rise depending on brown dwarf spectral type (they actual share spectral classes with very low mass stars and giant gas planets), brown dwarfs are mainly infrared emitters. Additionally compact objects such as neutron stars or even cool white dwarfs, along with some possible low mass black hole unknown distribution, might too account for the missing needed matter. All these candidates will be reviewed on the possible candidates section. A very important tool for their study was gravitational lensing, a mechanism uncovered by general relativity that enabled researchers to probe mass in their local universe, as we will see in the coming section.

2.2. Gravitational Lensing

According to general relativity space and time are part of the same fabric, one on which the universe lies. This fabric is generally *flat* - this term here refers to how space-time is not affected by gravity which means light will always travel in straight lines. However that is not always the case, mass perturbs this fabric and thus observers in motion around a massive object have their trajectories changed because space-time has been locally distorted. Using this view, it is not massive objects that attract other lighter masses, but massive objects actually distort the fabric of space-time in which all other observers move, massive or not. Particles of null mass such as photons can then have their trajectories changed due the presence of a massive object which changes the usual Minkowski -*flat*- space-time configuration. If we think about light beams rather than single photons, the deflection caused by the presence of a mass would act as a lens for the beam; for an observer in front of a massive object taking photometric measurements of a source behind the huge mass, its image would contain two measurements of the same source, one of which was due to an image being created around the massive object. This virtual image is created because light beams away from the observers direction are deflected around huge masses in such a way that the original image is distorted into a ring like shape. If the observed source was directly behind the massive object - eclipsed by it - the distorted image would actually fill a

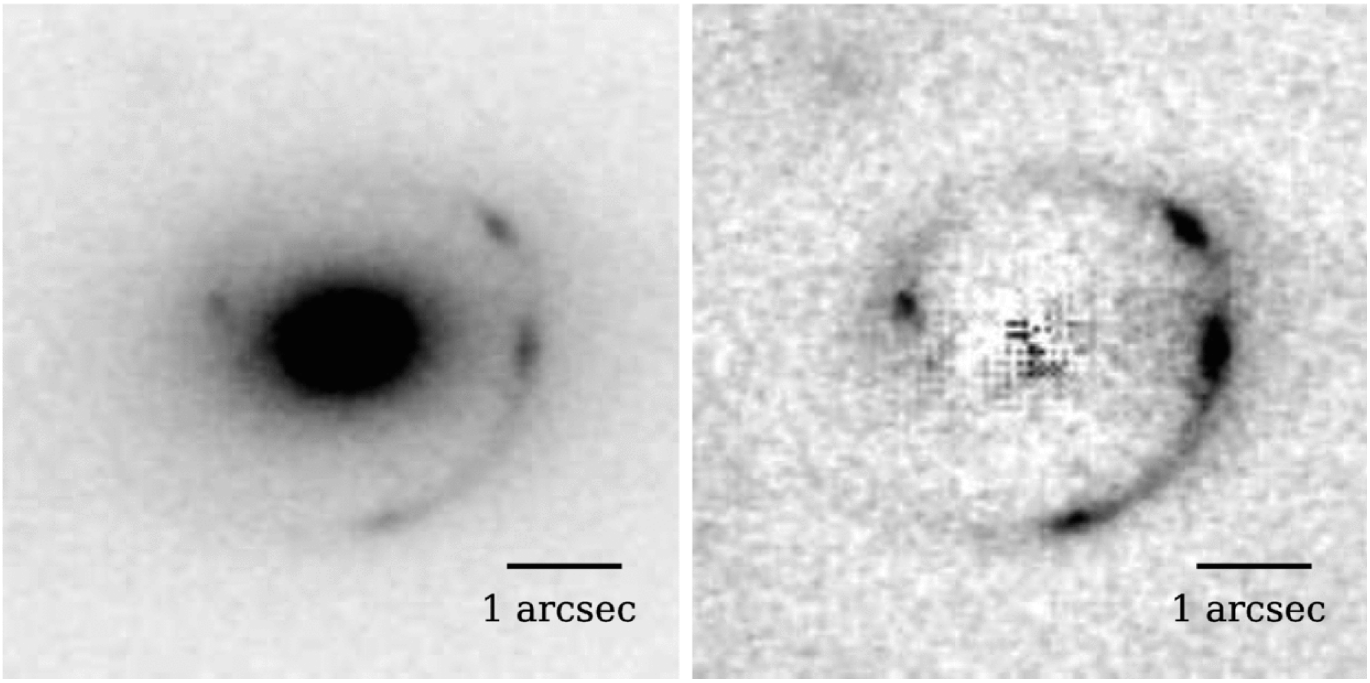

Figure 2. This is a science image from the SLACS Survey [7]. On the left panel the figure is a reduced image only but on the right the inner signal has been attenuated through subtraction of a B-spline model of the lensing galaxy for a clearer view of the ring structure.

whole ring; these phenomena are called Einstein rings. Since the conditions needed for a full Einstein ring are very difficult, most lensing detections are related to a partial ring detection.

Walsh et al. in 1979 [8] actually were the first astronomers to detect this phenomena, further testing general relativity through observations and uncovering a new astrophysical process from which information might be measurable. They found two different sources separated by 4.6 arcmin with very close redshifts, flux and spectra, which would be explained by the presence of a massive object that creates a virtual image of the same source in the plane of the observer. So to get scientific data such as the mass of the perturber, lets say a cluster of stars, we need to have a distant and powerful source as much directly behind the cluster as possible, in order for the Einstein ring effect to be greater as possible. These situations are not usual however some measurements have been made regarding this subject. The angular radius θ_E of the observed Einstein ring is related to the mass of the perturber and that relation can be expressed as follows [6]:

Theorem 4. *The radius of an arclet created through gravitational lensing, at the distance d_L away from the observer, of a source at a distance of d_S is*

$$\theta_E = \sqrt{\frac{4GM}{c^2}\frac{d_L S}{d_L d_S}} \tag{9}$$

Where $d_L S$ is the distance from the lensing (massive) object to the source of the incoming radiation.

Some researchers have been able to observe specially well resolved lens rings and obtain mass values for the cluster. Abell 370 and Cluster 2244-02 were found to need large amounts of dark matter in order to account for the observed lens effect[9]. Through an analysis of the Einstein rings the researchers were able to constraint the distribution of mass in the clusters and even the shape and size of the source being lensed. This distribution of masses not only confirmed the need for larges amounts of black matter but also was able to constraint the distribution of the dark matter in the clusters. For Abell 370 the dark matter should have a distribution different than that of luminous matter, however for Cluster 2244-02 they found the opposite could be true (galaxies), along with other configurations. Many more lens effects were observed: Hewitt et al. found the first actual lens ring in 1988 [10] [11], then researchers

starting detecting more complete rings as detector technology increase [12]. The Sloan Lens ACS (SLACS) Survey is one more recent effort using data from the Hubble Space Telescope which was able to confirm 85 grade "A" lens systems [7], one of which is presented on figure 2. In this survey the researchers think that the lens systems they have detected will allow them to probe the distribution of dark and luminous matter in the kpc-scale.

Gravitational lensing can also be used in the search for one type of dark matter: MACHOs. These objects have large masses that should cause gravitational lensing effects. This can only be done for the milky way, where these sources can be accounted for from an insiders perspective, as we look to sources behind the galactic plane. This way massive compact object on the way of the incoming light should be able to produce visible lensing effects and the distribution of MACHOs on the milky way should be then determinable. These issues are dealt with on the MACHOs section on possible candidates for dark matter.

2.3. Cosmological breakthrough: the impact of CMB and current cosmological observations

Cosmological knowledge grew a lot between the time dark matter's influence begun being studied and now. The Big Bang theory became the most universally accepted theory of cosmology, cemented by general relativity and particle physics related studies. As the BBT goes, the universe started from a very hot and dense state, in which all the elemental particles that compose the universe were initially coupled together, in a thermal relativistic fluid state. From a certain point on, the universe started slowing the expansion and thus particle species were able to decouple from the fluid. Photons are one one of the species coupled to this thermal relativistic fluid, as are all of the particles in the Standard Model of Particle Physics and their decoupling period is of extreme physical importance; it is related to an epoch of cosmological history called recombination. Another important time in the history of dark matter research is the Hadron Epoch, during which the first nuclei formed. Since both concepts are related, we will give a brief context on the Big Bang cosmological model.

After the Big Bang, the universe started expanding very rapidly with all particles staying in thermal equilibrium with each other - **Quark Epoch**. This first very rapid expansion is a very important cosmological mechanism called **Inflation**, needed to explain deviations from isotropy in our current universe, being that we know it must have started in a highly homogeneous state. We will come back to the importance of Inflation later on, however Inflation theories are state of the art cosmology and should be able to predict how the large scale configuration of the universe eventually evolved into its current state, which although mainly isotropic still shows small deviations that are not well explained today. The expansion driven by inflation eventually stopped allowing the universe to cool. 10^{-6} seconds after the Big Bang was cool enough to allow quarks to form hadrons, which can either be baryons for a combination of 3 flavors of quarks, or mesons for a combination of a quark and an anti-quark; this is know as the **Hadron Epoch**. Baryonic matter was thus created in the form of baryon/anti-baryon pairs, dominating the mass of the universe at the time and maintaining the matter and anti-matter ratio in equilibrium. By the end of this Hadron Epoch, the temperature was not hot enough for the creations of these matter/anti-matter pairs, so the anti-baryons were mostly annihilated, leaving a residue number of baryons, as it is observed today. Theories able to describe the mechanisms that drive the baryon/anti-baryon number ratio to reach the asymmetrical feature we see today - almost no anti-matter is observed compared to baryonic matter - are named Baryogenesis theories, and are also a main topic of cosmological research. During the Hadron Epoch some processes permitted some light nuclei to form via 2 body processes of protons and neutrons. Some examples follow:

$$p + n \rightarrow \gamma + D \tag{10}$$

$$D + D \rightarrow p + T \tag{11}$$

$$D + D \rightarrow p + T \tag{12}$$

$$T + D \rightarrow n + He^4 \tag{13}$$

$$T + He^4 \rightarrow Li^7 + \gamma \tag{14}$$

Which explains the high abundance of lighter elements in the universe. These interactions are some of many that can lead up to the creation of lithium and beryllium and this process is called Big Bang Nucleosynthesis (BBN). The leftover baryons then have light nuclei with them, maintaining a constant ratio of deuterium to hydrogen until stellar

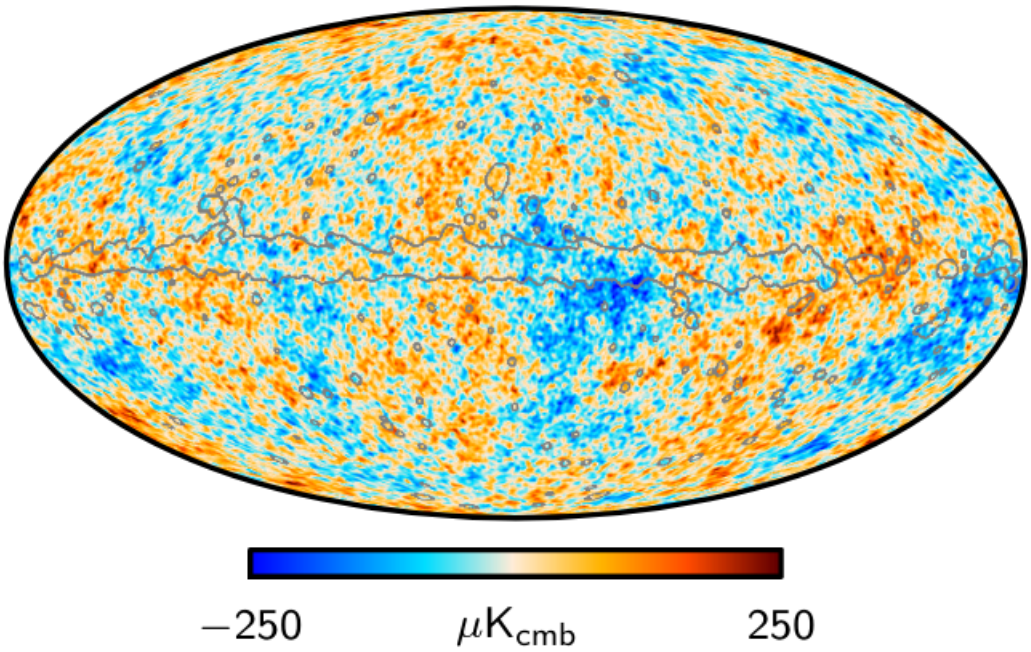

Figure 3. In this figure a representation of the CMB fluctuations in the observable sky obtained from the Planck Mission.[16]

objects were able to form very later on. This ratio is heavily dependent on the general baryon density. In order to make use of this, researchers looked at the most distant and ancient galaxies, where this ratio was most similar to that right after BBN. Using this technique the physical baryon density was found to account only for 20% of all matter [13][14]. The first cited source finds values for $\Omega_b h^2 \approx 0.022 \pm 0.002$ using two different methods for obtaining the deuterium density; other study from and observation of a quasar in 2006 finds a similar value of $\Omega_b h^2 \approx 0.0213 \pm 0.0017$ [15]. Observational data which can be explained by the big bang model infers again that baryonic mass should compose only around a fifth of all matter in the universe. Another particle species should then be dense enough in order for the missing matter to be accounted for. We will see how some candidate particle candidate fit into this point of view later on, for now we will resume the section on cosmological observational evidence of dark matter. After the BBN, electrons, protons and neutrons in the fluid are coupled via scattering processes but eventually the photons should decouple from the matter and start to travel freely in the universe. During the Hadron Epoch electrons - leptons in general - were coupled to the fluid along with the photons through weak interactions, contributing to a very high opacity of the universe due to Thomson scattering; another way to further illustrate this is to think on the photon free mean path, for example in the case of the sun, large nuclear densities cause photons to not be able to escape this core, however as the density falls with the radius, the mean free path of the photons is eventually enough to free it from the stellar atmosphere and travel the rest of the universe. At the end of the hadron epoch, leptons dominate the mass of the universe, however their decoupling is also inevitable. So eventually, the weak interactions that enabled the leptons to stay in thermal equilibrium are no longer supported by the temperature of the gas and a similar process to that of Baryogenesis happens, where most positrons are annihilated leaving a residue number of electrons.

This happens for all leptons, enabling some of these electrons to start binding to baryons in order to reach a lower energy state - Recombination. Electron-positron annihilation starts at around 0.5 Mev, some 6 seconds after the Big Bang, with the start of the first creation of light nuclei starting at around 0.1 MeV. At this time, free electrons are still enough to make the universe opaque, as we've discussed; however, as electrons are binded to nuclei in order to form atoms, the density of free electrons drops. Even more, the electrons that do bind to atoms should not bind at the fundamental energy state but at excited states and then relaxing to the fundamental state through photon emission. Some time before the photons are able to decouple, matter-radiation equality happens, indicating a new regime where radiation will dominated for a good while. After recombination, the Thomson scattering starts decreasing and eventually photons are able to decouple from the matter and the universe becomes transparent for the first time in its

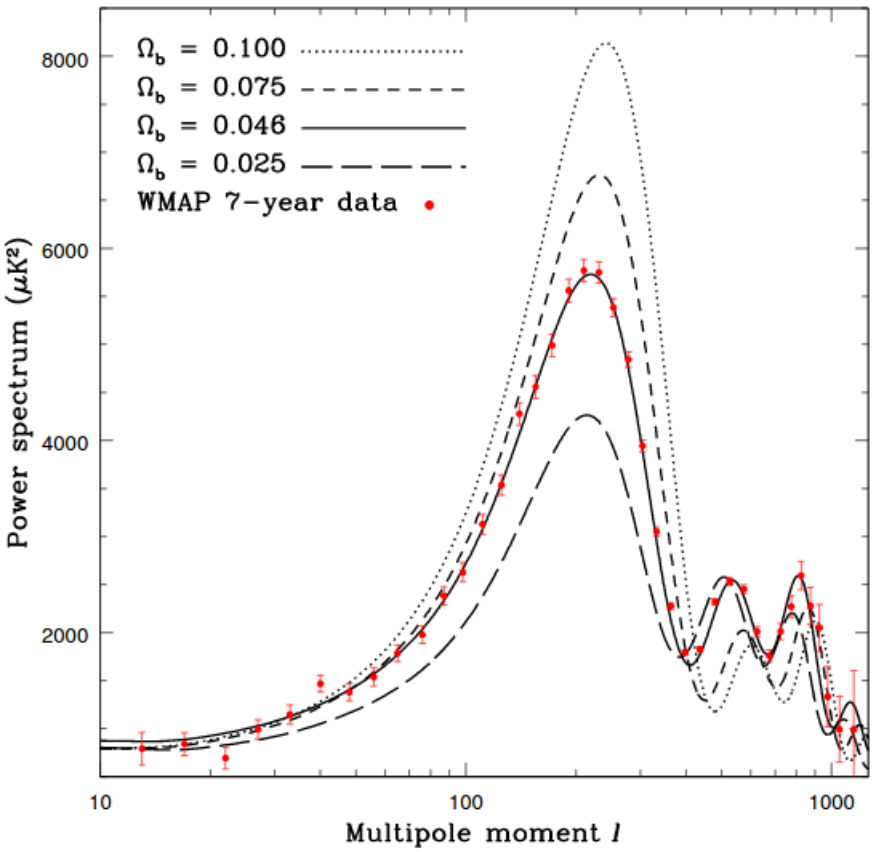

Figure 4. This plot illustrates the huge dependence of the CMB anisotropies on the baryon density using 7 years of WMAP data. Small differences in the baryon densitiy imply a large difference in the observed spectra. This way baryon density can be calculated, in the figure we see that the best fit for the data was a baryon density $\Omega_b = 0.046$ (solid line in the plot). Further data from the same Mission gives a matter density of around $\Omega_m \approx 0.3$ which implies a dark matter percentage of around 85%[18]

history. These photons, from the primordial light nuclei that formed in the BBN are called the Cosmic Microwave Background (CMB) and their signal can still be detected today at a temperature of $T = 2.73$K, bearing fluctuations on the fifth decimal order of magnitude[17] [18]. This signal was first found by Penzias and Wilkinson in 1965 [19] and has ever since been a central observational evidence of the big bang and the surface of last scattering. From the fluctuations present in the CMB one can derive the density of matter in the universe at the time of last scattering and even the baryon density. From these two values one may estimate how much dark matter exists in the universe. Dark matter was found again to be the primary component of the universe's matter component by missions studying the CMB energy fluctuations; the first mission to discover the fluctuations was COBE [17] (COsmic Background Explorer) but they have since been studied more in depth by the WMAP (Wilkinson Microwave Anisotropy Probe)[18] and Planck Missions[16]. The matter physical density as found to be $\Omega_m h^2 \approx 0.1314 \pm 0.0055$ and the baryon density as $\Omega_b h^2 \approx 0.02260 \pm 0.00053$ by WMAP and a representation of the CMB fluctuations from the Planck Mission 2015 results is presented in figure 3.

It is not explicit why baryonic matter density can be extracted from CMB fluctuations. It is related to how dark matter was not part of the photon-baryon fluid as it should have decoupled earlier - sometime after the creation of the first baryons. Without dark matter in the fluid, CMB fluctuations were solemnly connected with the first density perturbations from inflations and the dynamics of the fluid. As so these fluctuations are highly connected with the baryons density and this parameter is extractable from CMB observations, as presented earlier. Figure 4 better expresses this relation between the CMB anisotropies and the baryons density - plot of 7 years of WMAP data. Here see how the spectrum is an almost perfect black body, corroborating the view that the universe is mostly isotropic.

However, these small fluctuations cannot account for the large present structure of the universe, as it would not have had time to evolve yet. This reason drove cosmological research into Inflationary theories, which as we have discuss try to explain initial perturbations due to a very rapid expansion of the universe at the Quark Epoch which are then magnified by dark matter, thus driving the evolution of the large structure of the universe. Dark matter here is a necessity, because the low CMB temperature fluctuations imply the creations of the first gravitational wells through other massive particles. This is yet another argument, although this time theoretical, which further enhances the plausibility that we need dark non-baryonic matter. It should explain how baryonic matter evolved into its current structure. Dark matter is then a cosmological necessity if we are to continue employing the Big Bang model.

The search for these particles which could account for dark matter is one of the most important scientific searches of our day. Until today, no particle or large structure detections of dark matter have been found. We do not know what sort of particle we should exactly be looking for and how it could interact with our universe, excluding that it is massive and non-luminous. In the following sections we will give a brief overview of the most promising dark matter candidates. Although MACHOs have been discredited already through the essay, we give an overview on some studies which cemented their exclusion as dark matter candidates. These objects still drove dark matter research for some years and as such are important knowledge to overview. For non-baryonic particle candidates we will focus on WIMPs but we also look into some exotic possibilities since exoticness here mainly speaks for current theory popularity.

3. Possible types of dark matter

3.1. Brown Dwarfs and MACHOs

The first well argument for dark matter as we have preview came in the form of baryonic matter. Many different types of cold baryonic matter were known at the time of the first velocity measurements and thus became the primary source of interest on dark matter studies. Such objects which were talked of being able to compose the majority of dark matter ranged from sub-stellar objects to compact objects such as neutron stars, very cold white dwarfs or even stellar black holes. The population of these objects on galaxies was not well known at the time, as so the need for a thorough detection effort in order to catalog these more exotic bodies was in need.

The MACHO collaboration [20] and the EROS-2 Survey [21] were some of these efforts. They probed the Large Magellanic Cloud (LMC), which is a satellite galaxy of the milky way, in order to look for *micro-lensing* events, which are a process due to gravitational lensing in which the flux of an observed distant source changes due to the presence of a closer massive body. For both these missions the researchers aimed to find MACHOs in the milky way halo that could distort sources from the LMC. MACHO analyzed 11.9 million stars in the LMC and over the course of 5.7 years only 13-17 microlensing events were detected. For the MACHO population to be able to account for all the dark matter we would need around 30-40 events; for comparison for the known population of stars we would expect 2-3 microlensing events. The Macho collaboration thus found that around 20% of dark matter could be accounted for (see figure 5 for a representation of the results), however the EROS-2 survey, which also looked into the LMC found very different values for the events: they observed 33 million stars during the course of 6.7 years and found only one microlensing candidate, concurring with the expected value for the known population of stars. Other studies such as the SuperMACHO survey also find a dozen candidates, supporting the MACHO survey [22].

All these results arrive at the same conclusion: baryonic dark matter forms cannot account for the needed amount of dark matter. This, along with the cosmological knowledge we have derived earlier can finally objectively exclude these objects from dark matter state of the art theories. However it is interesting because since we know that known dark baryonic configurations of matter should not account for 85% of missing matter, these studies now give insight into how dark matter can cause microlensing effects in the galactic halo. For all these low amounts of events, it is most safe to say that dark matter should not exist in the same configurations that we see baryonic matter in (stars, planets, clusters).

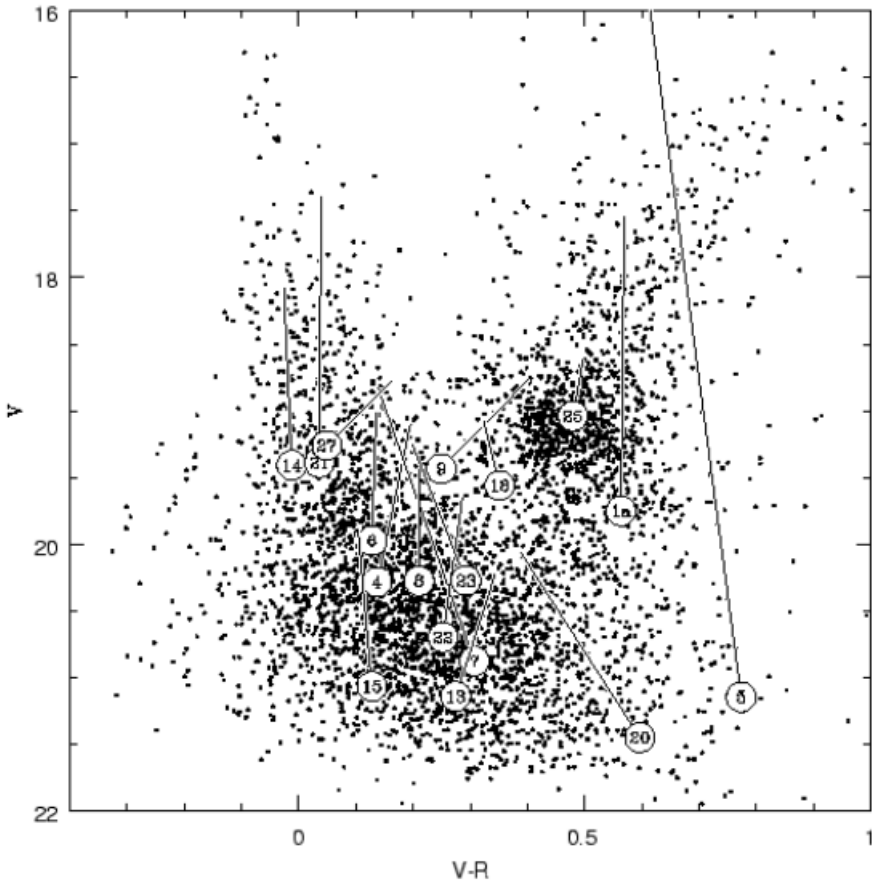

Figure 5. This is a color-magnitude diagram (CMD) from the MACHO collaboration's 5.7 year effort. It features the candidate MACHOS along with the 200 nearest MACHO candidate to each event. Each numbered circle denominates a microlensing candidate and its correspondent line segment shows how high the magnitude changed during the event.

3.2. Neutrinos and the problem of hot dark matter

Another possible candidate other than MACHOs indicated by Rubin et al. in 1983 was a massive neutrino. At the time his particle was though of not having mass at all; actually only very recently has an observable directly related to the individual mass, the sum of all 3 flavors, been measured [23]. Today, the Standard Model of particle physics accepts the mass of the neutrino into its theory and thus brings a viable candidate for dark matter, from an already tested and preconceived theory - this makes it an even more appetizing candidate. However the dreams does not stay long, first of all we would need to look into one of the neutrinos key characteristics: they are relativistic, however light and weakly interacting. The latter, unfortunately, cannot compensate for the former. If neutrinos actually exist in quantities that can explain dark matter, the evolution that they impose upon the universe does not corroborate with observations. A relativistic sort of dark matter - **hot dark matter** - would drive the evolution of the universe in a "top-down" formation where large scale structures form first and then condense and fragment into the configurations that we can see today. Well we know that galaxies can date back to some hundreds of million years after the Big Bang. In 2006 a galaxy with spectral redshift of 6.96 was found, which means galaxy formation dates back to at at least 750 Myrs after the Big Bang ($\approx$ 6% of the universes age!)[24]. Using this knowledge in numerical simulations we get that a bottom up formation process is way more likely [6][25].

Using cosmological knowledge from the CMB and large scale structure a team was able to constraint the neutrino density and their mass[26]! Their findings give an upper limit for both the density and mass observables as so:

$$\Omega_\nu h^2 < 0.0072 \tag{15}$$

Sfermions

Generation 1			Generation 2			Generation 3		
Particle	Mass (GeV)	Charge	Particle	Mass (GeV)	Charge	Particle	Mass (GeV)	Charge
up squark ($\tilde{u}$)	> 379	$+\frac{2}{3}$	charm squark ($\tilde{c}$)	> 379	$+\frac{2}{3}$	top squark ($\tilde{t}$)	> 92.6	$+\frac{2}{3}$
down squark ($\tilde{d}$)	> 379	$-\frac{1}{3}$	strange squark ($\tilde{s}$)	> 379	$-\frac{1}{3}$	bottom squark ($\tilde{b}$)	> 89	$-\frac{1}{3}$
selectron ($\tilde{e}$)	> 73	-1	smuon ($\tilde{\mu}$)	> 94	-1	stau ($\tilde{\tau}$)	> 81.9	-1
e sneutrino ($\tilde{\nu}_e$)	> 95	0	μ sneutrino ($\tilde{\nu}_\mu$)	> 94	0	τ sneutrino ($\tilde{\nu}_\tau$)	> 94	0

Gauginos

Particle	Mass (GeV)	Description
Neutralinos ($\tilde{\chi}^0_{1-4}$)	> 46	Mixture of photino ($\tilde{\gamma}$), zino ($\tilde{Z}$), and neutral higgsino ($\tilde{H}^0$)
Charginos ($\tilde{\chi}^\pm_{1,2}$)	> 94	Mixture of winos ($\tilde{W}^\pm$) and charged higgsinos ($\tilde{H}^\pm$)
Gluinos ($\tilde{g}$)	> 308	Superpartner of the gluon

Figure 6. In this figure we can see the new particles added to the SM upon a SUSY extension. The most prominent dark matter candidate is the neutralino

$$m_\nu < 0.23eV \tag{16}$$

From this information we can take that neutrinos account for 7% of dark matter, which together with the highest possible value for the MACHO dark matter($\approx$ 20%) density still leaves the **majority** of matter with an unaccountable origin.

3.3. The search for the perfect WIMP : the neutralino

After we've dried out our existing theory's tools, we reach a region of boundary pushing physics. What physical processes would explain the existence of a WIMP, now that not theory in our physical paradigm does? Well, following a particle physics approach from now on - the only approach possible really - there are many extensions to the Standard Model of particle physics that explain most Standard Model Predictions while harboring a larger amount of existent elemental particles. If some of those particles happen to be highly non interactive and massive, they are a prime candidate for a dark matter particle. A very promising extension to the SM is that of supersymmetry (SUSY). This theory arises from overcoming what is called the Coleman-Mandula theorem, which states the most general symmetries that a Quantum Field Theory can have are Lorentz Invariance and Gauge Symmetries - these include but are not limited to, charge conservation, lepton number conservation, parity, etc. One symmetry in specifically is that of angular spin conservation; this prohibits a fermion into becoming a boson and vice-versa. However, somewhere in the mid 80s researchers stumbled upon a way to overcome this theorem and allow fermion-boson inter-conversion [6][27] which means that every fermion has a partner boson particle associated with it and vice versa as well. This would - and does - effectively double the number of particles in the SM, however this is not to be seen as sloppy or unnecessary, because the SM is known to have faults, mainly due to the hierarchy of its constituent particles and failure to predict the energy of the Higgs field in a vaccum in a natural way - see section B, Particle Candidates chapter by Garret et al. [6]. So SUSY is actually a very appealing theory from a theoretical point of view, being that its predictions regard a probing of higher energy scales than is permitted today.

Apart from solving the small Higgs mass and the hierarchical problems of the SM, SUSY also delivers dark matter candidates. All the new particles due to SUSY are presented in figure 6. From those, the candidate particles - weakly interacting, massive - are the gravitino, superpartneer of the graviton, the sneutrino, superpartner of the neutrino, and the neutralino, which corresponds to a more complex configuration of superpositions of neutral superpartners to the Higgs and Gauge bosons (photino and Higgsino, respectively). As so it happens, the neutralino's density is not sufficient to account for dark matter because it annihilates very early and the gravitino is relativistic, which means it has the same large scale problems as the neutrino. One particle candidate remains, the neutralino. The needed density of neutralinos can be explained by a new type of symmetry, R-parity, which enables the lightest supersymmetric partner to never decay.

The neutralino is the dark matter candidate for a Standard Model SUSY extension. Its detection rates are high enough so that data is attainable in the laboratory but not in sufficient numbers to rule them out as a candidate. One

can say that the neutralino is indeed the most promising WIMP, however other forms of dark matter might be possible as we will talk about in the next and final section.

3.4. Some exotic examples of candidate particles

It is worth mentioning that we have since come to the conclusion that dark matter will be explained by a new theory of particle physics. Most likely, this theory will have a new approach on gravity, either characterizing the first range of energies where gravity starts being important or actually unifying gravity with the other 4 forces of nature. String theory, for example, is a quantum theory of gravity which is inherently supersymmetric. Many new theories were developed in the 70s through the early 2000s that could explain what we see and observe in a different way, they are just not falsifiable yet and thus remain as an intricate mathematical delicacy. Some of these theories have possible dark matter candidates that should be noted, mainly due to how fast researchers could turn away from the neutralino because of exclusion or technologically unachievable goals.

One of these particles is the axion, which was first formulated in order to solve the strong CP problem. It states that the neutron could have a dipole moment that was never observed because of a term in the strong force lagrangian [6][28]. Since this dipole has never been observed, it has been hypothesized that there is a symmetry which prevents this dipole from appearing -this is similar to how gauge symmetries keep the photon massless. Additionally, the original authors propose that this symmetry breaks slightly and as a consequence a new particle of very light mass arises, the axion. This axion can exist in large amounts and has a hypothesized mass around the μeV. Axions research is actually pretty varied. Constraints on axions have been put through finely tuned radio frequency cavity observations and even by observing how red giants cool[**?**]! Additionally if axions really exist and we have a SUSY theory for how the universe works then the axino is the lightest supersymmetrical partner has thus the most promising dark matter candidate.

One last dark matter candidate comes from theories of extra dimensions, which started in the 1920s when Kaluza and Klein first wrote down the equations of Einstein in 5 dimensions and recovered 4 dimensional gravity, Maxwell's equations for a scalar field and a new scalar particle. This drove a wave of theories known as Kaluza-Klein theories which aimed at Grand Unification of physics. In the midst of the particle physics growth they were forgotten because they seemed impractical, however in the 90s interest re-grew when scientist began researching this possibility again, trying to push the boundaries of the theory. One thing that was found was that if the theories compactify the extra dimensions it is possible that in order for particles to move freely between these dimensions a set of states called Kaluza-Klein states appear. Each particle is then associated with an infinite amount of Kaluza-Klein states. It is also postulated that a new symmetry akin to that of the axion CP problem can arise, allowing the possibility for a lightest Kaluza-Klein particle can actually be stable and account for dark matter. As Garret et al point out, the first excitation state of the photon is highly used as the LKP.

4. Conclusion

Dark matter is a research topic on the frontier of physical knowledge. It is a necessary knowledge to obtain in order for humanity to understand the large structure of our universe, a key piece into the real composition of the universe and maybe the only real concept that unifies quantum and gravity research. Because of this, every hypothesis is actually a state of the art physical problem, not only a cosmological one. Be it a WIMP, an axion or a Kaluza-Klein particle, dark matter is real and exists in large amounts in our universe. It most likely played a large part into the large structure evolution of our universe and the implications of its existence have only began being theorized. The following years will be most satisfying for dark matter research, cosmology and physical knowledge in general. There is work to be done, mainly in direct detection methods for dark matter, since there are few trustworthy processes, but we will see the truth unfold.

References

1. Kuiper, G.P. The Empirical Mass-Luminosity Relation. *Astrophysical Journal* **1938**, *88*, 472. doi:10.1086/143999.
2. Oort, J.H. The force exerted by the stellar system in the direction perpendicular to the galactic plane and some related problems. *Bulletin of the Astronomical Institutes of the Netherlands* **1932**, *6*, 249.
3. Zwicky, F. Republication of: The redshift of extragalactic nebulae. *General Relativity and Gravitation* **2009**, *41*, 207–224. doi:10.1007/s10714-008-0707-4.
4. Rubin, V.C. Dark matter in spiral galaxies. *Scientific American* **1983**, *248*, 96–106. doi:10.1038/scientificamerican0683-96.
5. Begeman, K.G. HI rotation curves of spiral galaxies. I. NGC 3198. *AAP* **1989**, *223*, 47–60.
6. Garrett, K.; Dūda, G. Dark Matter: A Primer. *Advances in Astronomy* **2011**, *2011*, 968283, [arXiv:hep-ph/1006.2483]. doi:10.1155/2011/968283.
7. Auger, M.W.; Treu, T.; Bolton, A.S.; Gavazzi, R.; Koopmans, L.V.E.; Marshall, P.J.; Bundy, K.; Moustakas, L.A. The Sloan Lens ACS Survey. IX. Colors, Lensing, and Stellar Masses of Early-Type Galaxies. *Astrophysical Journal* **2009**, *705*, 1099–1115, [arXiv:astro-ph.CO/0911.2471]. doi:10.1088/0004-637X/705/2/1099.
8. Walsh, D.; Carswell, R.F.; Weymann, R.J. 0957+561 A, B: twin quasistellar objects or gravitational lens? *Nature* **1979**, *279*, 381–384. doi:10.1038/279381a0.
9. Bergmann, A.G.; Petrosian, V.; Lynds, R. Gravitational Lens Models of Arcs in Clusters. *Astrophysical Journal* **1990**, *350*, 23. doi:10.1086/168359.
10. Hewitt, J.N.; Turner, E.L.; Schneider, D.P.; Burke, B.F.; Langston, G.I. Unusual radio source MG1131+0456: a possible Einstein ring. *Nature* **1988**, *333*, 537–540. doi:10.1038/333537a0.
11. Lynds, R.; Petrosian, V. Luminous Arcs in Clusters of Galaxies. *Astrophysical Journal* **1989**, *336*, 1. doi:10.1086/166989.
12. King, L.J.; Jackson, N.; Blandford, R.D.; Bremer, M.N.; Browne, I.W.A.; De Bruyn, A.G.; Fassnacht, C.; Koopmans, L.; Marlow, D.; Wilkinson, P.N. A complete infrared Einstein ring in the gravitational lens system B1938+666. *Monthly Notices of the Royal Astrophysical Society* **1998**, *295*, L41–L44, [arXiv:astro-ph/astro-ph/9710171]. doi:10.1046/j.1365-8711.1998.295241.x.
13. Cyburt, R.H. Primordial nucleosynthesis for the new cosmology: Determining uncertainties and examining concordance. *PRD* **2004**, *70*, 023505, [arXiv:astro-ph/astro-ph/0401091]. doi:10.1103/PhysRevD.70.023505.
14. Bauer, M.; Plehn, T. Yet Another Introduction to Dark Matter. *arXiv e-prints* **2017**, p. arXiv:1705.01987, [arXiv:hep-ph/1705.01987].
15. O'meara, J.M.; Burles, S.M.; Prochaska, J.X.; Prochter, G.E.; Bernstein, R.A.; Burgess, K.M. The Deuterium-to-Hydrogen Abundance Ratio toward the QSO SDSS J155810.16–003120.0*. 2006.
16. Planck Collaboration. Planck 2015 results. XI. CMB power spectra, likelihoods, and robustness of parameters. *AAP* **2016**, *594*, A11, [arXiv:astro-ph.CO/1507.02704]. doi:10.1051/0004-6361/201526926.
17. Smoot, G.F.; Bennett, C.L.; Kogut, A.; Wright, E.L.; Aymon, J.; Boggess, N.W.; Cheng, E.S.; de Amici, G.; Gulkis, S.; Hauser, M.G.; Hinshaw, G.; Jackson, P.D.; Janssen, M.; Kaita, E.; Kelsall, T.; Keegstra, P.; Lineweaver, C.; Loewenstein, K.; Lubin, P.; Mather, J.; Meyer, S.S.; Moseley, S.H.; Murdock, T.; Rokke, L.; Silverberg, R.F.; Tenorio, L.; Weiss, R.; Wilkinson, D.T. Structure in the COBE Differential Microwave Radiometer First-Year Maps. *ApJl* **1992**, *396*, L1. doi:10.1086/186504.
18. Jarosik, N.; Bennett, C.L.; Dunkley, J.; Gold, B.; Greason, M.R.; Halpern, M.; Hill, R.S.; Hinshaw, G.; Kogut, A.; Komatsu, E.; Larson, D.; Limon, M.; Meyer, S.S.; Nolta, M.R.; Odegard, N.; Page, L.; Smith, K.M.; Spergel, D.N.; Tucker, G.S.; Weiland , J.L.; Wollack, E.; Wright, E.L. Seven-year Wilkinson Microwave Anisotropy Probe (WMAP) Observations: Sky Maps, Systematic Errors, and Basic Results. *The Astrophysical Journal Supplement Series* **2011**, *192*, 14, [arXiv:astro-ph.CO/1001.4744]. doi:10.1088/0067-0049/192/2/14.
19. Penzias, A.A.; Wilson, R.W. A Measurement of Excess Antenna Temperature at 4080 Mc/s. *Astrophysical Journal* **1965**, *142*, 419–421. doi:10.1086/148307.
20. Alcock, C.; Allsman, R.A.; Alves, D.R.; Axelrod, T.S.; Becker, A.C.; Bennett, D.P.; Cook, K.H.; Dalal, N.; Drake, A.J.; Freeman, K.C.; Geha, M.; Griest, K.; Lehner, M.J.; Marshall, S.L.; Minniti, D.; Nelson, C.A.; Peterson, B.A.; Popowski, P.; Pratt, M.R.; Quinn, P.J.; Stubbs, C.W.; Sutherland, W.; Tomaney, A.B.; Vand ehei, T.; Welch, D. The MACHO Project: Microlensing Results from 5.7 Years of Large Magellanic Cloud Observations. *Astrophysical Journal* **2000**, *542*, 281–307, [arXiv:astro-ph/astro-ph/0001272]. doi:10.1086/309512.

21. Tisserand, P.; Le Guillou, L.; Afonso, C.; Albert, J.N.; Andersen, J.; Ansari, R.; Aubourg, É.; Bareyre, P.; Beaulieu, J.P.; Charlot, X.; Coutures, C. Limits on the Macho content of the Galactic Halo from the EROS-2 Survey of the Magellanic Clouds. *AAP* **2007**, *469*, 387–404, [arXiv:astro-ph/astro-ph/0607207]. doi:10.1051/0004-6361:20066017.
22. Becker, A.C.; Rest, A.; Stubbs, C.; Miknaitis, G.A.; Miceli, A.; Covarrubias, R.; Hawley, S.L.; Aguilera, C.; Smith, R.C.; Suntzeff, N.B.; Olsen, K.; Prieto, J.L.; Hiriart, R.; Garg, A.; Welch, D.L.; Cook, K.H.; Nikolaev, S.; Clocchiatti, A.; Minniti, D.; Keller, S.C.; Schmidt, B.P. The SuperMACHO Microlensing Survey. Gravitational Lensing Impact on Cosmology; Mellier, Y.; Meylan, G., Eds., 2005, Vol. 225, *IAU Symposium*, pp. 357–362, [arXiv:astro-ph/astro-ph/0409167]. doi:10.1017/S1743921305002164.
23. Mertens, S. Direct Neutrino Mass Experiments. Journal of Physics Conference Series, 2016, Vol. 718, *Journal of Physics Conference Series*, p. 022013, [arXiv:nucl-ex/1605.01579]. doi:10.1088/1742-6596/718/2/022013.
24. Iye, M.; Ota, K.; Kashikawa, N.; Furusawa, H.; Hashimoto, T. A galaxy at a redshift z = 6.96. *Nature* **2006**, *443*, 186–188, [arXiv:astro-ph/astro-ph/0609393]. doi:10.1038/nature05104.
25. Bond, J.R.; Efstathiou, G.; Silk, J. Massive Neutrinos and the Large-Scale Structure of the Universe. *PRL* **1980**, *45*, 1980–1984. doi:10.1103/PhysRevLett.45.1980.
26. Spergel, D.N.; Verde, L.; Peiris, H.V.; Komatsu, E.; Nolta, M.R.; Bennett, C.L. First-Year Wilkinson Microwave Anisotropy Probe (WMAP) Observations: Determination of Cosmological Parameters. *ApJl* **2003**, *148*, 175–194, [arXiv:astro-ph/astro-ph/0302209]. doi:10.1086/377226.
27. Wess, J.; Bagger, J.; Nath, P. Supersymmetry and Supergravity. *Physics Today* **1984**, *37*, 78. doi:10.1063/1.2916416.
28. Peccei, R.D.; Quinn, H.R. CP conservation in the presence of pseudoparticles. *PRL* **1977**, *38*, 1440–1443. doi:10.1103/PhysRevLett.38.1440.

Proceedings

Prospects for the unification of dark matter and dark energy using negative mass particles

João Dias [1]

[1] Affiliation 1; fc47913@alunos.fc.ul.pt

Received: date; Accepted: date; Published: date

Abstract: Dark matter and dark energy constitute about 95% of the Universe and by now we still dont know what they are. About a century ago, Einstein proposed the idea of gravitationally repulsive negative masses to explain the expansion of the Universe and since then it was forgotten. In this essay, I will resume the findings of a recent modified model which suggests that the continuous creation of negative masses can reproduce both the cosmological constant, believed to explain dark energy ,and the flattened rotation curve of galaxies, thus providing a way to unify both these mysterious components of the Universe. I will show you some recent results of the first 3-dimensional N-Body simulations of the evolution of large scale structure and formation of halos in the galaxies, incorporating negative masses. Some predictions of this model can be tested against several observations, namely of distant supernovas, of the cosmic microwave background and of galaxy clusters.

Keywords: negative masses; N-body simulations;dark matter halo; rotation curve of galaxies; structure formation; runaway motion

---

1. Introduction

Negative masses are not a new concept and first arises in the time of Einstein as a way to produce a static universe, which was the standard universe at the time. As gravitational forces tend to push things inward , Einstein thought a repulsive force was needed in order to avoid the collapse of the universe. One could say that a negative mass is a mass with negative sign, however in the context of General Relativity , where the source of gravitation is the stress-energy tensor, different observers in different reference frames can attribute different signs to the quantities involved in this tensor (density,density flux,mass, mass flux,etc), such that we can see that the definition of negative mass is not a trivial thing.

It is thought that this matter can violate one or more energy conditions of the theory of General Relativity. Energy conditions are boundary conditions to the equations.

In particular it is said to violate the positive energy condition, however this condition is not necessary for the internal consistency of the General Relativity of Relativity.

In fact the concept of mass can have different meanings in physics: the ability of matter to produce gravity (active gravitational mass), the response of matter to gravity (passive gravitational mass),the resistance of matter to accelerate (inertial mass) and it's energy equivalent.

In order to not violate the equivalence principle,we assume that the inertial and passive gravitational masses of these particle are all equal in magnitude and sign, in resemblance with positive regular matter. This will be assumed in the model presented in the rest of this essay.. More details about the compatibility with General Relativity can be found in Bondi (1957).

Let's begin by investigating the fundamental properties of negative masses.

Contrary to positive masses, the negative will repel all surroundings masses.

The most astonishing property comes from positive-negative mass pairs, when the particles have equal mass in magnitude, as they seem to violate the conservation of energy and momentum.

Imagine a body of positive mass and a body of negative mass separated by empty space. Using the language of Newtonian Mechanics, the positive body will attract the negative one, while the negative body will repel the positive body.If we confine the motion to the line of centers then we would expect the pair to experience an uniform acceleration, assuming they have absolute equal mass values (Figure 1).

The particles seem to generate a runaway motion, simply because the total mass of the system is zero. This way, it seems possible to accelerate the system to the speed of light.

In fact, as bizarre as this behaviour may seem, it does not contradict the classical laws of conservation of energy and momentum.

Consider the case of conservation of momentum. When two objects are at rest, the total momentum of the system is zero. If we induce a certain velocity in the system, the total momentum of the system remains zero, simply because the momentum of the negative mass particle is negative.

$$\Sigma P = P_+ + P_- = (+M)v + (-M)v \tag{1}$$

In the case of conservation of energy , if we start with a pair of opposite masses at rest and then accelerate them to velocity v, because the kinetic energy of the negative particle is also negative , the total energy will still equal zero.

$$2\Sigma E = 2E_+ + 2E_- = (+M)v^2 + (-M)v^2 \tag{2}$$

Given these basic properties how can they explain both dark energy and dark matter?

For the case of dark matter, quite naturally, negative mass emerges has a very good candidate, because the repelling gravitational forces between negative particles do not allow material to coalesce and form structure. Also, because of the repealing forces, they can push together regular matter and help galaxies and larger structures to form, forming an halo of negative particles encircling positive mass galaxies.

In the case of dark energy, imagine , like Einstein did, that we have negative patches of mass spread across the Universe. As they repel each other that can lead, quite naturally, to cosmic expansion. One argument against this reasoning is that , as regular matter, negative matter must dilute as the Universe expands,and so it can't explain cosmological expansion, simply because we know that dark energy has constant density (w=-1) from observations. However, this question can be solved.

One interesting consideration about the introduction of negative masses is that is introduces symmetry to the Universe. In fact , very-well understood physical forces can be modeled through division into two opposing polarised states. That is the case, for example, for electric charges (+ and-) and quantum information (0 and 1). Given the fact that cosmological models all assume a positive mass cosmology, in order to search for evidence for the model, requires a complex and long analysis of the various observations that make the ground for the current ΛCMD accepted model, but in light of the hypothesis of the existence of the illusive negative masses.

It is worth noting that negative masses are often used to speculate about the possibility of the existence of wormholes or even the construction of an Alcubierre drive, like those in Star Trek.

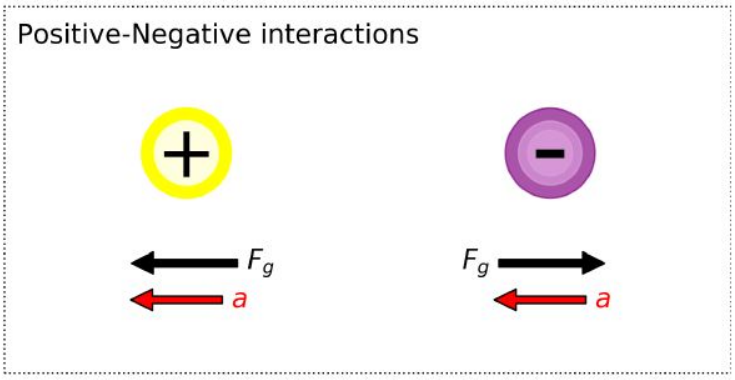

Figure 1. Schematic representation of the gravitational interaction between positive (yellow) and negative particles (purple). The black arrow represents the gravitational force (black), $F_g = -GM_1M_2/r^2$ felt by the particle and the red vector the acceleration of each particle, a=M/g. Taken from Farnes [1]

2. Theoretical results

Let's begin by considering the Einstein's Field Equations:

$$R_{\mu\nu} - \frac{1}{2}Rg_{\mu\nu} + \Lambda g_{\mu\nu} = \frac{8\pi G}{c^4}T_{\mu\nu}, \tag{3}$$

where $R_{\mu\nu}$ is the Ricci curvature tensor, R is the scalar curvature, $g_{\mu\nu}$ is the metric tensor, Λ is the cosmological constant , G is Newton's gravitational constant, c is the speed of light in the vacuum and $T_{\mu\nu}$ is the stress-energy tensor. The Friedmann equation, assuming a FLRW homogeneous and isotropic Universe, and the stress-tensor of a perfect fluid, is:

$$(\frac{\dot{a}}{a})^2 = \frac{8\pi G}{3}\rho + \frac{\Lambda c^2}{3} - \frac{kc^4}{a^2} \tag{4}$$

and the acceleration equation is:

$$\frac{\ddot{a}}{a} = \frac{-4\pi G}{3}\left(\rho + \frac{3p}{c^2}\right) + \frac{\Lambda c^2}{3} \tag{5}$$

where a is the scale factor, $H \equiv \frac{\dot{a}}{a}$ is the Hubble parameter , ρ is the total mass density of the Universe, p is the pressure, k is the curvature parameter or intrinsic curvature of space , and k/a^2 is the spatial curvature in any time-slice of the Universe.k=0 corresponds to a flat Universe, k=-1 to a open universe and k=1 to a closed universe. The pressure can be related to the density via the equation of state $p = \omega\rho$, where ω is a constant. For the negative mass, $\omega = 0$, which means the pressure is negligible. However, it can be shown that with constant creation of negative matter $\omega = -1$, reproducing the equation of state of dark energy. The content of the Universe can be separated in the following fractional parts:

$$\Omega_{M+} + \Omega_{M-} + \Omega_r + \Omega_\Lambda = \Omega \tag{6}$$

where $\Omega = 1 - \Omega_k$ and the density fractions Ω_i include positive masses M+, negative masses M-, radiation r, curvature k, and the cosmological constant Λ .In the conventional model, it is implicitly assumed that $\Omega_{M-} = 0$ and $\Omega_\Lambda > 0$.

2.1. Negative mass cosmology

Negative mass cosmology has $\mid \Omega_{M-} \mid > \mid \Omega_{M+} \mid$, a universe less than empty. Let's consider the case for a matter-dominated universe with $\Lambda = 0$. Considering eq. (4)), if ρ is negative , then the solutions exist only for k=-1, the opened universe case. The Friedmann equation can be written as:

$$(\frac{\dot{a}}{a})^2 = H^2 = \frac{8\pi G}{3}\rho_- + \frac{c^2}{a^2} \tag{7}$$

For a matter dominated cosmology with positive cosmological constant, if $\rho < 0$, then we can have the cases: k=-1,k=0,k=1. The other case is when $\Lambda < 0$, which leads again to solutions with the condition k=-1. Rewriting eq. (6) we have :

$$\Omega_{M+} + (\Omega_{M-} + \Omega_\Lambda) = 1 - \Omega_k, \tag{8}$$

We see that there exists a degeneracy between Ω_{M-} and Ω_Λ such that $\Omega_{degen} = \Omega_\Lambda + \Omega_{M-}$.
From observations,the equation of state parameter of Ω_{degen} is close to 1 .

2.2. Matter creation

Matter creation is not a new concept and has multiple references in the literature. To give two examples, we have steady-state theory of the Universe (Bondy Gold 1948; Hoyle 1960), and particle production at the expense of a gravitational field (Prigogine et al. 1988).

Let's assume the particle creation is adiabatic and happens in a universe with spatial curvature. The new stress-energy tensor becomes:

$$T'_{\mu\nu} = T_{\mu\nu} + C_{\mu\nu} \tag{9}$$

where $T_{\mu\nu}$ is the energy-momentum tensor for a fluid with equation of state $p = (\gamma - 1)\rho$, where γ is a constant, and $C_{\mu\nu}$ is the energy-momentum tensor related to the particle creation , such that

$$C_{\mu\nu} = P_C(g_{\mu\nu} + u_\mu u_\nu) \tag{10}$$

We can know write Einsteins equations as :

$$R_{\mu\nu} - \frac{1}{2}Rg_{\mu\nu} + \Lambda g_{\mu\nu} = \frac{8\pi G}{c^4}(T_{\mu\nu} + C_{\mu\nu}), \tag{11}$$

The matter creation pressure P_C can be written as:

$$P_C = \frac{-\Gamma}{3H}(\rho + p) \tag{12}$$

where $\Gamma(t)$ is the creation rate, i.e., the rate of change of the particle number in a physical volume V containing N particles (Pan et al. 2016; Paliathanasis, Barrow, Pan 2017).

The relation between ω_{eff} and $\Gamma(t)$ can be show to be:

$$\omega_{eff} = \frac{P}{\rho} = -1 + \gamma(1 - \frac{\Gamma}{3H}) \tag{13}$$

where $P = p + P_C$ and γ is constant. From this equation we see that different effective fluids and different gravitational effects can be provided by varying $\Gamma(t)$. This demonstrates that the creation of matter modifies the equation of state parameter. For a constant creation rate of $\Gamma = 3H$, one gets $\omega = -1$, effectively yielding an equation of state equivalent to a cosmological constant.

2.3. Equivalence with the cosmological constant

Negative masses that are being constantly created do not undergo the typical dilution as the Universe expands. Thus, at large scales, these masses retain a constant density. Modifying Friedmann equation one gets:

$$(\frac{\dot{a}}{a})^2 = \frac{8\pi G}{3}(\rho_- + \rho_+) - \frac{kc^2}{a^2} \tag{14}$$

Noting that ρ_- is constant one can define $\Lambda = \frac{8\pi G\rho_-}{c^2}$, such that

$$(\frac{\dot{a}}{a})^2 = \frac{8\pi G}{3}\rho_+ + \frac{\Lambda c^2}{3} - \frac{kc^2}{a^2} \tag{15}$$

As these negative masses can take the form of a cosmological constant , one can deduce that they are a property of the vacuum, and not non-relativistic matter in the normal case.

To sum up, the final Einstein's Field Equations, including matter creation are

$$R_{\mu\nu} - \frac{1}{2}Rg_{\mu\nu} = \frac{8\pi G}{c^4}(T^+_{\mu\nu} + T^-_{\mu\nu} + C_{\mu\nu}) \tag{16}$$

where the conventional $\Lambda g_{\mu\nu}$ is represented by a modified gravity term $(T^-_{\mu\nu} + C_{\mu\nu})$.

2.4. Solutions to the Friedmann Equations

Before solving the Friedmann Equations, we must first consider the existence of a spherically symmetric metric for the case of negative masses, i.e., we must find an equivalent Schwarschild Solution for negative masses. Such a spherically symmetric solution does not exist and has a naked singularity at the mass position,i.e, a singularity with no horizon. According to Penrose (1969), the naked singularity is in violation of the weak cosmic censorship conjecture.

One possible solution to the Einstein's Field Equations, however, is simply to use the results of positive regular matter, but instead we have $\rho = \rho_+ + \rho_-$.

This is the case for the solutions presented bellow. In a negative matter dominant universe the positive mass term in Friedmann Equation is negligible, so we have

$$(\frac{\dot{a}}{a})^2 = \frac{\Lambda c^2}{3} - \frac{kc^2}{a^2} \tag{17}$$

By definition $\rho < 0$ hence $\Lambda < 0$,which implies from eq. (17) that k=-1. Solving for the scale factor we have

$$a(t) = \sqrt{\frac{-3}{\Lambda c^2}} \sin \sqrt{\frac{-\Lambda c^2}{3}} t \tag{18}$$

and the Hubble parameter reads,

$$H(t) = \sqrt{\frac{-3}{\Lambda c^2}} \cot \sqrt{\frac{-\Lambda c^2}{3}} t \tag{19}$$

This solutions describe an Anti-de Sitter space (AdS) with a time varying Hubble parameter. This AdS universe has a cycle of expansion and contraction with a timescale of $\sqrt{\frac{-3\pi^2}{\Lambda c^2}}$. It is important to notice that this is a perplexing conclusion, because although negative masses are gravitationally repealing one another , the net cosmological effect seems to be for the negative energy associated with negative masses to make the universe recolapse. In other words, the universe is born in a Big Bang, then enters a phase of expansion followed by a phase of contraction which leads to a Big Crunch, and so on. This is called a cyclic cosmology. Another interesting aspect is that Λ seems to be fine tuned. If we increase the magnitude of Λ too much then the lifetime of the universe is too low to possible produce observers. Taking into account the value of Λ inferred from observation, $\mid \Lambda \mid \sim 0.3 \times 10^{-52} m^{-2}$, the lifetime of each cycle of the universe would be $\sim$ 105 Gyr. For the epoch we live on, 14 Gyr after the Big Bang, seems natural to observe the universe in an expanding phase. One notable point of interest is that the derived AdS space corresponds to one of most researched areas of string theory, the Anti-de Sitter/Conformal Field Theory correspondence (Maldacena 1999).

3. Simulations

I will present simulations in this essay from both Farnes [1] and Navarro [2]. The initial conditions in both Farnes and Navarro are the same, however there some important differences. In the case of Farnes, the simulations defined a gravitational force between two masses that dropped as the inverse of the distance d between the two masses,which gave rise to stronger forces at large distances. However, to re-run the simulations Navarro used a realistic Newtonian gravity with an inverse of d^2 dependence.

Another difference is the boundary conditions used. In Farnes, open boundary conditions are used, meaning the particles are free to spread beyond the frontier of the cubic box. Navarro instead used periodic boundary conditions, much more common, which allow to produce simulations that are automatically compliant with the cosmological principle, in the sense that the box is a typical region and there is no center, in particular, of the universe. For example, considering a homogeneous sea of negative masses particles, the open boundary conditions will make the initial box expand, as all particles repel each other., while in periodic boundary conditions the sea remains stable as all particles experience the same repulsive force from all directions. To simplify the simulations, cosmic expansion is also not considered, although it should be in the future.

3.1. Flattening of the rotation curve of galaxies

The standard galaxy rotation scenario can be described as a case where a positive mass test particle, of mass M_+, is located a distance r from the galactic center. For a stable circular orbit , the gravitational force is equal to the centripetal force, which provides

$$\frac{GM_+M_*}{r^2} = \frac{M_+v^2}{r} \tag{20}$$

The tangential velocity of the stars v around the center of the galaxy as a function of radius r can then be written,

$$v = \sqrt{\frac{GM_*}{r}} \tag{21}$$

This expression defines what is know as a keplerian rotation curve.

However, very few galaxies show evidence for a keplerian rotation curve . H_α and radio HI observations of galaxies both indicate that rotation curves remain essentially flat out to several tens of kpc, thus proving evidence to the existence of dark matter (Rubin Ford 1970;Rubin, Ford Thonnard 1980; Rubin et al. 1985.)

Let's now consider the following. We have a galaxy composed of positive matter surrounded by an halo of constantly created negative matter, in other words , the positive particles are embedded in a negative fluid that resembles a cosmological constant. We assume that the mass of the galaxy is concentrated at the center.

One important step is to examine the Newtonian limit of the field equations, i.e. when we are in the weak field limit and v«c. Writing the Poisson equation we have

$$\nabla^2\phi = 4\pi G\rho_+ - 4\pi G\rho_{vac} = 4\pi G\rho_+ - \Lambda c^2 \tag{22}$$

where ϕ is the scalar potential and ρ_+ is the positive mass density.

The solution is

$$\phi(r) = -\frac{GM_*}{r} - \frac{\Lambda c^2}{6}r^2 \tag{23}$$

which gives the potential a distance r from the galactic center.In the limit $\Lambda = 0$, we retrieve the know potential for Newton's Law of Gravitation. Equation (21) is then modified to become,

$$v = \sqrt{\frac{GM_*}{r} - \frac{\Lambda c^2}{3}r^2} \tag{24}$$

If we put $\Lambda = 0$, naturally we obtain the standard rotation curve, but for non-zero values of Λ the curve is modified in such a way that it increases linearly towards the outskirts of a galaxy , in such a way that $v \propto (\mid \Lambda^{1/2} \mid c/\sqrt{3})r$. Some studies found that most rotation curves are rising slowly even at the farthest measured point (Rubin, Ford, Thonnard 1980). So there is s consistency between the theory and the observations. Some models of galaxy curves are presented in figure 2.

The calculated value of Λ in the vicinity of galaxy is larger in magnitude than that of the intergalactic medium. This stems from the fact that the negative masses coalesce into a diffuse halo-like structure.

From the simulations of Farnes, we see that the radial velocity profile for the stars follows a flattened rotation curve, taking into account the uncertainties of the measurements.

Despite an initial excitement with these calculations, we have to take into account the following simplifications that were made in Farnes: (1) in reality, galaxies have a radially-dependent mass profile and don't have all mass at the center; (2) a typical galaxy has separate bulge, halo and disk, none considered in the model ; (3) the halo mass profile may also be asymmetric, contrary to the simplification used in calculations of Farnes.

Navarro re-run the simulations and used the stellar dynamics produced to plot the radial velocity profile of the stars in the galaxy. Contrary to Farnes, he found out that the orbital velocity of stars drop with the distance r from the center, which clearly does not support the claim that negative masses can reproduce the flattening of the rotation curves of galaxies. The plot is on figure 3 .

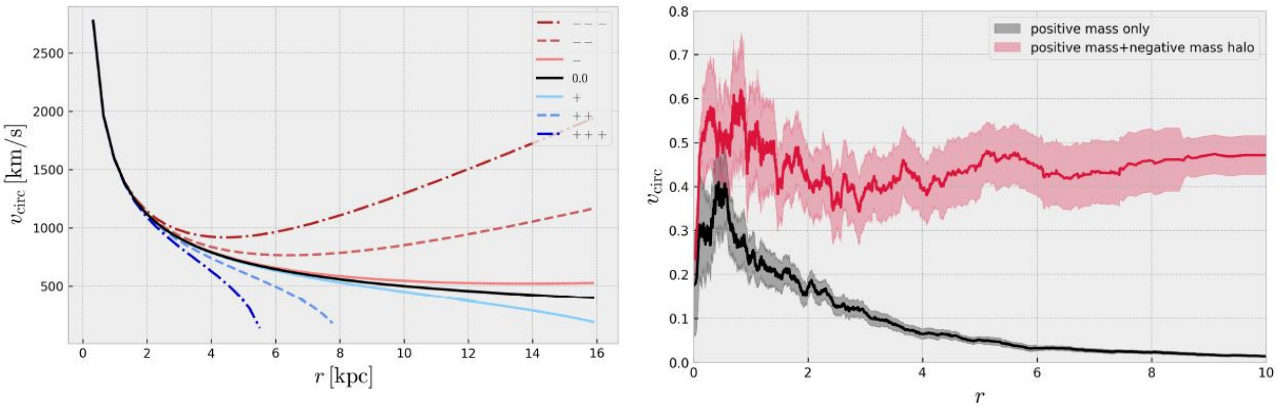

Figure 2. Left: Predicted circular velocity as a function of radius, for a galaxy of similar size and mass to the Milky Way and that is influenced by a cosmological constant. The displayed rotation curves are for increasing magnitudes of a positive (in blue) and a negative (in red) cosmological constant. The Keplerian curve with $\Lambda = 0$ is also shown (in black). **Right:** Circular velocity in function of the radius, extracted from the simulations. Taken from Farnes [1]

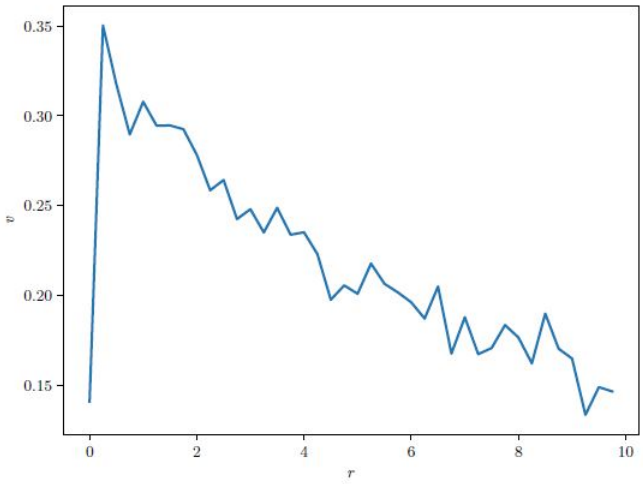

Figure 3. Average orbital velocity as a function of radial distance to the galactic center. Taken from Navarro [2]

3.2. Formation of dark matter halo

To test the formation of dark matter halos from negative masses it's necessary to do N-body 3D simulations. The first simulation I present was done by Farnes (2018) and seems to reproduce a dark matter halo.

The properties of his simulation were the following. The positive mass galaxy is initialized with spherical symmetry in accord with the Hernquist model (Hernquist 1990). The galaxy had a total of 5000 particles and total mass set to $M_+ = 1$. This patch of positive mass is inserted in a cube with volume 200^3 of particles of negative mass. All particles, both positive and negative, had zero initial velocity and were uniformly distributed in position. The negative mass patch had a total of 45000 particles and a total mass set to $M_- = 3$. Also, the positive galaxy was set to have a radius and mass equivalent to that of the Milky Way galaxy ($R = 15kpc, M = 5.8 * 10^11 M_{sun}$). Finally, the simulation was run for a total time of 21.5 Gyr.

The results show two major processes. In the first process, the negative particles in the outskirts of the cube are repealed by other negative ones such that the cube expands. In the second process, near the central positive galaxy, the negative masses will be attracted and slushed to and from either side of galaxy until they reach an dynamical equilibrium, forming an halo that surrounds the positive galaxy and extends out to several galactic radius.

Observations of galaxies typically indicate an approximately constant dark matter density in the inner parts of galaxies. However, simulations of positive mass dark matter show a steep power-law behaviour. This is know as the cuspy halo-problem (de Blok 2010).

In general, in simulations for positive mass particles, these accumulate in a central region thanks to the inward gravitational attraction, but in the case of negative matter that doesn't happen because of the repealing action, and so the simulations of these particles show an homogeneous distribution of negative particles, which seem to resemble that of the observations. In figure 4, the magnitude of the simulated negative mass density profile is compared to both the cuspy Navarro–Frenk–White(NFW) profile derived from standard N-body simulations with positive mass dark matter (e.g. Navarro, Frenk, White 1997), and to the non-cuspy, observationally motivated, Burkert density profile (Burkert 1995).

We can see that negative mass has the potential to provide at least a partial solution to the cuspy-halo problem.

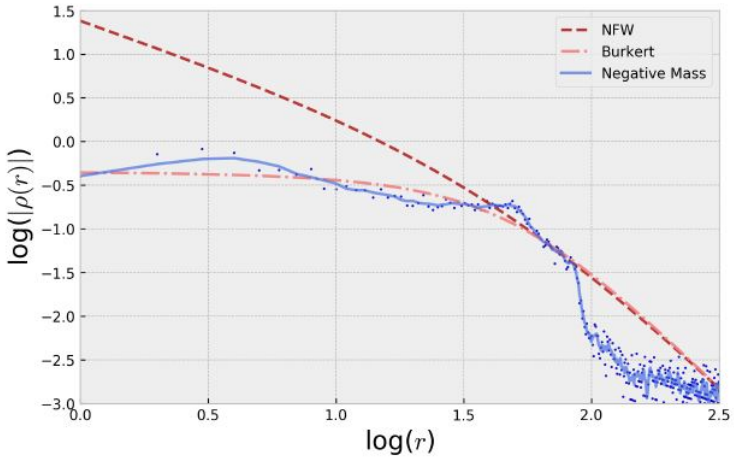

Figure 4. Plot of the magnitude of the density profile as a function of radius from the galactic centre, as extracted from the N-body simulations. (1) in blue we have the empirically determined density profile for negative masses (2) in dark red,the profile for NFW (3) in light red,the profile based on observations (Burket). Taken from Farnes [1]

Navarro tried to derive an analytical solution to the radial density profile of the spherical negative mass halo, before re-running the simulations. He assumed a initial constant density ρ_i^H for the halo and no initial velocity for the particles. At any given time , the amount of halo particles contained in a spherical shell of radius r and thickness dr is given by the number of particles that have fallen from the higher layers, balanced by those that have fallen from the opposite side of the halo , crossed the origin and are moving towards r. Then he calculated the probability that a particle that originated at shell r′ is inside r at any given time is the ratio of the time the particle spends at r divided by the time it needed to fall and reach that position,

$$P(r',r)dr = \begin{cases} 0, & r' < r \\ \frac{d\tau}{T}, & r < r' < R^H \end{cases} \tag{25}$$

with

$$\frac{d\tau}{T} = \frac{dr}{v(r',r)}, T = \int_0^{r'} \frac{dr''}{v(r',r'')} \tag{26}$$

where v(r′,r) is the velocity that particles that departure from r′ have when they reach r. Then it's necessary to solve the following equation for the halo radial density profile,

$$4\pi r^2 \rho^H(r)dr = \int_r^{R^H} \rho_i^H 4\pi r'^2 P(r',r)dr'dr = \int_r^{R^H} \rho_i^H 4\pi r'^2 \frac{1}{v(r',r)} \frac{1}{\int_0^{r'} \frac{dr''}{v(r',r'')}} dr'dr \tag{27}$$

To solve this equation , we need an expression for the velocity v(r′.r). Given the symmetry of the problem, we may express the gravitational field as,

$$g(r) = -G\frac{-m(r)}{r^2} \tag{28}$$

where G is the gravitational constant, m(r) is the cumulative mass at distance r from the center of our galaxy. This expression is valid for both negative and positive masses and the acceleration is also equal to g, so we can write the following:

$$v^2(r', r) = -2G\int_{r'}^{r} \frac{m(r'')}{r''^2} dr'' \tag{29}$$

Given the two last equations, we can find a solution for $\rho^H(r)$, One possible solution is,

$$\rho^H(r) = -\rho_0^H e^{-kr} \tag{30}$$

The radial density profile obtained in Navarro simulations is showed in Figure 5. The simulation reproduces the analytical solution of an exponentially decreasing density.

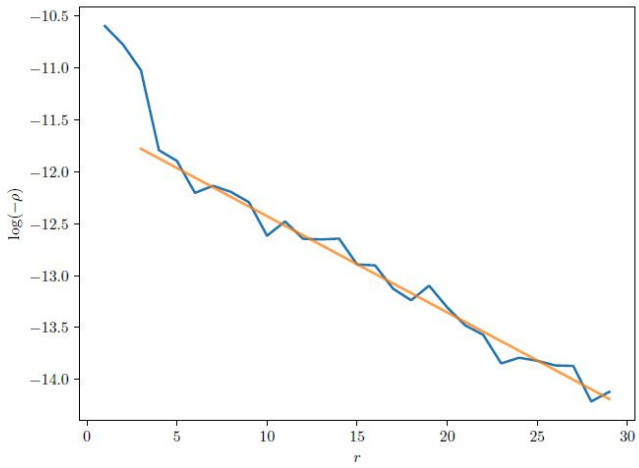

Figure 5. Radial density profile of the negative-mass halo in the galactic simulation. The axis of ordinates is logarithmic. The orange line shows an exponential density profile for reference. Taken from Navarro [2]

Although in both simulations halos of negative mass around the galaxies were produced, Navarro argued that the ratio of halo to core mass generated was between 0.3 and 0.8 , while in reality dark matter halos are four to five times more massive that their baryonic counterparts. As we can see, the halos simulated were too light. In fact, what happens is that the halo particles can only be held together due do the positive mass galaxy, giving some stability to the system. This only happens if the core mass is bigger that the halo mass, producing a total net force towards the core. If we are in the opposite situation, then the outer layers of the halo will experience a total net force outwards, which will cause those same layers to disperse to intergalactic space.

Another problem with the formation of the halo is it's shape. From the Navarro simulations, it can be seen that the form of the halo is not spherical, but is rather elongated towards a certain direction, corresponding to the direction of runaway motion. This shape can be observed in figure 7, on the right image. The physical mechanism behind this motion is explained in the section about Runaway motion.

The simulations from Farnes and Navarro concerning the formation of a dark matter halo are presented in figures 6 and 7,respectively.

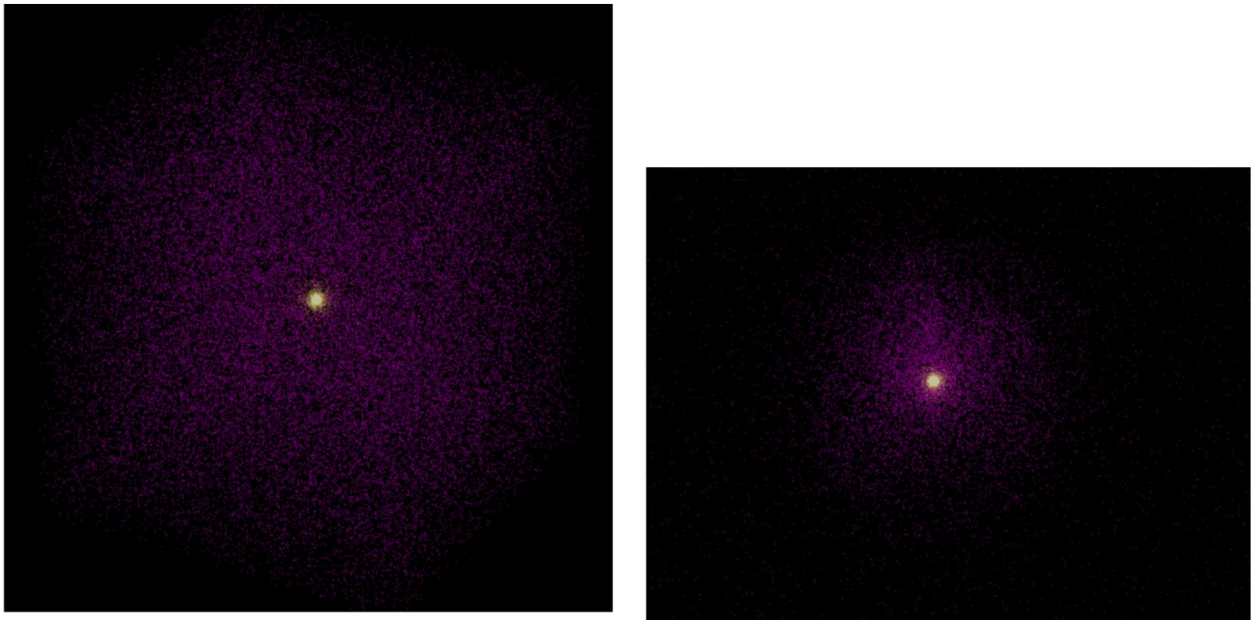

Figure 6. N-body simulations showing the formation of a non-cuspy dark matter halo from an initially motionless particle distribution of 45,000 negative masses (in purple), that surround a Hernquist-model galaxy of 5,000 positive masses (in yellow). Taken from Farnes [1].

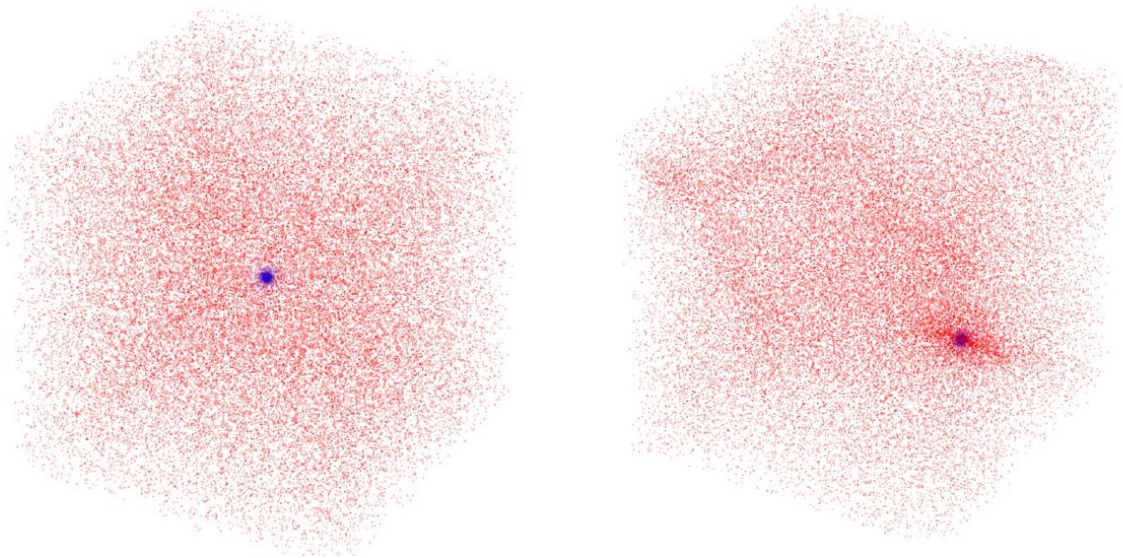

Figure 7. Simulation of the formation dark matter halos. Red points represent positive masses and blue represent negative particles. On the left, there is an initial spherical distribution of positive mass particles embedded in a uniform distribution of negative masses. On the right we can see an halo formed around the positive mass , however it is not spherical, but has a rather elongated shape [2].

3.3. Structure Formation

To test the hypothesis of the possibility of structure formation from negative masses, Farnes created the following model.

We have a volume of 200^3 . We set equal amounts of positive and negative particles, 25 000 each , and place them uniformly distributed in this volume. The total mass of the cube is +0.0, assuming $M_- = -1$ and $M_+ = +1$..The size of the simulation was 200 Mpc and was run for 21.5 Gyr.

The results were the appearance of a complex network that comprises filaments,voids and rich clusters. It is unclear, however, what was the dominant effect in formation of this structure: if the additional pressure from negative matter being attracted towards positive matter leading to more rapid structure formation comparing to our supposed positive matter universe; or if the expansion resulting from the negative masses repulsion property slows the formation process of structure.

The conclusion is that negative masses have the potential to allow the formation of structure, however more N-body simulation are needed in the future to compare the model results with the real observations of the large-scale filaments and voids properties.

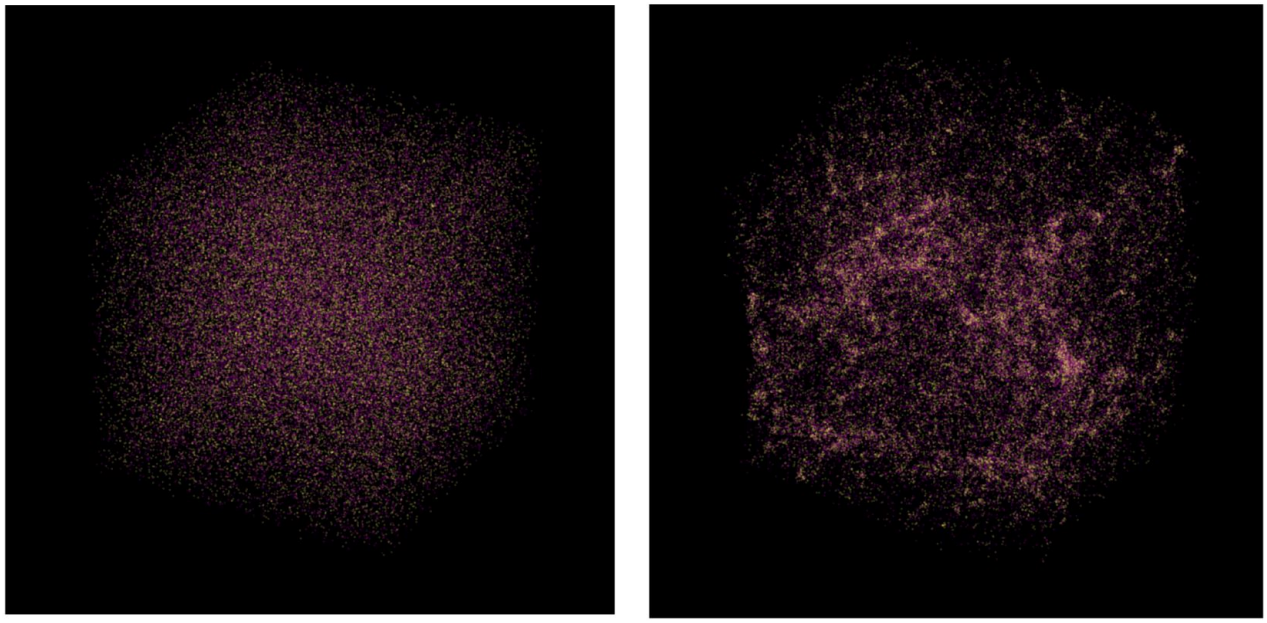

Figure 8. N-body simulations showing the formation of large-scale structure from an initially motionless, uniform, particle distribution of 25,000 positive masses (in yellow) and 25,000 negative masses (in purple). Taken from Farnes [1]

As a response, Navarro also tested the possibility of structure formation in a negative mass cosmology, however the results are quite different due to the periodic boundary conditions he used.

In open boundary conditions, the formation of structure is much faster than in periodic boundary conditions, because each point feels approximately the same force from all directions in the case of open boundary conditions.

Navarro used a box of 307 Mpc and a total of 25 000 particles. The total matter density was initially set to $2.6x10^{-27}kgm^{-3}$. In the first simulation, all the particles had positive mass, while in the second 84% of the particles had negative mass. The number of negative particles dominates and shows that the net effect is such that the mutual repulsion between the particles will smooth out inhomogeneities. Only later on, the positive masses begin to coalesce and attract the negative ones. This can be seen in figure 9.

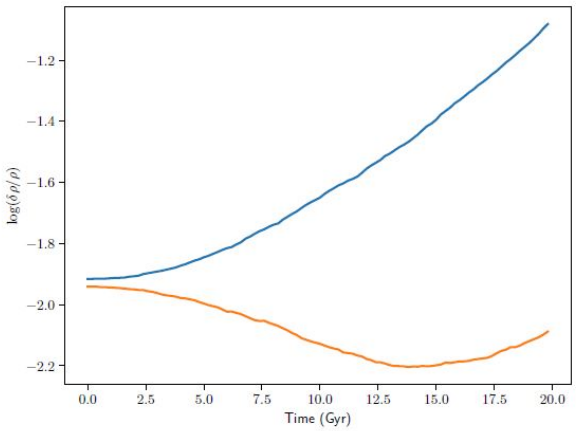

Figure 9. Matter density contrast in function of time for two different simulations. Blue: all matter is positive mass. Orange: 84% of matter has negative mass. We can see than near 15 Gyr the "orange" universe starts to aggregate matter after a period of density decreasing. Taken from Navarro [2]

4. Runaway motion

The prediction of gravitational dipoles accelerating to a speed c has been one of the strongest arguments against the existence of such an exotic type of matter (Bonnor 1989). This is due to the knowledge that conventional massive particles can't accelerate to the speed of light and we also don't observe those relativistic particles.

For the first part, from a theoretical point of view, negative mass particles respect the conservation of energy and momentum laws. Second, some observations indicate the existence of ultra-high energy cosmic rays whose origin is unclear (Pierre Auger Collaboration2017), but are extra-galactic in origin.

In summary, Farnes argument was that the possible existence of runaway motion was a constraint of his model and not a problem. Also, in the simulations he didn't observe this effect, so he concluded that the runaway motion , if it happens, is very rare and the runaway particles must be highly-scattered thanks to large scale Brownian motions (Landis 1991).

In order to test his conclusion, he admits that more extensive simulations with a greater number of particles could help constrain better the rate at which runaway particles form and also their density, which in turn could be compared with the density and distribution of ultra-high energy cosmic-rays from independent observations.

Navarro performed more simulations, with the starting conditions and properties described in the beginning of this chapter. However, he described a problem. Despite the center of mass being initially at rest, it keeps gaining acceleration in a random direction during the entire run. He perceived this as a "galaxy scale" runaway motion. Although in the beginning, the total force exerted on the positive mass core by the negative mass halo is zero, thanks to the situation of spherical symmetry, a slightly perturbation in the position of a bunch of negative particles creates an instability in the system that starts the runaway motion.

In mathematical language, the system is in equilibrium if the second derivative of the gravitational potential, at the origin of the system, is positive. So let's check this out,

$$\frac{d^2\phi(r)}{dr^2} = -\frac{dg(r)}{dr} = G\frac{d}{dr}(m(r)\frac{1}{r^2}) = G\frac{dm(r)}{dr}\frac{1}{r^2} - Gm(r)\frac{3}{r^2} \tag{31}$$

Approximating the mass using the density at the origin, $m(r) \sim \frac{4}{3}\pi r^3\rho_0$ Substituting in eq. (31), we get,

$$\frac{d^2\phi(r)}{dr^2} = 4\pi G\rho_0 - 4\pi Gr\rho_0 \tag{32}$$

and for r=0,

$$\frac{d^2\phi(r)}{dr^2}(r=0) = 4G\pi\rho_0 \tag{33}$$

Because $\rho_0 < 0$, the second derivative of ϕ is negative and so we have an unstable equilibrium. That is what we can observe in figure 10.

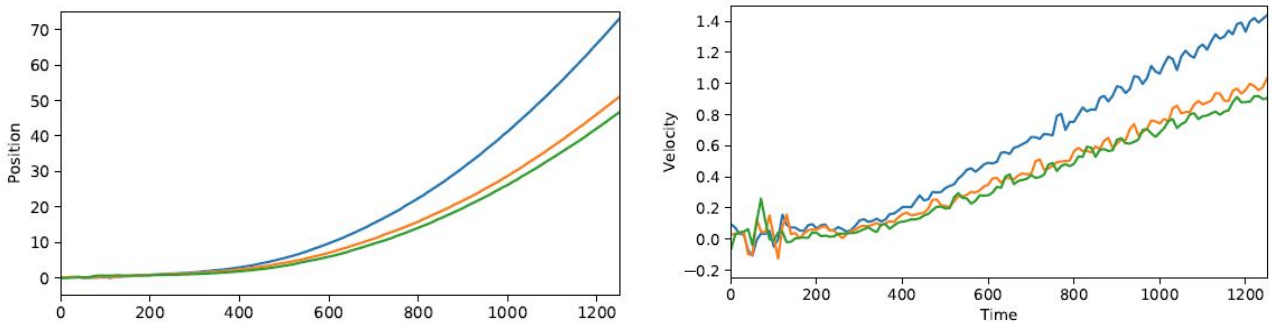

Figure 10. Left: Evolution of the position of the galactic core center of mass as a function of time. The blue, orange and green lines represent,respectively, the x,y and z axis coordinates. **Right:** Velocity components of the center of mass of the core as a function of time. We observe that after an initial period of stability and galactic size growth, the core begins a runaway motion of constant acceleration.Taken from Navarro [2]

5. Observational evidence

From the chapters above, we see that there is possibility that negative masses can explain both the flattening of the rotation curves of galaxies and also behave, in large scales, as a cosmological constant, as proved by the calculations. A starting point to search for evidence for this model is to look in the literature for results that may be in agreement with the model.

5.1. Supernova observations of the acceleration of the Universe

There is degeneracy between Ω_- and Ω_Λ, so in a standard ΛCMD cosmology, where we assume from the beginning $\Omega_- = 0$, it is natural to infer a positive cosmological constant instead of a negative density parameter.

Since the 1990's we know, with high confidence, from observations of high-redshift supernovas, that the universe is expanding due to a positive cosmological constant (Riess et al. 1998; Perlmutter et al. 1999). In the latest work by Perlmutter, is is assumed that $\Omega_M < 0$ has a probability of zero. In Riess et al, a definition was used such that negative values for the current deceleration was generated by a positive constant, instead from "unphysical, negative mass density".

Re-running their analysis without this definition, and demanding that $\Omega_\Lambda \equiv 0$, it forced them to relax the requirement that $\Omega_M \geq 0$. Then, the results read $\Omega_M = -0.38 \pm 0.22$ and $\Omega_M = -0.52 \pm 0.20$, according to the fitting procedure used. Despite the fact that by Occam's razor negative masses introduce more complexity to the problem,without necessity, is it also true that without constraining $\Omega_M \geq 0$ we are making one less assumption in the model.

5.2. CMB observations of a flat Universe

From CMB observations, we were able to measure the precision position of the first acoustic peak. The scale is about one degree, which points to a flat, k=0, universe (Spergel et al. 2003). This seems to rule out the open universe,k=-1,derived for negative masses.

One argument that protects the existence of negative masses is that the above curvature is a local result, resulting from the fact that the universe is exceptional large and at large scales has k=-1, however because of that we can't measure its value properly. As a side result, this type of argument also seems to allow any kind of geometry we want for the universe.

Accepting the position of the first peak from CMB measurements and comparing with the position of the peak calculated for a negative mass open universe with k=-1, we see that it should be located at a much smaller angle that observed.

The ratio of the angular distances for the negative mass universe and the universe at redshift z=1100 (last scattering surface) is

$$\frac{d_A^-(a)}{d_A^{\Lambda CMD}(a)}(z=1100)=169 \tag{34}$$

We know that the angular position of the first CMB peak is defined by the angle under which the sound horizon is seen at recombination

$$\theta=\frac{\chi_S(z_*)}{d_A(z_*)} \tag{35}$$

where $\chi_S(z_*)$ is the sound horizon, $d_A(Z_*)$ is the angular distance and z_* is the redshift of the last scattering surface.

In an expanding universe, the sound horizon can be written,

$$\chi_S=\int_0^t c_s\frac{dt'}{a(t')}, \tag{36}$$

where c is the speed of light, a(t) is the scale factor evolution in time and c_s is the speed of sound.

In a universe of negative and positive masses, the sound creation mechanisms are significantly altered. It happens that in this kind of cosmology,sound is generated in the interface between negative and positive patches of mass. It can be shown that the most important epoch for sound generation is the quark-gluon phase transition, corresponding to a temperature $T\sim 170MeV$ (Benoit-Lévy Chardin,2012). Also according to the same authors, the acoustic waves only propagate in the plasma while positive and negative masses are in contact. Using this formalism we obtain the position of the first CMB peak,

$$l_a\sim\pi\frac{d_A}{\chi_S(z_*)}\sim 160. \tag{37}$$

The standard result is $l_a\sim 360$

This means that within a factor of 2, the negative matter cosmology can reproduce the position of the first CMB peak, having the potential to be consistent with CMB observations.

The precise value of l_a can be modified by several factors associated with negative masses. For example, in the interface between negative and positive regions, as they are in contact, that could give rise to runaway motion and possible annihilation of positive-negative pairs.

During the formation of sound waves, both matter creation and the exact physical properties of negative masses must be taken into account. This factors could modify the value of l_a and could also help constrain the position of the second and third peaks of the CMB, comparing the results with data. All these question have not be considered until the moment of writing.

In conclusion, the model has a very good fit to the data, however by allowing dark matter and dark energy to have negative energy, it may possible to fit the data with the modified model.

5.3. Galaxy clusters data

Galaxy clusters had a important role in establishing the current ΛCMD model (e.g. Allen, Evrard & Mantz 2011). Several results in the literature have hinted on the presence of negative matter in clusters.

For example, Chandra measurements on the merging cluster Abell 2034 founds hints of a negative mass and therefore did not plot the data (Kempner, Sarazin, Markevitch 2003); regions in the mass profile in the galaxy NGC 4636 gave "unphysical" negative masses (Johnson et al. 2009); in the NGC 3411 galaxy group the total mass was found to decline with increasing radius - requiring material with negative mass (O'Sullivan et al. 2007), and a number of strong and weak gravitational lensing studies found indications of negative masses (Liesenborgs, De Rijcke, Dejonghe 2006; Diego et al. 2007). These findings may be due to systematic errors or biases , however, together with the above possible evidence, is at least reasonable to consider the possibility of existence of negative matter and reanalyse these studies.

5.4. Discussion

The current most accepted model of the universe is the model with cold dark matter and a cosmological constant. It can be said that negative mass cosmology is a modified model, with positive-positive interactions corresponding to baryons, positive-negative interactions corresponding do dark matter and negative-negative interactions corresponding do dark energy. In a way, we could reparameterise the standard $\Omega_b + \Omega_{CMD} + \Omega_\Lambda$ as $\Omega_{++} + \Omega_{+-} + \Omega_{--}$.

An important aspect of the negative mass dominated cosmology is a universe with negative spatial curvature and with a negative cosmological constant ($k = -1, \Omega_M < 0$ and $\Lambda < 0$)

In the face of the enormous evidence supporting the ΛCMD model it seems unwise to postulate and defend the existence of negative masses. In fact, all recent results point to a flat universe,k=0, filled with positive matter and a positive cosmological constant ($\Omega_M > 0$ and $\Lambda > 0$). We must consider, however, that all these results stemmed from the assumption that all mass in the universe is positive.

At least in a skeptical and curious point of view, its interesting to explore the possibility of existence of such exotic matter and even if we find out it isn't true, at least the results obtained may be in the future important for some other theory. String theory for example has no way of finding observational evidence with our current technology, however, the mathematical ideas and results may somehow be useful to construct other theories in the future. Quantum theory is also a very weird theory, but we know it's correct and one of the most tested and accepted theories of the present, so why can't we consider the case for negative masses?

Some important aspects to study in the future, in order to construct a more complete model of a negative mass dominant universe are the following:

- Validate the theory through the direct capture and detection of a negative mass particle. Particles with runaway motion would be highly scattered due to Brownian motion and would produce an isotropic background on the sky. It is possible that this background turns out to be consistent with the observations of ultra-high energy cosmic-rays.
- Models with particles whose inertial mass does not have the same sign as the gravitational mass.
- Negative matter can be modelled as matter or vacuum energy. Some interesting ideas propose that space-time is a large-scale condensate arising from more fundamental constituents (e.g. Liberati Maccione 2014). There is a change that negative masses may be interpreted as a quantised form of energy associated with space-time itself.
- Reconcile the presented theory with Standard Model of Particle Physics and figure out if negative masses could be generated by the Higgs mechanism or even if a Grand Unification Theory is possible upon the introduction of negative masses in the theory.
- In the know theories of quantum gravity, the carrying particles are gravitons and have mass zero and spin 2. According to these theories, the negative particles would attract each other and not repel. So, one path to discover would be the possibility of composite states of gravitons, bounding positive and negative masses together.

References

1. Farnes, J.S.; A unifying theory of dark energy and dark matter: Negative masses and matter creation within a modified framework;Astronomy & Astrophysics; **2018**; arXiv:1712.07962v2
2. Navarro, H.Socas.; Can a negative-mass cosmology explain dark matter and dark energy?; Astronomy & Astrophysics; **2019**; arXiv:1902.08287v2

Proceedings

The expansion of space and the cosmological red shift

Johannes Brinz

[1] johannesbrinz@web.de

Received: 27.01.2020

Abstract: One new concept of general relativity theory is that of an expanding space. The objective of this work was to examine what it actually means, that space is expanding and how such an expansion could be measured. Since expansion is usually measured with respect to space, providing an constant outer reference frame it is not obvious on first sight, what an expansion of space might be. This questions were examined first adopting a classical point of view and than changing to an relativistic understanding of the universe. The conclusion drawn in this article is, that expansion of space only makes sense in general relativity and describes the expansion of the commoving space with respect to physical space. The expansion of space becomes measurable using the concept of the cosmological red shift.

---

1. Introduction

General relativity radically changed the view scientists have on space and time. One major aspect of general relativity is the curvature of space time and the expansion of space. Both are concepts which are very different from our conception of the world, which makes them difficult to grasp for beginners. Most physics students take lectures in general relativity and for a deep understanding it is important to clear the terminology and the basic ideas. The question the present work tries to answer is the following: *What does it mean, that space is expanding?* It therefore takes a philosophical perspective on the subject of space, time, space time and the basic concepts of general relativity.
The present work is divided in three parts. The first part is supposed to make clear the problem of thinking of an expanding space. It deals with the conception of space and time in classical mechanics. Three problems are discussed separately: First the question how physics would change in an expanded space. Second how and if it is possible to experimentally proof such an expansion from a classical point of view. Third the question of an possible reference frame against which the expansion of space could be measured.
The second part discusses the expansion of space in special and general relativity. The main argument here is, that only the concepts of a curved space time and the distinction in commoving and physical space make the idea of an expanding space possible. Expansion of space means an expansion of the commoving space with respect to the physical space.
The third and last part of the present work answers the question how to measure the expansion factor. It therefore deals with the cosmological red shift. The author tries to make explicit how the cosmological red shift is connected to the curvature of space time and the expansion of space. In this context again the distinction in physical and commoving space becomes important.
The derivations of this work follow roughly the "No-nonsense introduction to general relativity"[1] by Sean M. Carroll, the third part of "Cosmology" by Daniel Baumann[2] and the second part of "Cosmology" by David Tong [3].

2. The classical conception of space and time

Lets at first take a look at the topic from a classical point of view. In classical mechanics space is a three dimensional object with a x, y and z component. No what does it mean to say, that three dimensional space is expanding? The point I want to argue for is, that it does not mean anything. And this for three reasons. First from a practical point

---

[1] Sean M. Carroll, *A No-Nonsense Introduction to General Relativity*, Enrico Fermi Institute and Department of Physics,University of Chicago, 2001 pp. 2-5. http://courses.theophys.kth.se/SI2370/Carroll$_G R_s ummary.pdf$(23.01.2020)
[2] Daniel Baumann, *Cosmology- Part III Mathematical Tripos* pp. 8. http://theory.uchicago.edu/ liantaow/my-teaching/dark-matter-472/lectures.pdf (24.01.2020)
[3] David Tong, *Cosmology- Part II Mathematical Tripos* pp 13 - 15, http://www.damtp.cam.ac.uk/user/tong/cosmo/one.pdf (27.01.2020)

of view, expanding space has no consequence on the actual physics of the universe. Second a epistemic problem arises. A classical theory proposing space was expanding would be irrefutable and therefore unscientific. Thirdly the meaning of the term "expansion" implies the existence of an outer reference frame, which is not given in the case of an expanding three dimensional space.

What does it mean, that an expansion of the three dimensional space would have no consequences on the physics of the universe? This means, that all objects would behave exactly the same as in a not-expanded space. All equations would yield exactly the same results as in a non-expanded space. from within the three dimensional universe no change would be recognizable and an outer perspective cannot be adopted, since every observer itself must be within the universe. Lets take a look at a very simple example. A car driving with a certain velocity along the x axis. It starts at $x = 0\,m$ and wants to reach a place at $x = 100\,m$. Lets assume, the car has a constant velocity of $v = 10\,\frac{m}{s}$. It is easy to see, that it takes the car exactly $10\,s$ to arrive at its destination. Now what exactly would happen if the space would have expanded? The lines which represent the $10\,m$ marks, the $20\,m$ marks, etc. would have grown further apart, the size of the car would have increased, and so forth. But those are changes only visible from the outside. From the inside perspective nothing changes. In both cases the car drives exactly one $10\,m$ line per second and therefore reaches its destination at exactly $t = 10s$. Also all the other parameters stay the same: the size and the weight of the car, the distance, etc. The physics of the system did not change. The difference between the two systems can only be observed from an outer perspective, not from within the system itself. In case of the universe being the system and space being stretched, such an outer perspective does not exist.

This in mind, one might argue, that space is not itself a physical object, but rather a theoretical concept. Following the argumentation of Immanuel Kant[4] space is an a priori concept, which makes the description of physical objects possible in the first place. We are not able to imagine an outer world without the concept of a three dimensional space in which physical objects are located. It is impossible to do physics without the conception of a three dimensional space. Therefore the idea of space precedes every empirical knowledge and can itself not be physical. This gives rise to another problem from an scientific point of view. The claim that space was expanding becomes irrefutable. There can be no empirical evidence, which proves or disproves this claim. In philosophy of science there is a vast agreement, that scientific theories cannot be proven for good. It was Karl Popper[5] who first argued, that general theories cannot be proven by singular instances of observation. An infinite amount of observations would be necessary to prove a general claim. No matter how many observations confirm the claim, that all swans are white, it is always possible that the next swan observed is black. It is therefore only possible to falsify general claims such as scientific theories and the best scientific theories are those, which are easy to falsify, but not yet falsified. Theories which are immune against empirical falsification, as are most conspiracy theories, are not scientific. The claim now, space was expanding, cannot be falsified empirically and therefore is unscientific.

Further following Kants arguments, the concept of space not only precedes every empirical knowledge but also every inner experience ("innere Erfahrung"[6]) and thus even theoretical concepts. If we imagine for example a geometric object, lets say a cube, we do so *in space*. We are not capable of imagining geometrical objects without imagining space. Now it is easy to imagine a cube expanding or contracting, even though it is only a theoretical concept. But it is not possible to imagine space itself expanding, because the idea of space must already be established before the geometrical operations of expansion and contraction can even be thought of. The expansion of a straight line can be thought of as the relative motion of its staring end ending point. But what would the expansion of a line segment of space it self be? Its staring end ending point are per definition fixed in space and no relative motion is possible. Space is a necessary condition for every empirical and theoretical conception. It simply does not make sense to speak of the expansion of space form a Kantian point of view.

---

4 Immanuel Kant, *Critique of Pure reason* B 38/39.
5 Karl Popper, *The logic of scientific discovery*, 1934.
6 Immanuel Kant, *Critique of Pure reason* B 66.

3. Expansion of space in special and general relativity

3.1. Special relativity

The discovery of the special relativity theory changed the view scientist look at time and space profoundly. Special relativity claims, that there are not two separate concepts of space and time, but rather one four dimensional space-time. Objects do not move in space as a function of time. Motion reduces to segments of space-time, sets of points in a non Euklidean four dimensional Minkowski space. Special relativity implies, that different observers do not agree on the distance between two events, nor on the time having past between them. What they do agree on is the so called space time interval ds, which is defined as follows. [7]

$$\begin{aligned} \mathrm{d}s^2 :=& \eta_{\mu\nu}\mathrm{d}x^\mu \mathrm{d}x^\nu && (1)\\ =& -c^2\mathrm{d}t^2 + \mathrm{d}x^2 + \mathrm{d}y^2 + \mathrm{d}z^2. && (2) \end{aligned}$$

Following the Einstein notation and $\eta_{\mu\nu}$ being the so called Minkowski metric.

$$\eta_{\alpha\beta} = \begin{pmatrix} -1 & 0 & 0 & 0 \\ 0 & 1 & 0 & 0 \\ 0 & 0 & 1 & 0 \\ 0 & 0 & 0 & 1 \end{pmatrix} \tag{3}$$

[8] Equation (2) now puts the spatial coordinates x, y and z in a relation with the time coordinate (ct). This maybe answers the question for an outer reference frame. It might mean that expansion of the spatial coordinates of the space time becomes possible in the sense of an expansion with respect to a certain time interval $\Delta(ct)$, the physical distance, light travels in a certain time interval. Nevertheless, expansion of space becomes more interesting in the context of general relativity.

3.2. General relativity

The expansion of space is a consequence of the general relativity and follows directly from the concept of a curved space time. In the centre of general relativity stands the Einstein equation.[9]

$$G_{\mu\nu} = \frac{8\pi G}{c^4} T_{\mu\nu} \tag{4}$$

$$R_{\mu\nu} - \tfrac{1}{2} R g_{\mu\nu} = \frac{8\pi G}{c^4} T_{\mu\nu} \tag{5}$$

[10] Where R is the Ricci curvature tensor, R is the scalar curvature, g is the metric tensor, G is Newton's gravitational constant, c is the speed of light in vacuum, and $T_{\mu\nu}$ is the stress–energy tensor. The Einstein equation connects the curvature of the space time on the left hand side to the energy distribution of the universe on the right hand side.
Here now may be the answer to the question in what sense space can expand. Figure 1 shows a schematic illustration of the curved space time.

---

[7] Sean M. Carroll, *A No-Nonsense Introduction to General Relativity*, Enrico Fermi Institute and Department of Physics,University of Chicago, 2001 p 3. http://courses.theophys.kth.se/SI2370/Carroll$_G R_s ummary.pdf$(23.01.2020)

[8] Sean M. Carroll, *A No-Nonsense Introduction to General Relativity*, Enrico Fermi Institute and Department of Physics,University of Chicago, 2001 pp. 3. http://courses.theophys.kth.se/SI2370/Carroll$_G R_s ummary.pdf$(23.01.2020)

[9] Sean M. Carrolll, *A No-Nonsense Introduction to General Relativity*, Enrico Fermi Institute and Department of Physics,University of Chicago, 2001 pp. 11-16. http://courses.theophys.kth.se/SI2370/Carroll$_G R_s ummary.pdf$(23.01.2020)

[10] Sean M. Carrolll, *A No-Nonsense Introduction to General Relativity*, Enrico Fermi Institute and Department of Physics,University of Chicago, 2001 p 14. http://courses.theophys.kth.se/SI2370/Carroll$_G R_s ummary.pdf$(23.01.2020)

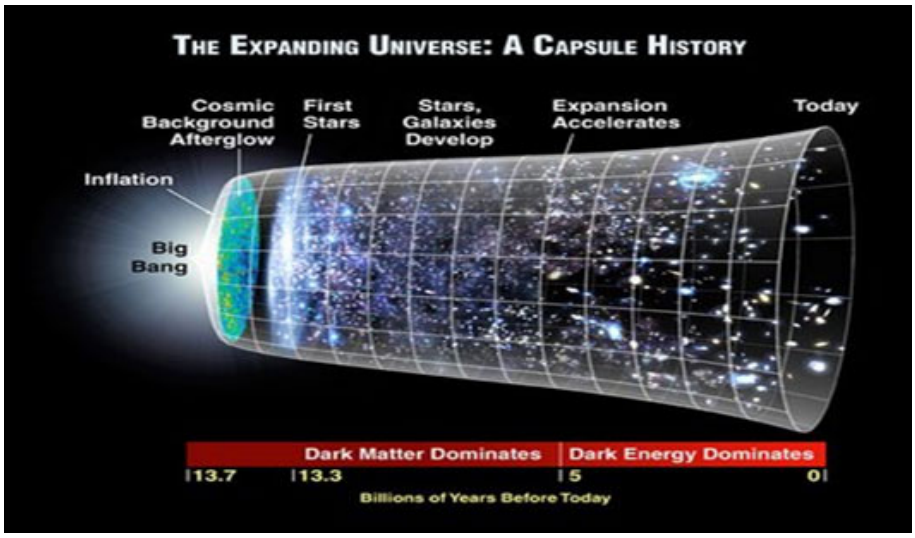

Figure 1. Illustration of the space time of the universe[11]

This has become very famous and illustrates very nicely the problem of visualising and understanding the expansion of space. This for one reason: It lacks coordinates. The y axis represents the time. But in which coordinate system is the space measured? It obviously cannot be the commoving space itself, since than we would see a tube. Nevertheless it is important to remember, that while figure 1 presents space time as an Euklidean space, relativity theory regards space time as a non-Euklidean space.

An other and maybe more promising approach to the expansion of space is the mathematical approach. Therefore the next part of this work will be dedicated to mathematical deduction of the expansion factor of the three dimensional space.
In order to solve the Einstein equation, lets assume, that the universe is homogeneous and isotropic. The solution of the Einstein equation under this assumptions is called the Friedman-Lemaitre-Robertson-Walker-metric. For reasons of simplicity and clarity, all calculations[12] are done in natural units ($c = \hbar = 1$). The assumption of an homogeneous and isotropic universe yield three possible curvatures of three dimensional space.

1. Flat Euklidean space with line element:

$$dl^2 = dx^2 = \delta_{ij} dx^i dx^j \tag{6}$$

2. Positively curved space creating a three dimensional surface of a sphere embedded in four dimensional Euklidean space:

$$dl^2 = dx^2 + du^2, \qquad a^2 = u^2 + x^2 \tag{7}$$

   Where a is the radius of the sphere.
3. Negatively curved space creating a three dimensional hyperboloid embedded in four-dimensional Lorentzian space $\mathbb{R}^{3,1}$:

$$dl^2 = dx^2 - du^2, \qquad -a^2 = u^2 - x^2 \tag{8}$$

   Where a is an arbitrary constant.

[12] The deductions follow broadly Daniel Baumann, *Cosmology- Part III Mathematical Tripos*, pp. 5-8. http://theory.uchicago.edu/ liantaow/my-teaching/dark-matter-472/lectures.pdf (24.01.2020)

In order to derive the sale factor for the expansion of space it is enough to focus on one of the above cases. This will be the case of the spherical space. For reasons of convenience it is common to rescale the coordinates $x \to ax$, $u \to au$. The line element then looks as follows.

$$dl^2 = a^2(dx^2 + du^2) \tag{9}$$
$$1 = u^2 + x^2 \tag{10}$$

(9) and (10) together yield:

$$dl^2 = a^2(dx^2 + \frac{xdx}{1-x^2}) \text{ .}^{13} \tag{11}$$

Now it is common to transform x into spherical coordinates. This is not necessary in our case. It is enough to introduce the idea of the commoving coordinates ω. The substitution goes as follows.

$$d\omega^2 = dx^2 + \frac{xdx}{1-x^2} \tag{12}$$

Which yields:

$$dl^2 = a^2 d\omega^2 \tag{13}$$

It is important to note, that the flat and the negatively curved space would yield exactly the same relation. The case of the spherical universe was only chosen because it is the most illustrative one. One important fact is, that by transforming the coordinates x became uniteless while a carries the unite of length. Integrating both sides of (13) and assuming, that a may depend on time yields the following equation.

$$l(t) = a(t) \cdot \omega \tag{14}$$

In this relation now lies the meaning of expansion of space. The term on the left hand side stands for the measurable physical lenght $l(t)$, while the right hand side is divided into the the time dependent scale factor $a(t)$ and the time independent uniteless commoving length ω. Of prime importance is the distinction between *commoving* and *physical* space. Figure 2 shows the difference.

It is the commoving space, which expands with respect to the physical space![15]. The commoving space is a theoretical concept, whereas the physical space represents space as we perceive it. It is important to make clear of which of the two concepts we are talking, when we speak of "space". Now it becomes possible, that two objects, which have no relative velocity in the *commoving* space, move away from each other in the *physical* space, because the *commoving* space stretches. Here the terminology is ambivalent. "Distance" for example can mean "distance in physical space" ($l[m]$) or "distance in commoving space" ($\omega[-]$). This ambiguity may cause confusion when it comes to the meaning of an expanding space.

---

[15] See David Tong, *Cosmology- Part II Mathematical Tripos* pp 10 - 11, http://www.damtp.cam.ac.uk/user/tong/cosmo/one.pdf (27.01.2020)

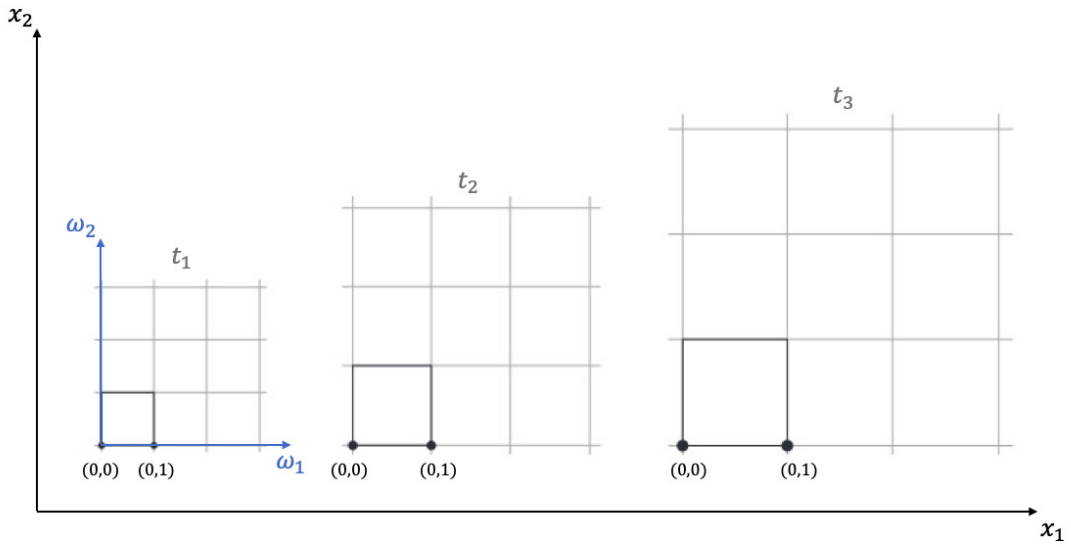

Figure 2. Expansion of the commoving space with respect to the physical space.[14]

4. Cosmological red shift

Now that the terminology is clearer and the understanding of an expanding space has improved, there is one question left to answer. How is it possible to measure the expansion of (commoving) space? The answer is the cosmological red shift. It is defined using the difference of the wavelength of the emitted and the observed wave.

$$z = \frac{\lambda_{\text{obsv}} - \lambda_{\text{emit}}}{\lambda_{\text{emit}}} .^{16} \tag{15}$$

The cosmological red shift differs from the red shift caused by the Doppler effect insofar, that it is not caused by a motion in commoving space, but rather by the expansion of commoving space itself. It can be derived[17] from the space time interval.

$$ds^2 = -dt^2 + dl^2 = -dt^2 + a(t)^2 d\omega^2 \tag{16}$$

Lets look at a light wave emitted from a point of arbitrary distance ω and observed at distance $\omega = 0$. Two consecutive maxima of the light wave are emitted at t_{e1} and t_{e2} and absorbed at t_{a1} t_{a2}. The associated wave lengths then are

$$\lambda_e = c\,(t_{\text{e2}} - t_{\text{e1}}) \tag{17}$$
$$\lambda_a = c\,(t_{\text{a2}} - t_{\text{a1}}) \tag{18}$$

Light always travels along so called null world lines[18] with

$$ds^2 = -dt^2 + a(t)^2 d\omega^2 = 0 \tag{19}$$

---

17 See David Tong, *Cosmology- Part II Mathematical Tripos* pp 10 - 15, http://www.damtp.cam.ac.uk/user/tong/cosmo/one.pdf (27.01.2020)
18 See James B. Hartle, *Gravity - An Introduction to Einsteins General Relativity*, Addison Wesley: Santa Barbara Ca, USA, 2003. p 178.

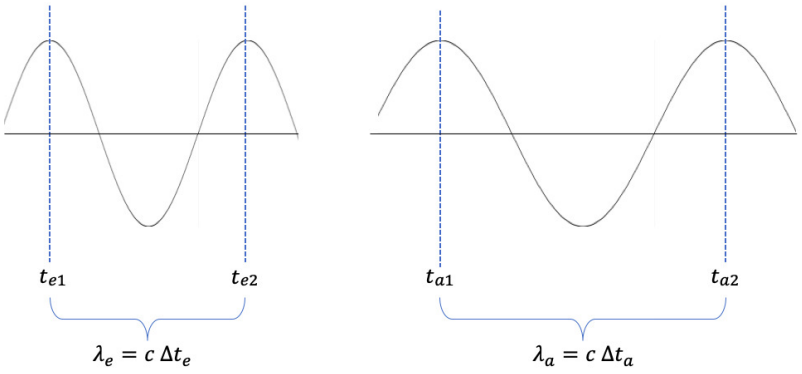

Figure 3. Light wave at t_e and t_a.

which yields

$$dt = a(t)d\omega \tag{20}$$

$$\Leftrightarrow \quad \frac{1}{a(t)}dt = d\omega\,. \tag{21}$$

[19]

The commoving distance traveled by the two maxima is per definition equal. By integrating both sides we get from equation (21)

$$0 = \omega_2 - \omega_1 == \int_{t_{e2}}^{t_{a2}} a^{-1}(t)\,\mathrm{d}t \; - \int_{t_{e1}}^{t_{a1}} a^{-1}(t)\,\mathrm{d}t\,. \tag{22}$$

Since both integrals are applied on the same function, it is possible to change the integration limits. Assuming a to be constant for small time differences this yields

$$0 = \int_{t_{a1}}^{t_{a2}} a^{-1}(t)\,\mathrm{d}t \; - \int_{t_{e1}}^{t_{e2}} a^{-1}(t)\,\mathrm{d}t = \frac{t_{a2} - t_{a1}}{a(t_{a1})} - \frac{t_{e2} - t_{e1}}{a(t_{e1})}\,. \tag{23}$$

Using equations (17) and (18) we get

$$\frac{\lambda_a}{\lambda_e} = \frac{t_{a2} - t_{a1}}{t_{e2} - t_{e1}} = \frac{a(t_{a1})}{a(t_{e1})}\,. \tag{24}$$

and finally the cosmological red shift caused by the expansion of the commoving space

$$z = \frac{\lambda_a - \lambda_e}{\lambda_e} = \frac{a(t_a)}{a(t_e)} - 1\,. \tag{25}$$

---

[19] See David Tong, *Cosmology- Part II Mathematical Tripos* p 14, http://www.damtp.cam.ac.uk/user/tong/cosmo/one.pdf (27.01.2020)

In most cases the time of absorbtion is the present time t_0. Usually the expansion factor of the present is set to one.[20] Equation (25) then reduces to

$$z = \frac{1}{a(t_e)} - 1 \,. \tag{26}$$

This equation directly links the measurable red shift to the expansion of the space. Expansion therefore can be proven experimentally.
The red shift results from the fact, that light travels in the physical space, while the emitter and the absorber are at fixed places in commoving space. Lets assume that the emitter and the absorber had a constant distance in physical space. This would yield the following equation.

$$l_1 = l_2 \tag{27}$$

.

From equations (16) and (19) we get

$$-dt^2 + dl^2 = 0 \;\Leftrightarrow dt = dl \,. \tag{28}$$

Together with equation (25) we get

$$0 = l_2 - l_1 = \int_{t_{\mathrm{a1}}}^{t_{\mathrm{a2}}} \mathrm{d}t \; - \int_{t_{\mathrm{e1}}}^{t_{\mathrm{e2}}} \mathrm{d}t = (t_{\mathrm{a2}} - t_{\mathrm{a1}}) - (t_{\mathrm{e2}} - t_{\mathrm{e1}}) \tag{29}$$

$$\Leftrightarrow \; t_{\mathrm{e2}} - t_{\mathrm{e1}} = t_{\mathrm{a2}} - t_{\mathrm{a1}} \,. \tag{30}$$

This again means, that the wave lengths are the same and the red shift therefore zero.

$$\lambda_a = \lambda_e \;\Leftrightarrow\; z = \frac{\lambda_{\mathrm{a}} - \lambda_{\mathrm{e}}}{\lambda_{\mathrm{e}}} = 0 \,. \tag{31}$$

This would be the case, when the the cosmological red shift is cancelled out by a blue shift caused by the Doppler effect of emitter and absorber moving towards each other. It is therefore of great importance to be clear about whether a statement applies to the commoving or the physical space.

5. Conclusions

The objective of this work was to answer the question, what it means, that space is expanding. First the possible problems of the conception of an expanding space were discussed. In the centre of the discussion was the question, whether space should be understood as the theoretical concept preceding all possible knowledge. The argument was, that it is not possible to imagine a universe without having a conception of space and time first. This is insofar linked to our question, that it would not make sense to speak of an expanding space if it was really a necessary condition for any conceptualisation of the world. There would be no referece frame against which such an expansion could be described.
Another problem which arose, was, if it is possible to experimentally determine an expansion of space. Since expansion is usually measured with respect to space, as a relative motion of the objects boundary points, it is not obvious, if the

[20] See David Tong, *Cosmology- Part II Mathematical Tripos* p 15, http://www.damtp.cam.ac.uk/user/tong/cosmo/one.pdf (27.01.2020)

expansion of space itself could be measured. The problem here is, that a the theory claiming space was stretching could not empirically verified nor falsified and therefore would lose its scientific character.
Both problems could be solved by adopting a relativistic perspective and by introducing the distinction between physical and commoving space. The claim that space is expanding then means, that the commoving space is expanding with respect to the physical space. In this conception it becomes possible to imagine two fixed points in (commoving) space actually moving away from each other. The physical distance created between two objects fixed in space can than be measured using the cosmological red shift. Light which travels through the expanding space changes its wave length. This change in wave length is directly related to the expansion factor of the universe and can be observed empirically.

References

1. Sean M. Carroll, *A No-Nonsense Introduction to General Relativity*, Enrico Fermi Institute and Department of Physics,University of Chicago, 2001. http://courses.theophys.kth.se/SI2370/Carroll_GR_summary.pdf (23.01.2020).
2. Daniel Baumann, *Cosmology- Part III Mathematical Tripos*. http://theory.uchicago.edu/ liantaow/my-teaching/dark-matter-472/lectures.p (24.01.2020)
3. David Tong, *Cosmology- Part II Mathematical Tripos*. http://www.damtp.cam.ac.uk/user/tong/cosmo/one.pdf (27.01.2020).
4. Immanuel Kant, *Critique of Pure reason* B 38/39.
5. Karl Popper, *The logic of scientific discovery*, 1934.
6. http://wethesikhs.com/wp-content/uploads/2015/11/expansion.jpg (23.01.2020).
7. James B. Hartle, *Gravity - An Introduction to Einsteins General Relativity*, Addison Wesley: Santa Barbara Ca, USA, 2003.

Proceedings

A review of CAMB: a CMB Boltzmann code to compute anisotropies in the cosmic microwave background

Luis Atayde [1]

[1] Instituto de Astrofisica e Ciencias do Espaco, Faculdade de Ciencias da Universidade de Lisboa,Edificio C8, Campo Grande, P-1749016, Lisboa, Portugal; luisbbatayde@gmail.com

Received: date; Accepted: date; Published: date

Abstract: *CAMB* is a FORTRAN code with a Python wrapper for computing anisotropies in the microwave background. We have the objective to learn the way the code works. With this objective in mind this essay start with a simple example for an Einstein Boltzmann system, were we try to derive the simplest case. Followed by the study of the mathematical theory inside the *CAMB* code. Finalizing by executing and experimenting the code for the simple case of ΛCDM case

Keywords: *CAMB*; Einstein-Boltzmann; power spectrum; perturbations,Cosmic Microwave Background,ΛCDM

1. Introduction

One essential part of the modern cosmology is the capability to constrain various properties of cosmological models using observations such has the Cosmic Microwave Background. This primordial variations in the radiation and matter are the seed to the temperature anisotropies and galaxy distribution respectively.

One way to study the CMB is to study the perturbations and if one want's to research more about cosmological perturbations on large scales(for each model), one should expand the most important fields to the linear order around a homogeneous and isotropic background. This cosmological fields are the space time metric, the many components of the energy density, the pressure, the momentum , the phase space densities of relativistic component, and others. One must then change these linearised fields with the cosmological evolution; using the Einstein field equation, the conservation of energy momentum tensor and the Boltzmann equations. By the end one can associate the background equations and the first order evolution equation to understand how a set of initial conditions will evolve.

We do all this so we can derive a set of spectra. Here is the power spectrum of matter fluctuations at conformal time τ,for example;

$$\langle \delta_M^*(\tau, \mathbf{k}')\delta_M(\tau, \mathbf{k})\rangle \equiv (2\pi)^3 P(k,\tau)\delta^3(\mathbf{k}-\mathbf{k}') \ , \tag{1}$$

we derived the energy density of matther, ρ_M near its average value, $\bar{\rho}_M$, $\delta_M = (\rho_M - \bar{\rho}_M)/\bar{\rho}_M$,and taken its Fourier transform.

After that we can calculate the angular power spectrum

$$\langle a^*_{\ell' m'} a_{\ell m}\rangle = C_\ell^{TT}\delta_{\ell\ell'}\delta_{mm'} \ , \tag{2}$$

which we can expand, $\delta T/T(\hat{n})$ in spherical harmonics such that

$$\frac{\delta T}{T}(\hat{n}) = \sum_{\ell m} a_{\ell m} Y_{\ell m}(\hat{n}) \ . \tag{3}$$

In general we are able to derive the angular power spectrum of polarization in the CMB, specially of the "E" mode, C_ℓ^{EE}, the "B" mode, C_ℓ^{BB} and the cross-spectra between the "E" mode and the temperature anisotropies, C_ℓ^{TE}, as well as the angular power spectrum of the CMB lensing potential, $C_\ell^{\phi\phi}$.

We could also derive background quantities.

2. Einstein-Boltzmann Equations

The evolution of perturbation in the universe can be described by the linear Einstein-Boltzmann. In this section we will start by focus in a more simple set of equations to describe the features of the matter power spectrum.

The primordial fluctuations were created during the inflationary period and are approximately scale invariant. With this we have already our initial condition, now we just need to know how it's going to evolve.

The coupled Boltzmann equations for radiative species governs the way that the cosmological perturbations evolve, while the matter species are dictated by the fluid equations and the Einstein equations dictate the metric.

Because we want study the CMB the most important statistic it's angular power spectrum C_l and for which the linearized approach is capable to determine. But just because we are only going to work with linear order that doesn't mean it's going to be easy.

There are many reason for the Einstein-Boltzmann system be a difficult system to develop. The fact that the equations consider the effect of a diverse set of physical processes that have various time scales, it brings that some variables can have a high rate of fluctuation, mean while others can bee much more flat at the same regime. The parameters of the system end up being time dependent. And due to the different physical factors (dark matter, baryons, photons and neutrinos), the system has generally many perturbations. In the end even while being a linear system is very difficult, requiring advance numerical solvers to treat the different regimes of evolution.

So lets investigate how the dark matter power spectrum evolves, so we are going to simplify the set of variables. ρ_r and ρ_m respectively are the density of radiation and matter. Θ_0 and Θ_1 respectively are the monopole and dipole moments. We will define the matter perturbations with overdensity δ and the irrotational peculiar velocity v.

Using conformal Newtonian gauge and let's do purely scalar metric perturbations "with no anisotropic stresses"

We can then write the metric perturbation, for the metric $ds^2 = -(1-2\Phi)dt^2 + a^2(1+2\Phi)\delta_{ij}dx^i dx^j$, with only one scalar potential Φ. In this simple case we have that the coupled Boltzmann, fluid and Einstein equations are

$$\frac{d\Theta_0}{d\eta} + k\Theta_1 = -\frac{d\Phi}{d\eta}, \tag{4a}$$

$$\frac{d\Theta_1}{d\eta} - \frac{k}{3}\Theta_0 = -\frac{k}{3}\Phi \tag{4b}$$

$$\frac{d\delta}{d\eta} + ikv = -3\frac{d\Phi}{d\eta} \tag{4c}$$

$$\frac{dv}{d\eta} + \frac{1}{a}\frac{da}{d\eta} = ik\Phi \tag{4d}$$

$$k^2\Phi + 3\frac{1}{a}\frac{da}{d\eta}\left(\frac{d\Phi}{d\eta} + \frac{1}{a}\frac{da}{d\eta}\Phi\right) = 4\pi G a^2\left[\rho_m\delta + 4\rho_r\Theta_0\right]. \tag{4e}$$

where $d\eta = dt/a$ is the conformal time , a is the scale factor and k is the comoving wavenumber. This equations are in fourier space. So here we have equation (4e) which is the Einstein equation in conformal newtonian gauge. From the conservation of energy momentum we can get the equation (4c) and (4d) that can describe the density and the velocity of the fluid.The equation (4a) and (4b) will describe the monopole and dipole momentum equations.

There are five variables and correspondingly five initial conditions which, in general, may be specified independently. However for adiabatic initial conditions given by standard single-field inflation the relations are

$$\begin{aligned}
\Theta_0(k, a_i) &= \frac{1}{2}\Phi(k, a_i) \\
\Theta_1(k, a_i) &= -\frac{1}{6}\frac{k}{a_i H_i}\Phi(k, a_i) \\
\delta(k, a_i) &= 3\Theta_0 = \frac{3}{2}\Phi(k, a_i) \\
u(k, a_i) &= 3\Theta_1 = -\frac{1}{2}\frac{k}{a_i H_i}\Phi(k, a_i),
\end{aligned}$$

where a_i and H_i are the initial values of the scale factor and Hubble parameter and $\Phi(k, a_i)$ is the initial potential. In order to further simplify the system, we introduce new variables

$$y_1 = \Theta_0 + \Phi \tag{6a}$$
$$y_2 = 3\Theta_1 \tag{6b}$$
$$y_3 = \delta + 3\Phi \tag{6c}$$
$$y_4 = iv \tag{6d}$$
$$y_5 = \Phi \tag{6e}$$

and define the parameter

$$\epsilon \equiv \epsilon(k, a) = \frac{k}{Ha}. \tag{7}$$

Changing the time variable from η to $\ln a$, and noting that $\frac{d}{d\eta} = (Ha)\frac{d}{d\ln a}$, the system given by eq.4 can be re-written as

$$\dot{y}_1 = -\frac{\epsilon(k,a)}{3} y_2 \tag{8a}$$
$$\dot{y}_2 = \epsilon(k,a)\left[y_1 - 2y_5\right] \tag{8b}$$
$$\dot{y}_3 = -\epsilon(k,a) y_4 \tag{8c}$$
$$\dot{y}_4 = -y_4 - \epsilon(k,a) y_5 \tag{8d}$$
$$\dot{y}_5 = \frac{1}{2}\left[\Omega_m(a) y_3 + 4\Omega_r(a) y_1 - \left\{3\Omega_m(a) + 4\Omega_r(a) + \frac{2}{3}\epsilon^2(k,a) + 2\right\} y_5\right], \tag{8e}$$

The initial conditions become

$$y_1(k, a_i) = \frac{3}{2} y_5(k, a_i) \tag{9a}$$
$$y_2(k, a_i) = -\frac{1}{2}\epsilon(k, a_i) y_5(k, a_i) \tag{9b}$$
$$y_3(k, a_i) = \frac{9}{2} y_5(k, a_i) \tag{9c}$$
$$y_4(k, a_i) = -\frac{1}{2}\epsilon(k, a_i) y_5(k, a_i). \tag{9d}$$

3. *CAMB*

CAMB (Code for Anisotropies in the Microwave Background). *CAMB* is a Python and Fortran code for computing CMB, CMB lensing, lensing, galaxy count and dark-age 21cm power spectra, transfer functions and matter power spectra, and background cosmological functions.

Let's study the way that *CAMB*works inside. For these we will have to derive the multipole equations, solutions, and equations for C_l.

Thomson scattering and the geodesic equation are the ones who will dictate the evolution of the photon multipole and it will be this way

$$\dot{I}_{A_l} + \frac{4}{3}\Theta I_{A_l} + D^b I_{bA_l} - \frac{l}{2l+1} D_{\langle a} I_{A_{l-1}\rangle} + \frac{4}{3} I A_{a_1}\delta_{l1} - \frac{8}{15} I\sigma_{a_1a_2}\delta_{l2} = -n_e\sigma_T\left(I_{A_l} - I\delta_{l0} - \frac{4}{3} I v_{a_1}\delta_{l1} - \frac{2}{15}\zeta_{a_1a_2}\delta_{l2}\right) \tag{10}$$

where I_{A_l} approximate to zero when $l < 0$ and

$$\zeta_{ab} \equiv \frac{3}{4} I_{ab} + \frac{9}{2}\mathcal{E}_{ab} \tag{11}$$

This is a source of anisotropic stress and E-polarization. if we pick the equation above and do the spatial derivative for $l = 0$, we get the equation for the density disturbance $D_a I$. So with all that we know the evolution equation for the polarization multipolar tensor are

$$\begin{aligned}\dot{\mathcal{E}}_{A_l} + \frac{4}{3}\Theta\mathcal{E}_{A_l} + \frac{(l+3)(l-1)}{(l+1)^2}\mathrm{D}^b\mathcal{E}_{bA_l} - \frac{l}{2l+1}D_{\langle a_l}\mathcal{E}_{A_{l-1}\rangle} - \frac{2}{l+1}\nabla\times\mathcal{B}_{A_l} &= -n_e\sigma_T(\mathcal{E}_{A_l} - \frac{2}{15}\zeta_{a_1a_2}\delta_{l2}) \\ \dot{\mathcal{B}}_{A_l} + \frac{4}{3}\Theta\mathcal{B}_{A_l} + \frac{(l+3)(l-1)}{(l+1)^2}\mathrm{D}^b\mathcal{B}_{bA_l} - \frac{l}{2l+1}D_{\langle a_l}\mathcal{B}_{A_{l-1}\rangle} + \frac{2}{l+1}\nabla\times\mathcal{E}_{A_l} &= 0. \end{aligned} \quad (12)$$

The equations have to be then worked to scalar, vector and tensor harmonics to be used in the numerical solver.

As we said a decomposition to scalar,vector and tensor it's helpful to the comprehension as well to the code execution.To start we have to clarify that the m-type tensors, scalar ($m = 0$) is the density perturbations, vector ($m = 1$) is vorticity the and 2-tensor ($m = 2$) is gravitational waves.

We can describe a PSTF (projected symmetric and trace-free) tensor X_{A_l} as a sum of $m-$type tensors

$$X_{A_l} = \sum_{m=0}^{l} X^{(m)}_{A_l}. = X^l_{A_l} + \mathrm{D}_{\langle a}X^{l-1}_{A_{l-1}\rangle} + \cdots + \mathrm{D}_{\langle A_{l-1}}X^1_{a_l\rangle} + \mathrm{D}_{Al}X^0 \quad (13)$$

$X^{(m)}_{A_l}$ now will be written for each $l - m$ derivatives of a transverse tensor ($\nabla_i T^{ij} = 0$)

$$X^{(m)}_{A_l} = D_{\langle A_{l-m}}\Sigma_{A_m\rangle} \quad (14)$$

We have that $\mathrm{D}_{A_l} \equiv \mathrm{D}_{a_1}\mathrm{D}_{a_2}\ldots\mathrm{D}_{a_l}$ and Σ_{A_m} is first order, PSTF (projected symmetric and trace-free) and transverse $\mathrm{D}^{a_m}\Sigma^m_{A_{m-1}a_m} = 0$. The 'scalar' component is $X^{(0)}$, the 'vector' component is $X^{(1)}_a$, etc.

Because in General Relativity there no association for $m > 2$ one only consider scalar, vectors and (2-)tensors. They evolve independently in linear orde.

Now for the numerical solver we must do an harmonic expansion in terms of zero order eignfunctions of the Laplacian $Q^m_{A_m}$ which is transverse for all indices,$\mathrm{D}^{a_m}Q^m_{A_{m-1}a_m} = 0$.

$$\mathrm{D}^2Q^m_{A_m} = \frac{k^2}{S^2}Q^m_{A_m}, \quad (15)$$

With this the scalar is Q^0, the vector is Q^1_a and so on.

In a flat universe the eigenfunctions can be represented by

$$Q^m_{A_m} \propto \epsilon_{A_m}e^{-ik\cdot x} \quad (16)$$

where ϵ_{A_m} is a constant symmetric, trace free tensor that is orthogonal to k, $k^a\epsilon_{aA_{m-1}} = 0$.

If required we can write eigenfunctions with positive and negative parity as $Q^{m\pm}_{A_m}$.

$$\mathrm{D}^2(\nabla\times Q_{A_m}) = \nabla\times(\mathrm{D}^2Q_{A_m}) = \frac{k^2}{S^2}\nabla\times Q_{A_m} \quad (17)$$

there is the relation by $\nabla\times$ operation. With this information we know that

$$\nabla\times\nabla\times Q^m_{A_m} = \frac{k^2}{S^2}Q^m_{A_m} \quad (18)$$

normalizing the $\pm$ harmonics

$$\nabla\times Q^{m\pm}_{A_m} = \frac{k}{S}Q^{m\mp}_{A_m}. \quad (19)$$

the way that it's build from $Q^{m\pm}_{A_m}$ as

$$Q^m_{A_l} \equiv \left(\frac{S}{k}\right)^{l-m} \mathrm{D}_{\langle A_{l-m}} Q^m_{A_m\rangle} \tag{20}$$

now substituting $X^{(m)}_{A_l}$ by X_{A_l}, we have

$$\begin{aligned} \mathrm{D}^2 Q^m_{A_l} &= \frac{k^2}{S^2} Q^m_{A_l} \\ \mathrm{D}^{a_l} Q^m_{A_{l-1}a_l} &= \frac{k}{S}\frac{(l^2-m^2)}{l(2l-1)} Q^m_{A_{l-1}} \\ \nabla \times Q^{m\pm}_{A_l} &= \frac{m}{l}\frac{k}{S} Q^{m\mp}_{A_l} \end{aligned} \tag{21}$$

where $l \geq m$. We can define dimensionless harmonic coefficient as

$$\begin{aligned} \sigma^{(m)}_{ab} &= \sum_{k,\pm} \frac{k}{S}\sigma^{(m)\pm} Q^{m\pm}_{ab} \quad & H^{(m)}_{ab} &= \sum_{k,\pm} \frac{k^2}{S^2} H^{(m)\pm} Q^{m\pm}_{ab} \\ q^{(m)}_a &= \sum_{k,\pm} q^{(m)\pm} Q^{m\pm}_a & E^{(m)}_{ab} &= \sum_{k,\pm} \frac{k^2}{S^2} E^{(m)\pm} Q^{m\pm}_{ab} \\ \pi^{(m)}_{ab} &= \sum_{k,\pm} \Pi^{(m)\pm} Q^{m\pm}_{ab} & I^{(m)}_{A_l} &= \rho_\gamma \sum_{k,\pm} I^{(m)\pm}_l Q^{m\pm}_{A_l} \\ \Omega_a &= \sum_{k,\pm} \frac{k}{S}\Omega^{\pm} Q^{1\pm}_a & A^{(m)}_a &= \sum_{k,\pm} \frac{k}{S} A^{(m)\pm} Q^{m\pm}_a \\ & & (D_a X)^{(m)} &= \sum_{k,\pm} \frac{k}{S} (\delta X)^{(m)\pm} Q^{m\pm}_a \end{aligned} \tag{22}$$

In here we have that the k dependence of the harmonic coefficient extinguish. The m and $\pm$ indices are extinguish for clarity. we expand multipoles in analogy with I_{A_l}. The heat flux are $q_i = (\rho_i + p_i)v_i$ (v_i is the velocity) while the total heat flux is given by the sum of them. $B^{(m)}_0 \equiv \Pi^{(m)}_B/\rho_\gamma$ quantifies the magnetic field

So the photon multipole equations when derived into harmonics

$$\begin{aligned} I'_l + \frac{k}{2l+1}\left[\frac{(l+1)^2-m^2}{l+1} I_{l+1} - l I_{l-1}\right] = & \\ - S n_e \sigma_T \left(I_l - \delta_{l0} I_0 - \frac{4}{3}\delta_{l1} v - \frac{2}{15}\zeta \delta_{l2}\right) & \\ + \frac{8}{15} k\sigma \delta_{l2} - 4h'\delta_{l0} - \frac{4}{3} kA\delta_{l1} & \end{aligned} \tag{23}$$

for which $l \geq m$, $I_0 = \delta\rho_\gamma/\rho_\gamma$, $I_l = 0$ when $l < m$. The equation for the neutrino multipoles (after neutrino decoupling) is

$$\begin{aligned} \mathcal{E}^{m\pm\prime}_l + k\left[\frac{(l+3)(l-1)}{(l+1)^3}\frac{(l+1)^2-m^2}{(2l+1)}\mathcal{E}^{m\pm}_{l+1} - \frac{l}{2l+1}\mathcal{E}^{m\pm}_{l-1} - \frac{2m}{l(l+1)}\mathcal{B}^{m\mp}_l\right] &= -S n_e \sigma_T (\mathcal{E}^{m\pm}_l - \frac{2}{15}\zeta^{m\pm}\delta_{l2}) \\ \mathcal{B}^{m\pm\prime}_l + k\left[\frac{(l+3)(l-1)}{(l+1)^3}\frac{(l+1)^2-m^2}{(2l+1)}\mathcal{B}^{m\pm}_{l+1} - \frac{l}{2l+1}\mathcal{B}^{m\pm}_{l-1} + \frac{2m}{l(l+1)}\mathcal{E}^{m\mp}_l\right] &= 0. \end{aligned} \tag{24}$$

We can found solutions to the Boltzman hierarchies using the line of sigh integrals

Because of simplicity lets just do for a flat universe

Lets do the solutions to Eq. 23 to facilitate in the right hand side we will set to zero

$$\Psi_l^m(k\eta) \equiv \frac{l!}{(l-m)!}\frac{j_l(k\eta)}{(k\eta)^m} \tag{25}$$

$j_l(x)$ is a spherical Bessel function. we can now use this to make the Green's function solution.

Because the solutions for the polarization is less obvious. Lets do the solution for each mode (m)

For vector modes ($m = 1$) the solutions are

$$I_l(\eta_0) = 4\int^{\eta_0} d\eta e^{-\tau}\left[Sn_e\sigma_T\bar{v}\Psi_l^1(\chi) + \left(k\bar{\sigma} + Sn_e\sigma_T\frac{\zeta}{4}\right)\frac{d\Psi_l^1(\chi)}{d\chi}\right] \tag{26}$$

$$E_l^{\pm}(\eta_0) = \frac{l(l-1)}{l+1}\int^{\eta_0} d\eta Sn_e\sigma_T e^{-\tau}\left[\frac{1}{\chi}\frac{dj_l(\chi)}{d\chi} + \frac{j_l(\chi)}{\chi^2}\right]\zeta^{\pm} \tag{27}$$

$$B_l^{\pm}(\eta_0) = -\frac{l(l-1)}{l+1}\int^{\eta_0} d\eta Sn_e\sigma_T e^{-\tau}\frac{j_l(\chi)}{\chi}\zeta^{\mp} \tag{28}$$

$\chi \equiv k(\eta_0 - \eta)$.

For tensors ($m = 2$) the solutions are

$$I_l(\eta_0) = 4\int^{\eta_0} d\eta e^{-\tau}\left[k\sigma + Sn_e\sigma_T\frac{\zeta}{4}\right]\Psi_l^2(\chi) \tag{29}$$

$$E_l^{\pm}(\eta_0) = \frac{l(l-1)}{(l+1)(l+2)}\int^{\eta_0} d\eta Sn_e\sigma_T e^{-\tau}\left[\frac{d^2j_l(\chi)}{d\chi^2} + \frac{4}{\chi}\frac{dj_l(\chi)}{d\chi} - \left(1 - \frac{2}{\chi^2}\right)j_l(\chi)\right]\zeta^{\pm} \tag{30}$$

$$B_l^{\pm}(\eta_0) = -2\frac{l(l-1)}{(l+1)(l+2)}\int^{\eta_0} d\eta Sn_e\sigma_T e^{-\tau}\left[\frac{dj_l(\chi)}{d\chi} + \frac{2}{\chi}j_l(\chi)\right]\zeta^{\mp}. \tag{31}$$

τ is the optical depth from η to η_0,

$\tau' = -Sn_e\sigma_T$.

Finally by taking the harmonic expansion of I_{A_l}, we know that the contribution to the C_l from type-m is

$$C_l^{TT(m)} = \frac{\pi}{4}\frac{(2l)!}{(-2)^l(l!)^2}\sum_{k,k',\pm}\langle I_{l,k}^{\pm}I_{l,k'}^{\pm}\rangle Q_{A_lk}^{\pm}Q_{k'}^{A_l\pm}. \tag{32}$$

4. ΛCDM example

The *CAMB* code can be used in to different ways we will invest more using the FORTRAN compiler because It's the more essential if one wants to modified the code for new cases not implemented yet. The first important point to know is the position of our files. On the main directory we have a folder called *fortran* this folder is where most of our tools when working in FORTRAN are.

Lets Start with the *Makefile_main* this is the file that is going to compile all the others files. If there are errors compiling it should be looked at for all the flags in this file and change for the ones that better suit the machine. Then we have the main file called *cmbmain.f90*, this is were the the linearized perturbation equations of general relativity, the Boltzmann equations and the fluid equations are in the code.

The file equations.f90 contains all the evolution equations of the background and perturbations. There are others files has *halofit.f90* (for the non linear evolution of cold dark matter power spectra) has well has *lensing.f90* (that does the lensing for the power spectrum)

In the folder this time *inifiles* is where the *params.ini* file is this file contain all the initial parameters.

This main files are going to be the most important when starting using *CAMB*.

To compile *CAMB* one must write the command make in the directory *fortran*. The *gfortran* compiler or the *ifortran* compiler will create a binary file in the same directory. This binary file will have the name of *camb*. To run this file one must point to *params.ini* file like this example "./camb params.ini". This command will start *CAMB*and 4 new files will be created with the results. By using some tools one can then create the following graphics

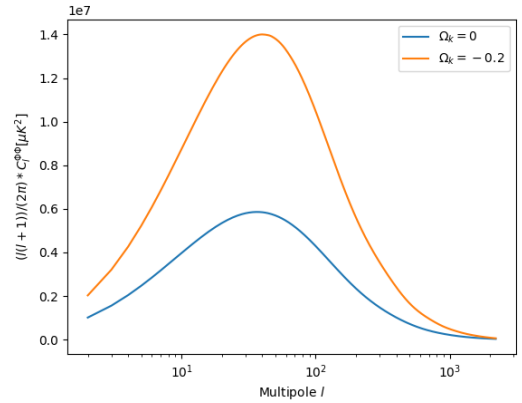

Figure 1. $\phi\phi$ power spectrum for ΛCDM

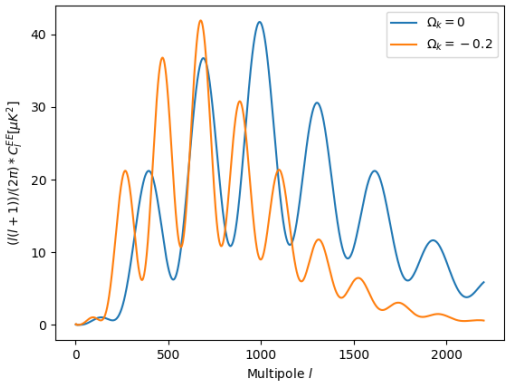

Figure 2. EE power spectrum for ΛCDM

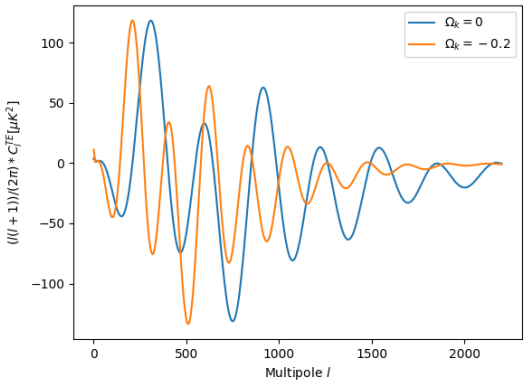

Figure 3. TE power spectrum for ΛCDM

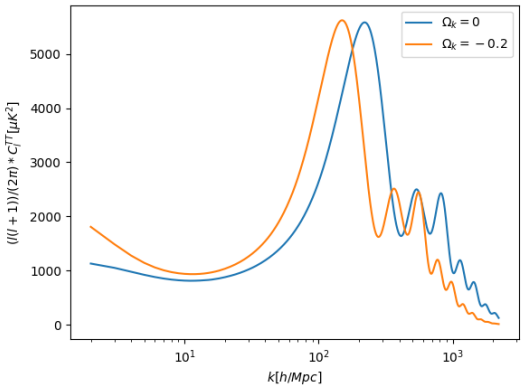

Figure 4. TT power spectrum for ΛCDM

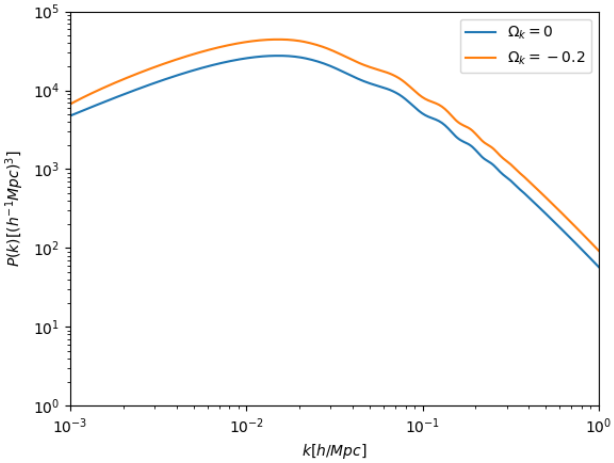

Figure 5. Matter power spectrum for ΛCDM

This figures were all created from the data created by *CAMB* and worked on using Python. This figures were done for two different initial conditions the first is for the case where the curvature is 0 and the second where the curvature density is negative. So we have a $\Omega_k = 0$ and $\Omega_k = -0.2$. We can see that for Figure(2), Figure(3) and Figure (4) there is a shift in the x axis for the left. Meaning that the maximums now happen in smaller *Multipole l*. While Figure(1) has a maximum higher than when $\Omega_k = 0$. Finaly in Figure (5) there is a shift in the y axis.

5. Conclusions

At the end the objective was achieved and the way the study of *CAMB* worked provided a balance for beginners to improve. This being it would have been interest if we have been able to work in other Einstein-Boltzmann codes like EFTCAMB,CMBFAST, hi_class, etc.

Funding: This research received no external funding

Acknowledgments:

Conflicts of Interest: The authors declare no conflict of interest.

References

1. Antony Lewis, T. CAMB Notes. **2014**, *4*, 1-25.
2. Antony Lewis, Efficient sampling of fast and slow cosmological parameters. prd **2013**, *4*, 1-103529.
3. Sharvari Nadkarni-Ghosh, The Einstein-Boltzmann equations revisited arXiv **2016**, *4*.

Proceedings

The Higgs mechanism and the electroweak phase transition: an introductory overview with an attempt of contextualization

Pedro Garcia [1]

[1] Faculty of Sciences of the University of Lisbon; 45808@alunos.fc.ul.pt

Received: date; Accepted: date; Published: date

Abstract: In order to better understand any process we must also try to understand the history of the developments of said process. In this work, I try to do an introductory overview, along with some historical contextualization, of the Higgs mechanism, or the Englert-Brout-Higgs-Guralnik-Hagen-Kibble mechanism, of the electroweak phase transition and all the major theoretical dependencies of these concepts, from superconductivity and spontaneous symmetry breaking to mexican hat potentials and the Higgs boson.

Keywords: Higgs mechanism; Electroweak phase transition; Superconductivity; Higgs boson

1. The Higgs mechanism

The first step to introduce the concept of the Higgs mechanism is to first understand how we can generate mass and spontaneously break symmetry. Let us break things down and build up from the basics with an analogous behaviour. We will see how this mechanism is just a relativistic version of what happens in a superconductor to pairs of electrons.

1.1. Symmetry breaking and superconductivity

Until 1960, there was no previously proposed connection between mass gain and symmetry breaking. That was until the work: Quasi-Particles and Gauge Invariance in the Theory of Superconductivity by Yoichiro Nambu [1]. But how is superconductivity related to symmetry breaking and mass gain?

Remember that superconductivity has at its core an attractive force between electrons that comes from the interaction between electrons and phonons. Since there is this attractive force between electrons, they are now coupled. This creates what it is called a Cooper pair, where both electrons have opposite momentum and spin. We can observe this in a Bose–Einstein condensate state, which is formed when a low-density gas of bosons is cooled to temperatures very close to absolute zero forcing a large fraction of bosons to occupy the lowest quantum state.

To better understand this, let us define a superconductor through a mathematical model. Thankfully, and even before 1957 when the theory for superconductivity was established, the Bardeen-Cooper-Schrieffer theory [2], someone already did that work for us in 1950. This is of course the Ginzburg-Landau model [3]. Here is its Hamiltonian, in natural units:

$$H = \int d^3x [\frac{1}{2m} D\phi^* \cdot D\phi + V(\phi)] \tag{1}$$

Here, ϕ represents the wave function of the aforementioned Cooper pairs as a condensate and has an effective charge of $2e$, since the Cooper pair involves two electrons. Here, as the temperature decreases and reaches a critical temperature T_c the ϕ field becomes very small and we can expand the potential $V(\phi)$ in a power series:

$$V(\phi) = \alpha\phi^*\phi + \frac{1}{2}\beta(\phi^*\phi)^2 \tag{2}$$

Note that the α and the β terms are dependent on temperature. And in a particular case, at the critical temperature T_c, the α term changes its sign. So, for a temperature lower than T_c, we have a negative α which gives us the following shape for the potential:

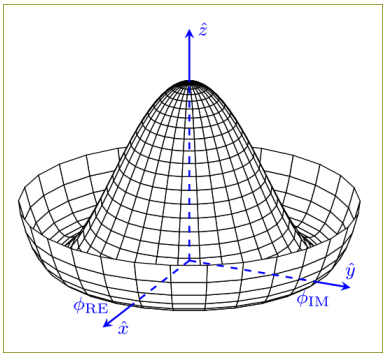

Figure 1. An example of the sombrero potential.

This is what it is called a sombrero potential, for obvious reasons. But for less obvious reasons, the minimum of this potential is not at $\phi = 0$, which is the symmetry point, but around this very symmetry point. This is what generates a symmetry break. But in this specific case it is a gauge symmetry break.

In electrodynamics, the field equations have a particular structure such that the electric field $E(t, x)$ and the magnetic field $B(t, x)$ can be expressed in terms of a scalar potential $A_0(t, x)$ and a vector potential $A(t, x)$. If we can describe the same electric and magnetic fields using those scalar and vector potentials, which can be related by a gauge transformation, then we call this gauge invariant. This is what falls apart. We can no longer use these gauge transformations used in this model:

$$A \to A + \nabla\lambda \tag{3}$$

$$\phi \to \phi e^{2ie\lambda} \tag{4}$$

So, around the sombrero, the magnitude of the number density of electronic pairs in the condensate, $|\phi|^2$, is well defined but its phase is not. This means that in this minimum there is a degeneracy in the lowest state.

Both Ginzburg-Landau [3] and later Bardeen-Cooper-Schrieffer [2] models do not respect gauge symmetry. At the time of this discovery it was seen at a flaw of these theories. However, this is now considered the first example of spontaneous symmetry breaking.

Back in 1960, Nambu showed how this symmetry break might be related with a specific energy gap [1]. Being that the electrons we considered are in these Cooper pairs, they suffer an attractive force. So, since the force between the electrons is attractive it would require energy to separate these pairs. This means the system is separated from the ground state by a non-zero energy gap, even if its momentum tends to zero. This was the way Nambu suggested that the masses of the elementary particles were created in a similar way, by breaking symmetries.

1.2. From superconductors to particles

Nambu suggested that if the superconducting ground state does not respect the symmetries in its theory, maybe, the vacuum state might not respect the symmetries regarding elementary particles acquiring mass.

In this case, Nambu predicted a theory that involved a massless fermion field $\psi(x)$, which Lagrangian was invariant under both symmetric and asymmetric phase changes:

$$\psi(x) \to e^{i\alpha}\psi(x) \tag{5}$$

$$\psi(x) \to e^{\alpha\gamma_5}\psi(x) \tag{6}$$

where $\gamma_5^2 = -1$. This means the Noether currents would also be conserved:

$$j^\mu = \overline{\psi}\gamma^\mu\psi \tag{7}$$

$$j_5^\mu = \overline{\psi}i\gamma^\mu\gamma_5\psi \tag{8}$$

He then proposed that, similarly to the the energy gap in the superconducting case, the mass would be a consequence of spontaneously breaking symmetry.

In 1961, Nambu and Jona-Lasinio developed a model with these proprieties [4] which had the following Lagrangian:

$$L = i\overline{\psi}\gamma^{\mu}\partial_{\mu}\psi + g[(\overline{\psi}\psi)^2 - (\overline{\psi}\gamma_5\psi)^2] \tag{9}$$

They assumed that, in the ground state or vacuum, the symmetry is broken spontaneously by a non-zero expectation value:

$$\langle 0|\overline{\psi}(x)\psi(x)|0\rangle \neq 0 \tag{10}$$

Similarly for what Nambu did to develop further on the ideas on superconductivity, they both showed that this broken symmetry would have has a consequence the nonzero mass for the nucleon which was the supposedly found quasi-particle in this case.

1.3. Goldstone's model

Previously, it was mentioned that the Higgs mechanism had relativistic proprieties. Expanding on that, one such theory was developed by Goldstone in 1961 [5]. This relativistic field theory, which also suffers spontaneous symmetry breaking, is based on a complex scalar field ϕ with the following Lagrangian:

$$L = \partial_{\mu}\phi^*\partial^{\mu}\phi - V(\phi) \tag{11}$$

Where,

$$V(\phi) = m^2\phi^*\phi + \frac{1}{2}\lambda(\phi^*\phi)^2 \tag{12}$$

It is important to remind that here natural units is used. Moreover, the metric here is (1,-1,-1,-1), m is the mass parameter and λ is the self-interaction coupling constant of the scalar field.

This model is invariant under a global change of phase:

$$\phi(x) \to e^{i\alpha}\phi(x) \tag{13}$$

If $m^2 > 0$, then this model represents a scalar field which only interacts with itself and from which derive particles and antiparticles with mass m.

If $m^2 < 0$, then we have a maximum of the potential at $\phi = 0$, which is the unstable equilibrium of the potential V which has the following form:

$$V(\phi) = -\frac{1}{2}\lambda v^2\phi^*\phi + \frac{1}{2}\lambda(\phi^*\phi)^2 \tag{14}$$

where $v^2 = -2m^2/\lambda$. V is the sombrero potential. Its minimum values are now spread on the circle:

$$|\phi|^2 = v^2/2 \tag{15}$$

So it is more than expected that in the ground or vacuum state the value of our field ϕ is different from zero. In this case, its magnitude would be approximately $v/\sqrt{2}$ but its phase would be random.

If we confined this system to a finite volume, the expected value of our field would be zero, as the true vacuum state would be a symmetric linear superposition of all these random-phase ground states. This does not happen in the superconduction case, even in a finite volume this symmetry would be broken. However, this field theory deals with infinite volumes, which results that all those random-phased ground states are mutually orthogonal, distinct cases disappear.

What does appear, though, are the Nambu-Goldstone bosons. These emerge if we choose a specific minimum of our field, where it is real and positive. Defining these shifted real fields as $\phi_{1,2}$ by:

$$\phi = \frac{1}{\sqrt{2}}(v + \varphi_1 + i\varphi_2) \tag{16}$$

the resulting Lagrangian is:

$$L = \frac{1}{2}[(\partial_\mu \varphi_1)^2 + (\partial_\mu \varphi_2)^2] - V \tag{17}$$

where:

$$V = -\frac{1}{8}\lambda v^4 + \frac{1}{2}\lambda v^2 \varphi_1^2 + \frac{1}{2}\lambda v \varphi_1(\varphi_1^2 + \varphi_2^2) + \frac{1}{8}\lambda(\varphi_1^2 + \varphi_2^2)^2 \tag{18}$$

This translates into two particles, one associated with ϕ_1, which has a mass of $v\sqrt{\lambda}$, and another one related with ϕ_2, which has no mass and corresponds to a variation on the phase angle. These second ones are what are called the Nambu-Goldstone bosons.

1.4. Nambu-Goldstone boson

Similarly to the Goldstone model [5], the model developed by Nambu and Jona-Lasinio [4] also predicts the existence of a massless particle of spin zero, the Nambu-Goldstone boson, which is a bounded state between a nucleon and a anti-nucleon. This comes from the broken chiral symmetry. When we apply to all the supposed particles a chiral rotation we are just traveling from one degenerate vacuum state to another. This means no energy is actually applied in this rotation. Since it already requires very little energy to vary spatially the chirality with a long wavelenght, when we consider that the energy tends to zero in the long-wavelenght limit, the mass of this particle is zero. The proof of this theory in relativistic terms was made in 1962 by Goldstone, Salam and Weinberg [6].

Nambu and Jona-Lasinio understood that, by breaking symmetry, the way they explained their nucleon would have as consequence the existence of a particle with zero spin and zero mass. No particle like this is known, so they suggested instead that the chiral symmetry was already broken. If they considered this, then the supposed "Nambu-Goldstone bosons" would acquire a small mass and might have been identified with as pions. And although this model was already replaced by other better models, this pion identification would be consistent with the Standard Model of today. Today what we have are no longer the nucleon quasi-particles associated with a potential field but a agglomerate of quarks that composes our matter. We still do not know if our quarks are in fact massless. If this were to be the case, as we have chiral symmetry in spin, we would also have chiral symmetry related with quantum chromodynamics and as consequence pions would became massless.

1.5. Concluding

The task of showing that the Higgs mechanism could work in a relativistic way was done independently by three research groups. This was shown in 1964, by the previous order, by Robert Brout and François Englert [7], by Peter Higgs [8] and by Gerald Guralnik, C. R. Hagen, and Tom Kibble [9]. Although they started working on this problem from different ways, they reached essentially the same conclusions. However, this mechanism is most known by the Higgs mechanism an not by the the Englert-Brout-Higgs-Guralnik-Hagen-Kibble mechanism because the simplest and most direct argument was the one of Higgs [8], where he developed his work based on the previously discussed Goldstone's model. It is important to mention that Higgs had also made important contributions before reaching his final model in the same year[10] where he explicitly notes that a specific gauge choice would remove the relativistic invariance of the theory, and so, one could not simply apply the Goldstone's theorem in that case. However, essentially the same model was considered by both the other groups. Englert and Brout [7], who published first, made calculations regarding the vacuum polarization in the lowest-order perturbation theory when said vacuum symmetry is broken. Finally, Guralnik, Hagen and Kibble [9], studied how could the Goldstone's theorem be avoided by using an operator-oriented approach.

After the busy year of 1964 however, other contributions were made to the overall theory. Higgs in 1966 studied his model in a more quantum mechanical way focusing on transition and decay amplitudes for the model in the lowest-order perturbation theory along with coupling this field with other symmetry breaking fields and trying to figure out what out outcome of this.

To sum up, the main purpose of the Higgs mechanism was to give mass to bosons, in this specific case the bosons W and Z. But as a consequence, it ended up also giving mass, arbitrarily to other fundamental particles of the Standard Model. So, any fermion that interacts with this field can acquire mass in terms of hv resulting from the non-zero expected value of this field. In the Standard Model, this mechanism ends up giving mass to leptons and quarks

alike. However, the masses are determined by arbitrary coupling constants related to how strongly a specific particle interacts with the Higgs field.

2. The Higgs Boson and its mass

Lets consider a simplification of the Higgs field H [11]:

$$V(H) = \mu^2 H^2 + \lambda H^4 + c_0 \tag{19}$$

where μ^2 is the negative mass parameter squared, λ is the Higgs field self-coupling and c_0 is an arbitrary normalization constant which is independent of H and which has no physical consequences. This potential is again our sombrero potential with a maximum value at $H = 0$ and two minimum values at $H = \pm v/\sqrt{2}$ where $v^2 = -\mu^2/\lambda$.

The Higgs potential is symmetric when we consider the $H <-> -H$ symmetry. But this is not the case when we consider its lowest energy state. In this case the symetry is spontaneously broken:

$$H = +v/\sqrt{2} <-> H = -v/\sqrt{2} \tag{20}$$

Keeping this in mind, it is postulated that our universe might have gone through a phase transition at a very early time after the Big Bang, which changed from a high temperature with a symmetric vacuum, a zero average Higgs field, to a low temperature when it rolled into one of the two minimum values which became the vacuum we have today. This transition is what is known as the electroweak phase transition.

The Higgs boson is the quantum of the Higgs field. The mass of this boson is given by the Higgs potential. Its mass is defined by the Higgs potential but here the mass is not clearly visible or a positive coefficient for that matter, since the coefficient μ^2 of the H^2 is negative. So to explicitly show the mass of the Higgs boson, we can devide the Higgs field in two different parts: one that is related to the Higgs particle, which varies around $H = v/\sqrt{2}$, and another part regarding the constant value $v/\sqrt{2}$:

$$H = (h + v)/\sqrt{2} \tag{21}$$

If we substitute this in the previous equation, along with $c_0 = \mu^4/(4\lambda)$ we get:

$$V(h) = 1/4\lambda h^4 + \lambda v h^3 + \lambda v^2 h^2 \tag{22}$$

The last term, $\lambda v^2 h^2$, has the form of the mass term $M_h^2 h^2/2$, which has a positive sign. This is what corresponds to the Higgs boson mass:

$$M_h^2 = 2\lambda v^2 = -2\mu^2 \tag{23}$$

This mass, however, only came much later, on the 4th of July of 2012, where the Higgs boson was finally discovered at the LHC with a mass of 125 GeV, later confirmed on 14th of March of 2013. This corroborated the idea that the Higgs field could not be zero in vacuum. Finally, for clarification, what we in fact observe at the LHC is where the location of the minimum is and how is the curve shaped at that specific minimum value. It is still unknown, however, the specific relation of the Higgs boson with the Standard Model. This is something that only future Physics might answer.

3. The electroweak phase transition

The electroweak phase transition is the phase transition where we swapped from higher-symmetry early-universe phase to a lower-symmetry one by symmetry breaking. Only after this phase transition are we able to make any distinction between the electromagnetic force and the weak force. This happening occurred at a very early stage of the universe, from around $10^{-12}s$ to $10^{-9}s$ after the Big Bang.

Consider the following Higgs potentials for several temperatures:

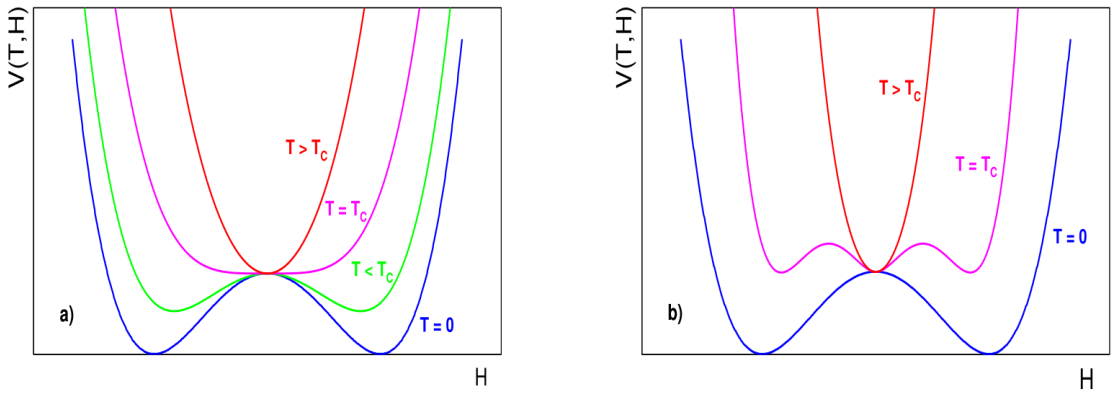

Figure 2. a) Higgs potential for different temperatures for second order phase transition. b) Higgs potential for different temperatures for first order phase transition.

Very shortly after the Big Bang, the Higgs potential took the form we see in b) of figure 2 at the critical temperature of $T_c = 160GeV$. As a result of this, the elementary particles of this early universe gained mass.

To better understand this, we can try to write the Higgs potential at that specific time using the finite temperature effective field theory [12]. This involves making a correction in terms of temperature, proportional to T^2, to the classical Higgs potential that we saw in equation 19. As a result, we get the following modified potential:

$$V(T,H) = V(H) + bT^2H^2 = (\mu^2 + bT^2)H^2 + \lambda H^4 \tag{24}$$

where b relates the particles of the Standard Model to the Higgs field.

Analogously, the relation $\mu^2 + bT^2 = -\lambda v^2 + bT^2$ has a similar effect to which of the α parameter when we looked at the superconducting case. Again, the following relations are established: $\alpha > 0$ for $T > T_c$; $\alpha = 0$ for $T = T_c = \sqrt{(\lambda v^2/b)}$; and $\alpha < 0$ for $T < T_c$. This potential is shown in a) of figure 2.

When the temperature is greater than the critical temperature, the potential is symmetric with its the minimum at $H = 0$. This represents the vacuum of a very early universe. When the temperature is equal to the critical temperature, the valley becomes flatter. When the temperature is smaller than the critical temperature, the potential now gets two minimum values, one at $H > 0$ and the other one at $H < 0$. When the temperature reaches the absolute zero, the two minimum values get to $H = \pm v/\sqrt{2}$ and the potential becomes identical with the one in b) of figure 2. This phase transition is a second order one.

If we consider a first order phase transition however, like in b) of figure 2, we can have three degenerate states when the temperature is equal to the critical temperature. We can achieve this by adding another temperature correction of the next order to the equation 24. This is important to consider because it has been shown that the electroeak phase transition has proprieties of both first and second order phase transitions [13]. Also, for cosmologists, the first order electroweak phase transition can be much more interesting to study since it is associated with the generation of gravitational waves, which can potentially be studied by new gravitational wave interferometers [14], and might also explain the asymmetry that we observe today regarding matter and antimatter in our universe.

4. Conclusions

I tried to the best of my ability, to provide context and overview of the Higgs mechanism, boson, electroweak phase transitions and possible analogies along the chronological order. While in hindsight, it may not have been the best choice of topic, since I am not very keen on particle physics, it was a great task that gave me much more insights, although still introductory, to the matter in question.

The Higgs field remains a not completely understood concept even though it has such a specific and important task in relationship with the other particles in the Standard Model. This field is responsible for the masses of elementary particles, it seems to be the source of great amounts of energy in the vacuum and it may have had an important role in the asymmetry of matter and anti-matter that we today observe in our universe.

Conflicts of Interest: None.

References

[1] Nambu, Y. Quasi-Particles and Gauge Invariance in the Theory of Superconductivity. *Phys. Rev.* **1960**, *117*, 648–663. doi:10.1103/PhysRev.117.648.

[2] Bardeen, J.; Cooper, L.N.; Schrieffer, J.R. Microscopic Theory of Superconductivity. *Phys. Rev.* **1957**, *106*, 162–164. doi:10.1103/PhysRev.106.162.

[3] Ginzburg, V.L.; Landau, L.D. On the Theory of superconductivity. *Zh. Eksp. Teor. Fiz.* **1950**, *20*, 1064–1082.

[4] Nambu, Y.; Jona-Lasinio, G. Dynamical Model of Elementary Particles Based on an Analogy with Superconductivity. I. *Phys. Rev.* **1961**, *122*, 345–358. doi:10.1103/PhysRev.122.345.

[5] Goldstone, J. Field Theories with Superconductor Solutions. *Nuovo Cim.* **1961**, *19*, 154–164. doi:10.1007/BF02812722.

[6] Goldstone, J.; Salam, A.; Weinberg, S. Broken Symmetries. *Phys. Rev.* **1962**, *127*, 965–970. doi:10.1103/PhysRev.127.965.

[7] Englert, F.; Brout, R. Broken Symmetry and the Mass of Gauge Vector Mesons. *Phys. Rev. Lett.* **1964**, *13*, 321–323. doi:10.1103/PhysRevLett.13.321.

[8] Higgs, P.W. Broken Symmetries and the Masses of Gauge Bosons. *Phys. Rev. Lett.* **1964**, *13*, 508–509. doi:10.1103/PhysRevLett.13.508.

[9] Guralnik, G.S.; Hagen, C.R.; Kibble, T.W.B. Global Conservation Laws and Massless Particles. *Phys. Rev. Lett.* **1964**, *13*, 585–587. doi:10.1103/PhysRevLett.13.585.

[10] Higgs, P.W. Broken symmetries, massless particles and gauge fields. *Phys. Lett.* **1964**, *12*, 132–133. doi:10.1016/0031-9163(64)91136-9.

[11] Melo, I. Higgs potential and fundamental physics. *European Journal of Physics* **2017**, *38*, 065404. doi:10.1088/1361-6404/aa8c3d.

[12] Carena, M.; Megevand, A.; Quirós, M.; Wagner, C. Electroweak baryogenesis and new TeV fermions. *Nuclear Physics B* **2005**, *716*, 319–351. doi:10.1016/j.nuclphysb.2005.03.025.

[13] Kajantie, K.; Laine, M.; Rummukainen, K.; Shaposhnikov, M. A non-perturbative analysis of the finite-T phase transition in SU (2) x U (1) electroweak theory. *Nuclear Physics B* **1997**, *493*, 413–438. doi:10.1016/s0550-3213(97)00164-8.

[14] Huang, P.; Long, A.J.; Wang, L.T. Probing the electroweak phase transition with Higgs factories and gravitational waves. *Phys. Rev. D* **2016**, *94*, 075008. doi:10.1103/PhysRevD.94.075008.

Proceedings

Formation of Primordial Black Holes

Pedro Martins [1]

[1] Faculdade de Ciências da Universidade de Lisboa; fc49539@alunos.fc.ul.pt

Received: 27-01-2019

Abstract: Primordial black holes (PBHs) are hypothetical structures thought to have been formed in the early stages of the Universe, as a result of quantum fluctuations on its density during the otherwise uniform expansion. It is thought that, aside from putting constraints on the spectrum of density fluctuations in the early universe, they could also present a solution for problems such as the dark matter problem, the domain wall problem, and the cosmological monopole problem. This article aims to review current information on PBH, focusing on their formation and evaporation, with eventual constraint being placed by recent studies.

Keywords: Cosmology; Primitive Universe; Black Holes.

---

1. Introduction

Usually, when discussing black holes, one would be referring to structures formed from the gravitational collapse of massive stars, resulting in a body of extremely high density.

Primordial black holes however, though also the result of great compression, are thought to be formed during the early expansion of the Universe, by quantum fluctuations of the density. A comparison of the cosmological density at a time t after the Big Bang with the density associated with a black hole of mass M shows that PBHs would have of order the particle horizon mass at their formation epoch (S. W. Hawking, 1971):

$$M_H \approx \frac{c^3 t}{G} \approx 10^{15} \left(\frac{t}{10^{-23} s} \right) g \tag{1}$$

One can see by the expression that PBHs have appear to have a great mass range, going as low as the Planck mass (10^{-5}g), in contrast with the minimum mass for regular black holes of around $1 M_\odot$. This prompted Hawking to study their quantum properties, leading to his discovery that black holes radiate like a black body with a temperature

$$T = \frac{\hbar c^3}{8\pi G M k} \approx 10^{-7} \left(\frac{M}{M_\odot} \right)^{-1} K \tag{2}$$

on a timescale

$$\tau(M) = \frac{\hbar c^4}{G^2 M^3} \approx 10^{64} \left(\frac{M}{M_\odot} \right)^3 y \tag{3}$$

Only black holes smaller than about 10^{15}g would have evaporated by the present epoch, so Eq.1 implies that this effect could be important only for black holes which formed before 10^{-23}s.

Hawking's study established a link between general relativity, thermodynamics and quantum theory, serving as a great advance for the study of the Primordial Universe.

2. PBH formation

It is clear that during the first moments after the Big Bang, the energy density of the Universe was extremely high. This however is not enough to create conditions for PBH formation, as the expansion should have occured in an homogeneous way (at the macro scale, that is).

Introducing quantum fluctuations in the density creates overly dense regions that could collapse and form a PBH, even in a spontaneous way in an homogeneous region. Their study could then impose important constraints on primordial inhomogeneities and parameters associated with phase transition.

2.1. Density fluctuations

As mentioned above, PBHs are thought to have formed from density fluctuations during the early stages of the Universe. As such, studying PHBs allows for limits to be placed on the spectrum of density perturbations. This is because, if PBHs do form directly from density fluctuations, the fraction of regions undergoing collapse at any epoch is determined by the root-mean-square amplitude ϵ of the fluctuations entering the horizon at that epoch and the equation of state p = wρ. Since we're analyzing the radiation-dominated period, we should expect deviations from $w = \frac{1}{3}$.

In (B. J. Carr and S. W. Hawking, 1974), it was assumed that the region which evolves to a PBH is spherically symmetric and part of a closed Friedmann model. In order to collapse against the pressure, the size of that region must be larger than the Jeans length at maximum expansion ($\sqrt{w}$ times the horizon size), and smaller than the horizon size, from beyond which it would form a separate closed universe and not be part of our Universe.

The first implication of this restriction is that a PBH forming at time t after the Big Bang should have of order the horizon mass given by Eq.1. Second, for a region destined to collapse to a PBH, one requires the fractional increase in density at the horizon epoch δ to exceed w. As determined in (B. J. Carr, 1975), if the density fluctuations have a Gaussian distribution and are spherically symmetric, the fraction of regions of mass M which collapse is

$$\beta(M) \sim \epsilon(M) exp\left[-\frac{w^2}{2\epsilon^2(M)}\right] \tag{4}$$

where ϵ(M) is the value of ϵ when the horizon mass is M. The PBHs can have an extended mass spectrum only if the fluctuations are scale-invariant (ϵ has to be independent of M). In this case, the PBH mass distribution is given by

$$\frac{dn}{dM} = (\alpha - 2)\left(\frac{M}{M_o}\right)^{-\alpha} M_o^{-2}\Omega_{PBH}\rho_{crit} \tag{5}$$

where $M_o \approx 10^{15}$ is the minimum mass limit due to Hawking radiation, Ω_{PBH} is the total density of the PBHs in units of the critical density (which depends on β) and the exponent α is determined by the equation of state:

$$\alpha = \left(\frac{1+3w}{1+w}\right) + 1 \tag{6}$$

For $w = \frac{1}{3}$ (radiation), we have $\alpha = \frac{5}{2}$, meaning that for PBHs larger than M, the density falls off as $M^{-1/2}$, and so most of the PBH density is contained in the smallest ones.

Scenarios conducted by Carr on the density fluctuations showed that although ϵ is approximately scale-invariant, the sensitive dependence of β on ϵ proves the importance of even tiny deviations from scale-invariance. If ϵ(M) decreases with M, then the spectrum falls off exponentially and most of the PBH density is contained in the smallest ones. If ϵ(M) increases with M, the spectrum rises exponentially and so PBHs could only be formed at large scales. For this last scenario to be true however, the microwave background anisotropies should be larger than observed, so it is not likely to happen.

Carr also determined the density parameter Ω_{PBH} associated with PBHs which form at a redshift z or time t to be related to β by

$$\Omega_{PBH} = \beta\Omega_R(1+z) \approx 10^{18}\beta\left(\frac{M}{10^{15}g}\right)^{-1/2} \tag{7}$$

where $\Omega_R \approx 10^{-4}$ is the density parameter of the microwave background. The (1 + z) factor arises because Ω_R scales with $(1+z)^4$ and Ω_{PBH} scales with $(1+z)^3$. Any limit on Ω_{PBH} therefore places a constraint on β(M) (Fig. 1) (Carr et al., 1994). The constraint for non-evaporating mass above 10^{15}g comes by taking Ω_{PBH} <1.

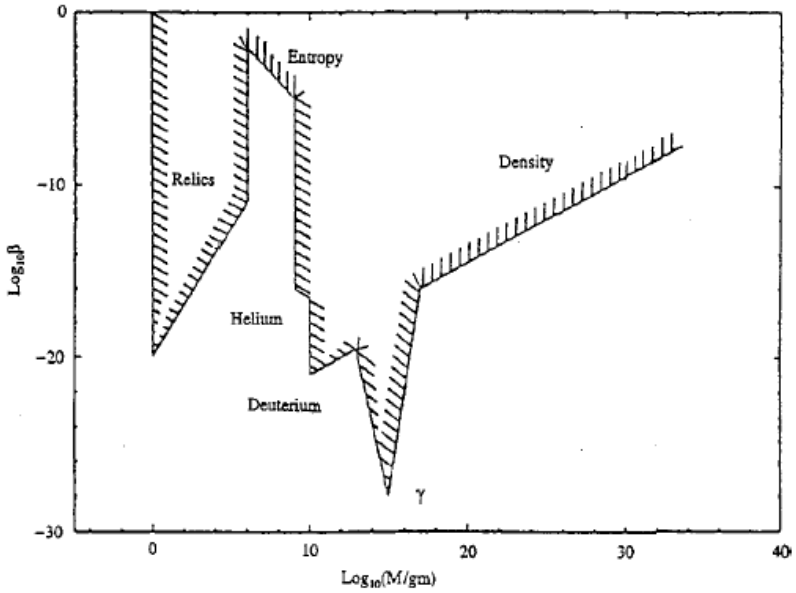

Figure 1. Logarithmic plot of the constraints on β(M) (B. J. Carr, 1994).

Stronger constrictions have been placed on this value by observational methods. Femtolensing of γ-ray bursts is probably the strongest of them. Usually, gravitational lensing causes the distortion of an object when its light passes through another with a strong gravitational field, acting like a lens and deflecting the light. However, in femtolensing the distortions are not visible, instead becoming noticeable by small variations in the frequency of the light received.

A limit of $10^{10} - 10^{15}$ was placed early on from observational data(D.N. Page andS. W. Hawking, 1976). In (A. Barnacka et al., 2012), the lack of femtolensing detections in data from the Fermi Gamma-ray Burst Monitor evidenced that the mass range $10^{14} - 10^{17}$ should not contribute to dark matter. This limit was latter removed by , by taking into account the extended nature of the object (A. Katz et al., 2018). The constraints below 10^6g are based on the assumption that evaporating PBHs leave stable Planck mass relics.

The constraints on β(M) can be converted into constraints on ϵ(M) using Eq.4 (Fig. 2). Also shown here are the non-PBH constraints associated with the spectral distortions in the CMB induced by the dissipation of intermediate scale density perturbations and the COBE quadrupole measurement. This shows that, in order to produce PHBs, the fluctuation amplitude needs to decrease with the scale.

T. Harada et al. (2013) was able to give a reliable analytic formula for the perturbation amplitude. As mentioned before, considering a spherical geometry, the radius of the dense region at maximum expansion should be

$$R_{a,max} = a_{max} \sin \chi_a \tag{8}$$

and be somewhere between the Jeans radius ($R_J = \sqrt{w} a_{max}$) and the horizon size a_{max}. Working in a closed Friedmann space (k=1), we have

$$\frac{a_{max}}{a_0} = \left(\frac{\Omega_0}{\Omega_0 - 1} \right)^{1/(1+3w)} \tag{9}$$

$$a_0 = (\Omega_0 - 1)^{-1/2} H_0^{-1} \tag{10}$$

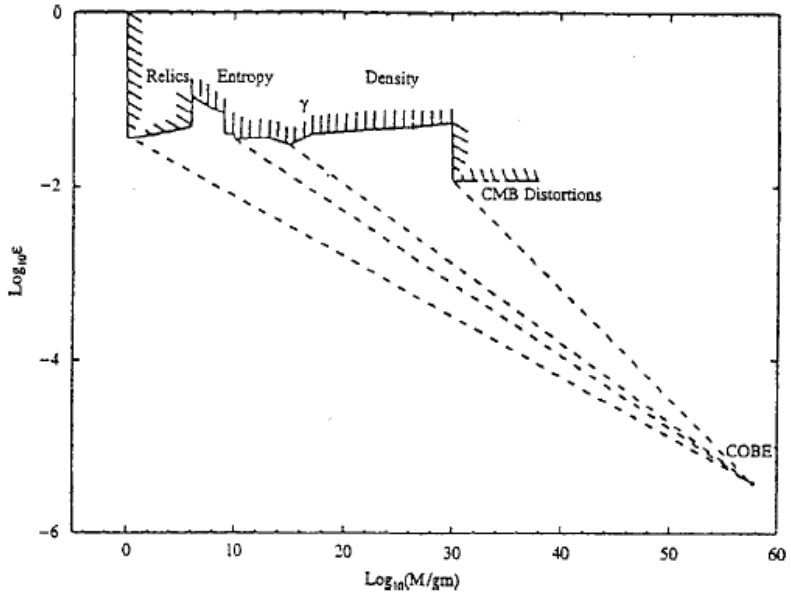

Figure 2. Logarithmic plot of the constraints on ϵ(M) (B. J. Carr, 1994).

Applying all these conditions to the constraint would result in the relation

$$w < (\Omega_0 - 1)\left(\frac{R_{a,0}}{R_{H_0}}\right)^2 < 1 \tag{11}$$

where the middle term corresponds to the fluctuation amplitude, δ_H^{UH}. A way to reduce the dependence of the result with the Jeans radius through numerical simulations (T. Harada et al., 2013) gives

$$\delta_{Hc}^{UH} = \sin\left(\frac{\pi\sqrt{w}}{1+3w}\right)^2, \delta_c = \left[\frac{3(1+w)}{5+3w}\right]\delta_{Hc}^{UH} \tag{12}$$

where δ_{Hc}^{UH} is the perturbation amplitude at the horizon crossing time in the uniform Hubble slice, and δ_c is the amplitude measure used in the simulations. With this formula, for a radiation fluid ($w = \frac{1}{3}$), we have $\delta_{Hc}^{UH} = 0.6203$ and $\delta_c = 0.4135$.

2.2. Inflation

Inflation has two important consequences for PBHs (B. J. Carr, 2005). Firstly, any PBHs formed before the end of inflation will be diluted to a negligible density. Inflation thus imposes a lower limit on the PBH mass spectrum:

$$M > M_{min} = M_P\left(\frac{T_{RH}}{T_P}\right)^{-2} \tag{13}$$

where T_{RH} is the reheat temperature and $T_P \approx 10^{19}$ GeV is the Planck temperature. The CMB quadrupole measurement implies $T_{RH} \approx 10^{16}$ GeV, so M_{min} certainly exceeds 1 g. On the other hand, inflation will itself generate fluctuations and these may suffice to produce PBHs after reheating. If the inflation potential is $V(\phi)$, then the horizon-scale fluctuations for a mass-scale M are

$$\epsilon(M) \approx \left(\frac{V^{3/2}}{M_P^3 V'}\right)_H \tag{14}$$

In the standard chaotic inflationary scenario, one makes the "slow-roll" and "friction-dominated" assumptions:

$$\xi = \left(\frac{M_P V'}{V}\right)^2 \ll 1, \eta = M_P^2 \frac{V''}{V} \ll 1 \tag{15}$$

Usually the exponent n characterizing the power spectrum of the fluctuations, $|\delta_k|^2 \approx k^n$, is very close to but slightly below 1:

$$n = 1 + 4\xi - 2\eta \approx 1 \tag{16}$$

and considering that ϵ scales with $M^{(1-n)/4}$, we can infer that the fluctuations are slowly increasing with scale. The normalization required to explain galaxy formation ($\epsilon \approx 10^{-5}$) would then predict the formation of PBHs on a smaller scale. However, if PBH formation is to occur, we need the fluctuations to decrease with the mass (n > 1) and, from Eq.15, this is only possible if the scalar field is accelerating fast enough that

$$\frac{V''}{V} > \frac{1}{2}\left(\frac{V'}{V}\right)^2 \tag{17}$$

If this condition is met, Eq.4 implies that the PBH density will be dominated by the ones forming immediately after reheating (B. J. Carr and J. E. Lidsey,1993).

In Fig. 3, we can observe constraints put on the value of n over time (B. J. Carr et al., 1994). Since each value of n corresponds to a straight line in Figure 3., any particular value for the reheat time t_1 corresponds to an upper limit on n. It also shows how the constraint on n is strengthened if the reheating at the end of inflation is sufficiently slow for there to be a dust-like phase.

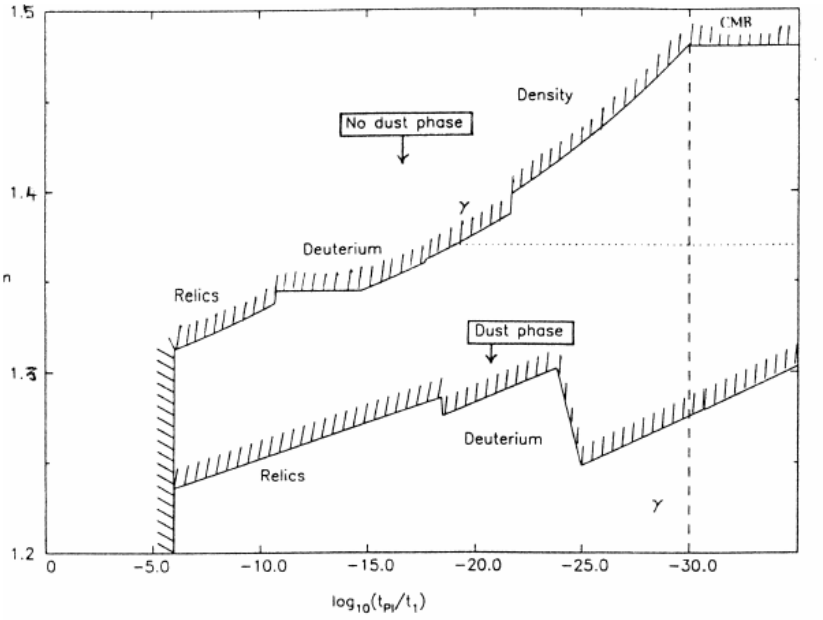

Figure 3. Logarithmic plot of the constraints on the spectral index n in terms of reheat time t_1 (B. J. Carr, 1994).

However, not all inflationary scenarios predict that the spectral index should be constant. By choosing the form of $V(\phi)$, one can get any spectrum for the fluctuations. For example, Eq.14 suggests that one can get a spike in the spectrum by flattening the potential over some mass range (since the function in divergent when V′ goes to 0). This idea was exploited by (Ivanov et al., 1994), who fine-tuned the position of the spike so that it corresponds to the mass-scale associated with microlensing observations.

Even if PBHs never actually formed as a result of inflation, studying them places important constraints on the many types of inflationary scenarios.

2.3. Other factors for PBH formation

Though fluctuations in density are viewed as the main mechanism in the formation of PBHs, there are some others worth mentioning, which could apply constraints to PHB mass. Following are brief, understandable reviews from B. J. Carr (2005).

2.3.1. Soft equation of state

Some phase transitions can lead to the equation of state becoming soft for a while. For example, the pressure may be reduced if the Universe's mass is ever channeled into particles which are massive enough to be non-relativistic. In such cases, the effect of pressure in stopping collapse is unimportant and the probability of PBH formation just depends upon the fraction of regions which are sufficiently spherical to undergo collapse. For a given spectrum of primordial fluctuations, this means that there may just be a narrow mass range - associated with the period of the soft equation of state - in which the PBHs form.

2.3.2. Collapse of cosmic loops

In the cosmic string scenario, one expects some strings to self-intersect and form cosmic loops. A typical loop will be larger than its Schwarzschild radius by the factor $(G\mu)^{-1}$, where μ is the string mass per unit length. If strings play a role in generating large-scale structure, $G\mu$ must be of order 10^{-6}. However, there is always a small probability that a cosmic loop will get into a configuration in which every dimension lies within its Schwarzschild radius. This probability depends upon both μ and the string correlation scale. Note that the holes form with equal probability at every epoch, so they should have an extended mass spectrum.

2.3.3. Bubble collisions

Bubbles of broken symmetry might arise at any spontaneously broken symmetry epoch and it is suggested that PBHs could form as a result of bubble collisions. However, this happens only if the bubble formation rate per Hubble volume is finely tuned: if it is much larger than the Hubble rate, the entire Universe undergoes the phase transition immediately and there is not time to form black holes; if it is much less than the Hubble rate, the bubbles are very rare and never collide. The holes should have a mass of order the horizon mass at the phase transition, so PBHs forming at the GUT epoch would have a mass of $10^3 g$, those forming at the electroweak unification epoch would have a mass of $10^{28} g$, and those forming at the QCD phase transition would have mass of around 1 solar mass.

2.3.4. Collapse of domain walls

The collapse of sufficiently large closed domain walls produced at a 2nd order phase transition in the vacuum state of a scalar field, such as might be associated with inflation, could lead to PBH formation. These PBHs would have a small mass for a thermal phase transition with the usual equilibrium conditions, and could be much larger if one invoked a non-equilibrium scenario. PBHs could therefore be suggested as a solution for the domain wall problem.

3. PBH evaporation

Originally, it was thought that black holes were bodies that only absorbed matter and energy around them, being essentially eternal. Of course, nowadays we know, they do release small amounts of energy through quantum effects near the black hole event horizon. This was first proposed by S. W. Hawking (1974).

3.1. Hawking radiation

In 1975, Hawking determined that black holes emit particles like black-bodies of temperature

$$T \approx \left(\frac{M}{10^{13} g}\right)^{-1} GeV \tag{18}$$

This however doesn't take into consideration charge or angular momentum, although there wouldn't be much difference, considering that both will be lost at a much shorter timescale than the mass. The rate at which a BH loses mass, according to Hawking, is

$$\frac{dM}{dt} = -5 \times 10^{25} \left(\frac{M}{g}\right)^{-2} f(M) g s^{-1} \tag{19}$$

where f(M) depends on the number of particle species light enough to be emitted by a BH of mass M. The lifetime of a BH is therefore

$$\tau(M) = 6 \times 10^{-27} f(M)^{-1} \left(\frac{M}{g}\right)^{3} s \tag{20}$$

f tends to 1 for holes larger than 10^{17}g and only emit "massless" particles (photons, neutrinos, etc). Holes in the mass range $10^{15}g < M < 10^{17}g$ also emit electrons, and those in the range $10^{14}g < M < 10^{15}g$ emit muons. This last range includes the critical mass for which the lifetime is the age of the Universe. Assuming $\tau = 13.7$ Gyr (B. J. Carr, 2005), we get $M_{crit} = 5 \times 10^{14}g$. For $M < 10^{14}g$, the BH can also emit hadrons through jets of quark and gluons.

J. H. MacGibbon and B. R. Webber (1990) where able to determine the present-day background spectrum of particles generated by PBH evaporations, by integrating over the lifetime of each BH of mass M and then over the PBH mass spectrum. O course, one must take into account that particles generated from smaller PBH will be redshifted due to their source evaporating earlier.

The results are plotted in Fig. 4, assuming an uniform PBH distribution around the Universe. As one can see, all the spectra seem to have a declination of E^{-1} for E < 100 MeV, due to fragmentation of jets, and E^{-3} for E > 100 MeV, due to final phases of evaporation at present time.

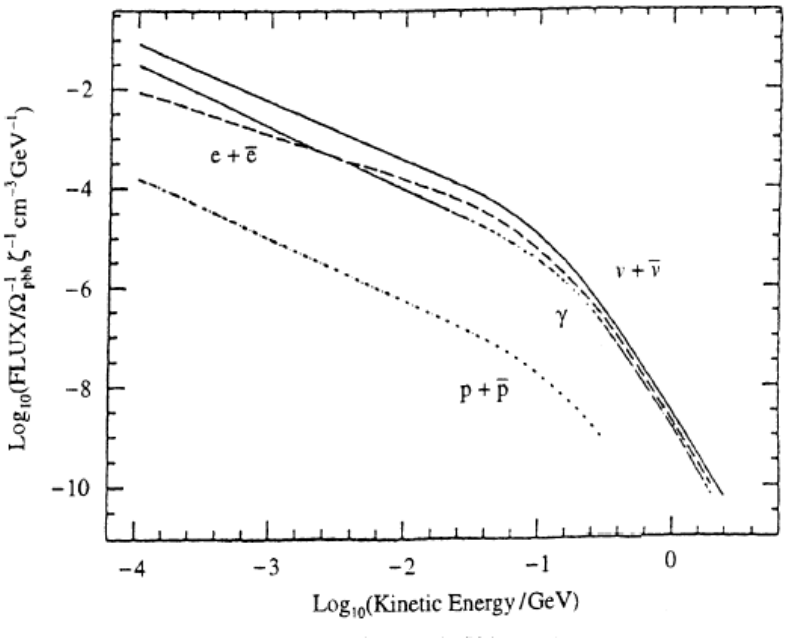

Figure 4. Logarithmic plot of the spectrum of particles from uniformly distributed PBHs (J.H. MacGibbon and B.R. Webber, 1990).

The situation is more complicated if we take into account that the PBHs evaporating at present time are clustered inside our own Galactic halo (B. J. Carr, 2005). In this case, any charged particles emitted after our galaxy's formation (PBHs somewhat smaller than M_{crit}) will have their flux enhanced relative to the photon spectra by a factor ξ which depends on the halo concentration factor and the time for which particles are trapped inside the halo by the Galactic magnetic field. At 100 MeV, we have $\xi \approx 10^3$ for electrons/positrons and $\xi \approx 10^4$ for protons and anti-protons.

3.2. Quantum scale PBHs

The formulae from the previous section are applicable only if the laws of gravity are approximately valid all the way down to the Planck scale. In particular, for black holes with masses below the Planck mass ($\sim 10^{-8}$ kg), they result in impossible lifetimes below the Planck time ($\sim 10^{-43}$ s). This is normally seen as an indication that the Planck mass is the lower limit on the mass of a black hole, meaning that the influence of extra dimensions becomes important at the energy scale of 10^{19}GeV. The study on formation and evaporation of black holes in particle accelerators could then prove useful. (B. J. Carr, 2005). In a model with large extra dimensions, the Schwarzschild radius itself depends on the dimension number:

$$r_S \approx \frac{1}{M_P}\left(\frac{M_{BH}}{M_P}\right)^{\frac{1}{1+n}} \tag{21}$$

where M_P is the modified Planck mass. Consequently, the temperature and lifetime will be given by

$$T_{BH} \approx \frac{n+1}{r_S}, \tau \approx \frac{1}{M_P}\left(\frac{M_{BH}}{M_P}\right)^{\frac{n+3}{n+1}} \tag{22}$$

Thus, the temperature is decreased relative to the standard 4-dimensional case and the lifetime is increased. The important qualitative effect is that a large fraction of the beam energy is converted into transverse energy, leading to large-multiplicity events with many more hard jets and leptons than what would otherwise be expected.

4. Conclusion

It is plausible that PBHs may have formed in the first moments of the Universe, mainly as the result of density fluctuations in the otherwise homogeneous expansion. Constraints on their mass and on the fluctuation amplitude can be placed by both mathematical and observational methods. The study of PBH formation in the early Universe can help place constraints on primordial inhomogeneities, phase transition parameters and inflation scenarios. By also considering the collapse of domain walls as a formation factor, one may suggest PBHs as a possible solution to the domain wall problem. On the other hand, the study of quantum-scale black holes in particle accelerators can help understand the influence of extra dimensions on the formation of small-scale PBHs.

References

1. Ali-Haïmoud, Y.; Kamionkowski, M. "Cosmic microwave background limits on accreting primordial black holes". *Phys. Rev. D* **2017**, *95*, 043534.
2. Barnacka, A. et al. "New constraints on primordial black holes abundance from femtolensing of gamma-ray bursts". *Phys. Rev. D* **2012**, *86*, 043001.
3. Carr, B.J.; Hawking, S.W. "Black Holes in the Early Universe". *Mon. Not. Roy. Astron. Soc.* **1974**, *168*, 399–416.
4. Carr, B.J. "The primordial black hole mass spectrum". *Astr. Jour.* **1975**, *201*, 1–19.
5. Carr, B.J. et al. "Black Hole Relics and Inflation: Limits on Blue Perturbation Spectra". *Phys. Rev. D* **1994**, *50*, 4853.
6. Carr, B.J. "Primordial Black Holes: Do They Exist and Are They Useful?". In *Inflating Horizon of Particle Astrophysics and Cosmology*; Universal Academy Press Inc and Yamada Science Foundation; 2005.
7. Harada, T. et al. "Threshold of primordial black hole formation". *Phys. Rev. D* **2013**, *88*, 084051.
8. Hawking, S.W. "Gravitationally collapsed objects of very low mass". *Mon. Not. R. Astr. Soc.* **1971**, *152*, 75–78.
9. Hawking, S.W. "Black hole explosions?". *Nature* **1974**, *248*, 30–31.
10. Hawking, S.W. "Particle Creation by Black Holes". *Com. Mat. Phy.* **1975**, *43*, 199–220.
11. Katz, A. et al. "Femtolensing by dark matter revisited". *Jour. Cos. Astro. Phys.* **2018**, *12*.
12. MacGibbon, J.H.; Webber, B.R. "Quark- and gluon-jet emission from primordial black holes: The instantaneous spectra". *Phys. Rev. D* **1990**, *41*, 3052–3079.
13. Page, D.N.; Hawking, S.W. "Gamma rays from primordial black holes". *Astr. Jour.* **1976**, *206*, 1–7.